UNRAVELLING NOVEL MOLECULAR TARGETS FOR PHOTOBIOMODULATION IN HUMAN HAIR FOLLICLE TOWARDS THE DEVELOPMENT OF MORE EFFECTIVE LIGHT-BASED THERAPIES FOR HAIR GROWTH

S.BUSCONE

PhD

2017

Unravelling novel molecular targets for photobiomodulation in human hair follicle towards the development of more effective light-based therapies for hair growth

Serena BUSCONE

Submitted for the Degree of

Doctor of Philosophy

Faculty of Life Sciences

University of Bradford

2017

Abstract

Unravelling novel molecular targets for photobiomodulation in human hair follicle towards the development of more effective light-based therapies for hair growth

Keywords: Hair follicle, hair growth, hair follicle stem cells, photobiomodulation, blue light, photoreceptors, Cryptochrome 1, Opsin 2, Opsin 3, circadian clock

Light and optical techniques have made a profound impact on modern medicine both in diagnostics and in therapy. Therapeutic action of light is based on photomechanical, photothermal, photochemical and photobiological interactions, depending on the wavelength, power density, exposure time and optical properties of tissue and cells. Last decade experienced a growing rise of commercial devices for management of hair growth, where all of them are based on low levels of light resulting into photobiological, non-thermal interaction of photons with cells, a process that recently has received an official term ‘photobiomodulation’. However, the design and analysis of the reported clinical studies are highly debated in a wider scientific community. The picture is further complicated by a virtual lack of proof about the exact molecular targets that mediate the physiological response of skin and hair follicles (HF) to low levels of light.

The goal of this project was to investigate the expression of light-sensitive receptors in the human HF and to study the impact of UV-free blue light on hair growth *ex vivo*. The expression of Cryptochromes 1 and 2 (CRY1, 2), Opsin 2 and 3 (OPN2 and OPN3), but not other Opsins 1, 4 and 5 was detected in the distinct compartments of skin and anagen HF. Evaluation of the physiological role of detected light-sensitive receptors on hair growth was performed by the modulation of photoreceptors activity in HF *ex vivo* model. HFs treated with KL001, a stabilizer of CRY1 protein that lengthens the circadian period, delayed HF anagen-catagen transition; while silencing of CRY1 induced premature catagen development accompanied by reduced cell proliferation. Silencing of CRY1 in the HF outer root sheath (ORS) cells in vitro caused downregulation of

genes involved in the control of proliferation; including the cyclin dependent kinase 6 (CDK6). OPN3 also had a positive effect on metabolic activity and proliferation of the ORS cells in vitro. OPN3 silencing resulted in the altered expression of genes involved in the control of proliferation and apoptosis. Investigated CRY1, OPN2 and 3 greatly absorb in the blue to green-region of the visible spectrum. This led us to investigate the effect of blue light on HF growth. Daily treatment with blue light (453 nm, 3.2 J/cm^2, 16 nm full width half maximum) prolonged anagen phase in HF *ex vivo* that was associated with sustained proliferation. In addition, blue light (3.2 J/cm^2) significantly stimulated proliferation of ORS cells *in vitro*. This effect was abrogated by silencing of OPN3.

To summarize, CRY 1, OPN 2 and OPN 3 are expressed in the distinct compartments of the HF, including HF stem cells. Blue light (453 nm) at low radiant exposure exerts a positive effect on hair growth *ex vivo*, potentially via interaction with OPN3. The further research should be conducted to decipher interactions between blue light and the investigated receptors in the HFs. In addition, the beneficial effect of blue light at low radiant exposure on hair growth raises a possibility of increasing therapeutic efficacy when combined with topical chemistry used for management of hair growth.

Acknowledgements

I would like first to acknowledge and offer my sincere thanks to my supervisor, Dr. Natasha Botchkareva for giving me the opportunity to be part of CLaSSiC project. Her guidance and support were invaluable throughout these years, and I had the chance to directly learn from her and get enthusiastic about the fascinating world of hair biology. I also would like to thank Dr. Andrei Mardaryev for his support as second supervisor within the Centre for Skin Sciences.

A special thanks to all the members of CLaSSiC team for their contribution to the project, in particular to Dr. Natallia E. Uzunbajakava, project supervisor at Philips Research, our industry partner within CLaSSiC. Her contribution to the present work, the Laser in Surgery and Medicine paper, and to all conferences attended over the past years has been fundamental.

Without the Marie Curie actions funding, this work would have not be possible, together with the opportunity of pursuing research under the exceptional guidance of a supervisory team of experts, sharing my work in the international scientific community and enjoy the experience of working abroad.

I’m especially grateful to Irene Castellano and Charles Mignon, great colleagues and friends over this PhD, Bianca Raaf for her exceptional technical support in Philips, all the colleagues in Botchkareva and Botchkarev lab, it felt always like home working with you.

Grazie finally to my family, without your support and love I could not be able to get through such an adventure, full of recognitions but also of hard times. Thank you my dear friends for always being present, even at distance and thank you Filippo to be the great partner in my life.

Author's declaration

I declare that the work in this dissertation was carried out in accordance with the requirements of the University's Regulations and Code of Practice for Research Degree Programs and that it has not been submitted for any other academic award. The work is the candidate's own work, except what was done in collaboration with, or with the assistance of others. Specifically, the author would like to mention that: the light treatment of hair follicle ex vivo and images collection was performed by Bianca Raafs, the statistical analysis of the mean survival time of hair follicle in response to light treatment was conducted by Jan W. Bikker, microarray and bioinformatics analysis was performed at the Center for medical research, University of Mannheim, by Carsten Sticht.

Table of Contents

List of figures

List of tables

List of abbreviations

7-AAD, 7-aminoactinomycin D

AA, alopecia areata

AE 13, Hair cortex cytokeratin

AE 15, Trichohyalin

AGA, androgenetic alopecia

APC, Allophycocyanin

APM, arrector pili muscle

BLOC1S2, Biogenesis of lysosomal organelles complex 1 subunit 2

BMP, Bone morphogenetic protein

BSA, Bovine serum albumin

CAV2, Caveolin 2

CD200, OX-2 membrane glycoprotein

CD34, Hematopoietic progenitor cell antigen CD34

CD49f integrin, Integrin alpha 6

cDNA, Complementary deoxyribonucleic acid

CK 14, Cytokeratin 14

COX, cytochrome C oxidase

DAPI , 4',6-diamidino-2-phenylindole

DP, dermal papilla

EDTA, Ethylenediaminetetraacetic acid

FBS, Fetal bovine serum

FDA, Food and Drug Administration

FDR, False discovery rate

FITC, Fluorescein isothiocyanate

FSTL1, Follistatin-like 1

GAPDH, Glyceraldehyde 3-phosphate dehydrogenase

GPCR, G-protein-coupled receptors

HaCaT, Immortalized cultured human keratinocytes cell line

HF, Hair follicle

HFSC, Hair follicle stem cells

HS, hair shaft

IRS, Inner root sheath

LED, Light-emitting diode

NIR, Near-infrared

NO, Nitric oxide

OPN1sw, Opsin 1 short wavelength

OPN1sw, Opsin 1 middle wavelength

OPN2, Opsin 2, Rhodopsin

OPN3, Opsin 3, Encephalopsin

OPN4, Opsin 4, Melanopsin

OPN5, Opsin 5, Neuropsin

ORS, Outer root sheath

PAK2, p21 protein (Cdc42/Rac)-activated kinase

PBM, Photobiomodulation

PBS, Phosphate-buffered saline

PCR, Polymerase chain reaction

PE, Phycoerythrin

PFA, Paraformaldehyde

qPCR, Quantitative polymerase chain reaction

RNA, Ribonucleic acid

ROS, Reactive oxygen species

RT-PCR, Reverse transcription polymerase chain reaction

RT-qPCR, Quantitative reverse transcription Polymerase chain reaction

SFNX1, Sideroflexin 1

SG, sebaceous gland

siRNA, Small interfering RNA

UBR5, Ubiquitin protein ligase E3 component N-recognin 5

ULBP1, UL16 binding protein 1

UVA, Ultraviolet A

UV-free, Ultraviolet-free

1 Introduction

1.1 Biology of the hair follicle

The hair follicle (HF) is one of the most complex “mini-organ” (Schneider et al. 2009) in the body and plays a variety of physiological roles: it is involved in the temperature regulation, immune defense, touch sensation, sexual selection, and wound repair (Ito et al. 2005; Stenn and Paus 2001). In addition, HF has also important functions in the social life of human; indeed hair loss can have a negative impact on people’s life. Different kinds of alopecia have been described; the most prevalent is androgenetic alopecia (AGA) that affect 50% of the male population by the age of 50 (Price 2003).The existing pharmacological treatments of AGA show some positive effects, but there is no definitive solution for this problem yet. This project aims to understand the biological effects triggered by low level laser therapy or photobiomodulation in the HF in order to develop more effective light-based solutions for the hair re-growth.

1.1.1 Hair follicle structure and cellular composition

Within the skin HFs are organized in pilosebaceous units composed of the HF, the sebaceous gland (SG) and the arrector pili muscle (APM). The SG is an acinar gland composed of lipid-filled sebocytes; it secretes sebum that, for example, helps making hair and skin waterproof (Schneider et al. 2009). The APM is a tiny smooth muscle that when contracted causes the ‘raising’ of the hair. The mature anagen HF can morphologically be divided into three regions: the infundibulum, isthmus and the hair bulb (Figure 1-1 A). The infundibulum represents the uppermost portion of the HF; it forms the junction between the HF and the epidermis and includes the opening of the hair canal to the skin

surface. The isthmus is the middle portion of the HF, which is situated between the SG duct opening and the attachment site for the APM; it harbors the bulge region (Figure 1-1 B) containing epithelial and melanocyte stem cells (Ohyama et al. 2006; Snippert et al. 2010). The lower portion of the HF, hair bulb, contains the hair matrix, consisting of the actively proliferating epithelial cells and pigment producing melanocytes, which envelopes an area of densely populated fibroblast cells called the dermal papilla (DP) (Paus and Foitzik 2004; Schneider et al. 2009) (Figure 1-1 C). The rapidly proliferating matrix keratinocytes contribute to the HF formation by generating the different cell lineages: the inner root sheath (IRS), including the companion layer, Henle's layer, Huxley's layer and cuticle and the hair shaft (HS), including the cuticle, cortex and the medulla (Schneider et al. 2009) (Figure 1-1 D). Functionally, the IRS serves as a rigid funnel-shaped protection covering the HS: the flattened corneocytes of the cuticle of the IRS overlap and interlock intimately with the cells of the cuticle of the HS ensuring that the IRS and the growing hair ascend upwards in the follicle together (Joshi 2011; Kreplak et al. 2001; Paus and Foitzik 2004). The outermost layer of the IRS, the companion layer, acts as a slippage layer allowing the HS to slide past the ORS and grow upwards (Paus and Foitzik 2004). The IRS is essential for the proper molding, adherence, and keratinization of the growing HS. The Flugzellen cells of Huxley's layer are postulated to function as nutritive canals between the not keratinized Huxley's layer and the ORS, bypassing the fully cornified and impermeable Henle's layer (Joshi 2011). Interestingly, in the condition described as loose anagen hair of childhood, premature keratinization of the IRS has been implicated in the loss of the anchoring function and subsequent deformation of the HS (Hamm and

Traupe 1989; Tosti and Piraccini 2002). The ORS is created from local progenitor cells located in bulge region and acts as a local paracrine signal source within the HF (Sequeira and Nicolas 2012). The bulge is clearly visible in mouse HFs, as a group of cells protruding from the side of the follicle; though in humans the bulge is not structurally distinct (Treuting and Dintzis 2011). Cells that are hosted in the bulge have the typical properties of epithelial stem cells: they are the slowest-cycling and longest-lived cells within the HF (Cotsarelis et al. 1990; Lyle et al. 1998). The stem cells are biochemically distinct cells and can be identified by molecular markers such as CD34 in mouse and CD200 in human HFs (Cotsarelis 2006; Ohyama et al. 2006).

The HF also contains neural crest-derived pigment producing melanocytes (Tobin and Bystryn 1996), Langerhans' cells that are dendritic antigen-presenting cells (Gilliam et al. 1998) , and Merkel cells, specialized neurosecretory cells (Kim and Holbrook 1995). Interestingly, these cells have the ability to repopulate the epidermis after injury. Also, they allow the HF to act as a sensory organ and immunologic sentinel for the skin: the HF detects mechanical stimuli relaying sensory information to the nervous system (Paus and Cotsarelis 1999). Langerhans' cells located at the opening of the HF detect surface pathogens and activate the immune system (Gilliam et al. 1998).

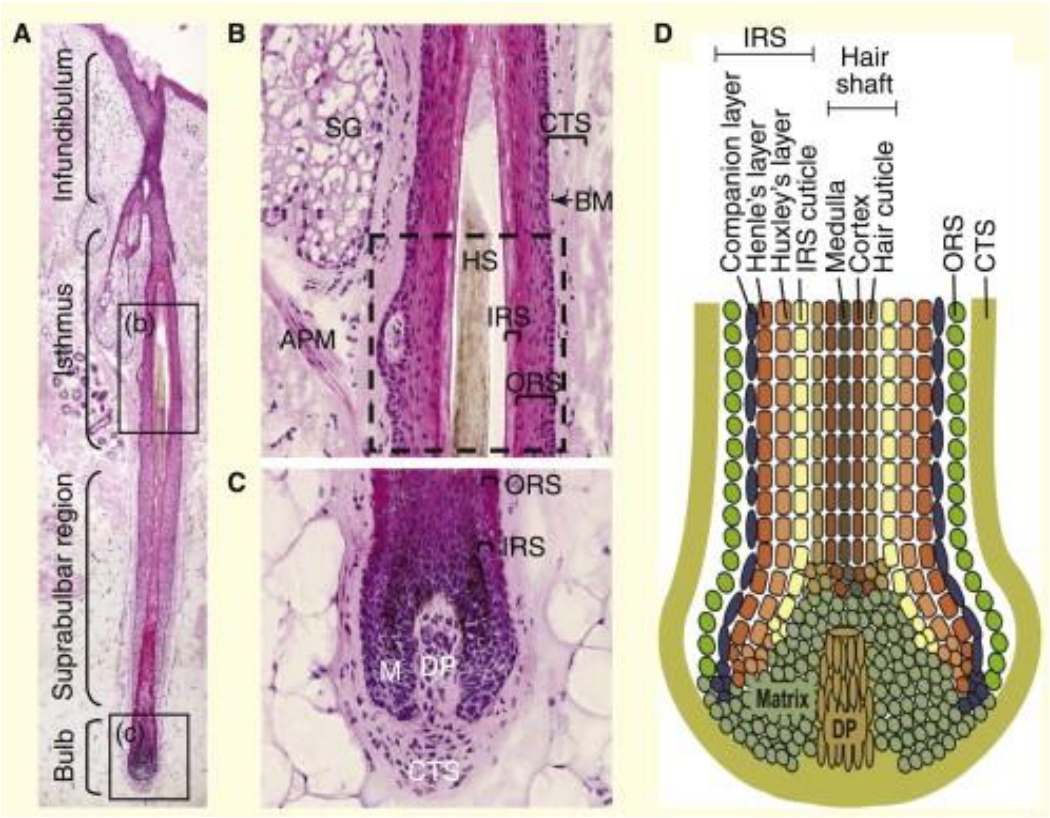

Figure 1-1 Histomorphology of the human hair follicle.

(A) Sagittal section through a human scalp HF (anagen VI) showing the permanent (infundibulum, isthmus) and anagen associated (suprabulbar and bulbar area) components. (B) High magnification image of the isthmus. The dashed square indicates the approximate location of the bulge. (C) High magnification image of the bulb. (D) Schematic drawing illustrating the concentric layers of the outer root sheath (ORS), inner root sheath (IRS) and shaft (HS) in the bulb. The IRS is composed of four layers: Companion layer (CL), Henle's layer, Huxley's layer, and the cuticle. (BM: basal membrane; APM: arrector pili muscle; CTS: connective tissue sheath; DP: dermal papilla; M: matrix; SG: sebaceous gland). Adapted from (Schneider et al. 2009)

1.1.2 Hair cycle

To produce a new HS the HF undergoes repetitive cycles consisting of active growth (anagen), regression (catagen) and relative resting (telogen) phases (Figure 1-3). In mice hair cycle occurs rapidly, moving in a caudal to rostral wave, with each cycle lasting around 25 days. The first two cycles follow well defined timings, allowing the hair cycle to be easily studied (Muller-Rover et al. 2001). The human hair cycle is much longer and asynchronous: anagen in scalp HF can last for up to 8 years. The duration of the anagen phase determines hair length (Cotsarelis 2006) and differs depending on body areas (Paus and Cotsarelis 1999).

Anagen involves the complete regeneration of the lower cycling portion of the HF, the HS factory (Figure 1-1 C). Historically the anagen phase has been divided into 6 different sub-phases by Chase et al (Chase 1965), which do not differ substantially in time except for the phase VI, the duration of which determine the length of the HS. During each anagen phase, HF produces an entire HS from tip to the root. An intense cross talk between DP cells and progenitor cells take place in order to trigger the anagen onset (Schneider et al. 2009). Transplantation studies have shown that DP cells from rodent vibrissae, when implanted into the hair less skin exhibit the capacity to form new HFs (Jahoda et al. 1984); this observation was later confirmed by another group, also showing that not only DP cells but also transplanted peribulbar dermal sheath cells were able to induce HF development (McElwee et al. 2003). At the onset of anagen, cells of the secondary hair germ, a structure that forms during the late catagen phase consisting of a population of progenitor cells (Ito et al. 2004), grow down into the dermis and form the distinct epithelial lineages.

Anagen I is associated with the activation of mitotic activity of the epithelial progenitors that migrate together with the DP downwards the dermis. In anagen II, a newly forming hair matrix begins to enclose the DP, while in anagen III-IV the matrix cells initiate their differentiation into at least 8 HF lineages. The newly forming HS begins to appear at anagen V and emerges from the skin at anagen VI (Muller-Rover et al., 2001). During anagen VI, hair matrix keratinocytes rapidly proliferate and act as suppliers of the cells to the HS. The melanogenesis is strictly coupled to anagen progression (Muller-Rover et al. 2001; Slominski et al. 2004).

Research published by Cotsarelis group identified putative stem cells in rodent HF as quiescent label-retaining cells (LRCs) in in-vivo studies (Cotsarelis et al. 1990). Bulge cells in adult mice generate all epithelial cells types within the intact follicle, as demonstrated by performing lineage tracing analysis of EGFP-labelled K15-positive bulge cells in mice (Morris et al. 2004). Transplantation of human scalp tissue onto immune-deficient mice confirmed that human HFSC are slowly-cycling in nature and with high proliferative potential and localized within the bulge area that is positive for cytokeratin 15 (K15) (Lyle et al. 1998). Ohyama et al work defined the bulge in the human HF (Ohyama et al. 2006). The group developed the method of navigated laser capture microdissection (N-LCM) to isolate bulge ORS cells and delineate biological distinctiveness of these cells by analyzing gene expression pattern (Ohyama et al. 2006). The analysis compared the profile of bulge cells with sub-bulge ORS cells: it revealed a new surface protein that now is considered as candidate bulge stem cells markers, CD200. The work highlighted several key differences between mouse and human gene expression in HF stem cells: in particular, CD34, which

is considered an excellent bulge cell marker in mouse (Trempus et al. 2003), is not the preferential marker of bulge stem cells in human HF. Instead, K15 and CD200 are preferentially expressed in human HFSC (Figure 1-2) (Cotsarelis 2006; Ohyama et al. 2006). When the supply of matrix cells declines, the differentiation of IRS and HS of the cycling portion regresses and the follicle enters the involution (catagen) phase (Paus and Foitzik 2004).

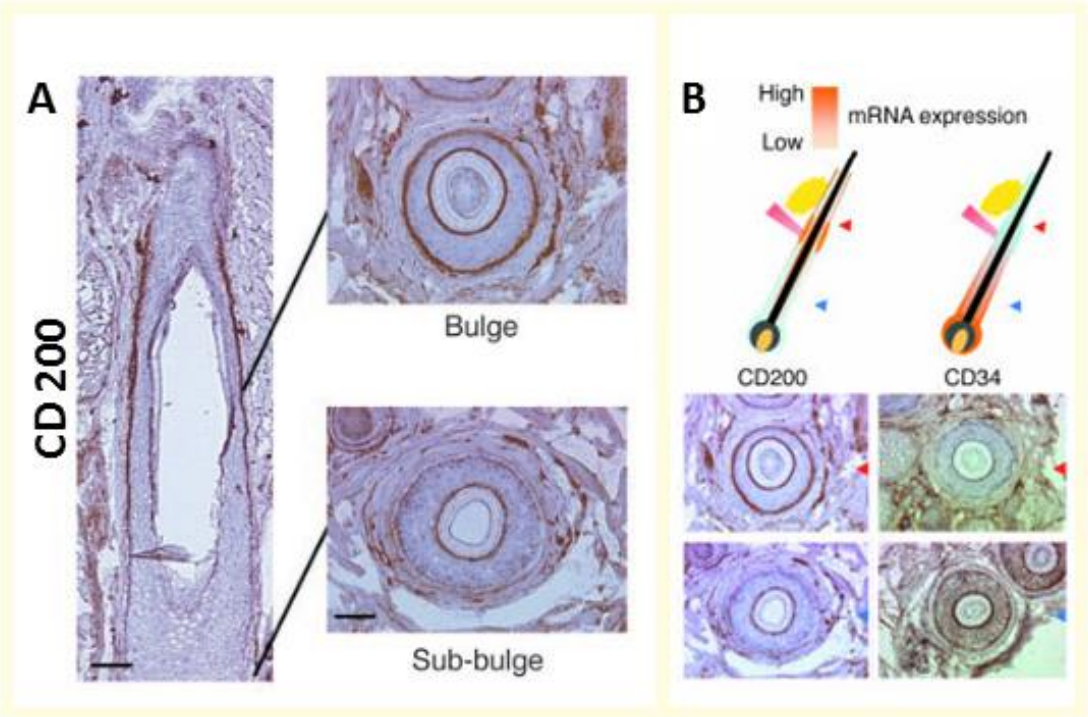

Figure 1-2 CD200 is a cell-surface marker for the bulge ORS cells

(A) CD200 is preferentially expressed on the defined bulge ORS and the companion layer of human anagen HF. (B) Upper panel illustrates the mRNA expression pattern of *CD200* and *CD34* in human HF. The orange gradient indicates the expression intensities of *CD200* and *CD34* transcripts. Lower panels demonstrate the expression pattern of each marker in the transverse sections of different levels of the same HF. Red and blue arrowheads indicate the levels of bulge and sub-bulge, respectively. Scale bars: 50 μm. (Adapted from (Ohyama et al. 2006)

Catagen is characterized by apoptotic-driven degradation of the lower cycling portion of the HF (Botchkareva et al. 2006; Schneider et al. 2009). The catagen phase involves the cessation of cell proliferation and pigmentation, loss of the layered differentiation of the lower follicle, extracellular matrix remodeling and shrinkage of the inferior follicle by the process of apoptosis (Schneider et al. 2009). Apoptosis distribution in HF during catagen has a wave pattern starting from the melanogenic area, propagating to the hair matrix and in late catagen to the central ORS, IRS and HS (Botchkareva et al. 2006). As the cycling portion regresses the DP, now a cluster of quiescent cells not affected by apoptotic events, comes into contact with the bulge region (Schneider et al. 2009). Contact between the DP and bulge cells is very important. Failure of these interactions in both, humans and mice, leads to the hair loss: for example, *hr* (*hairless)* gene mutation results in the disintegration of the DP and the HF epithelium during catagen that causes arrest of the HF cycling activity, development of the epithelial cysts and, eventually, hair loss (Ahmad et al. 1998; Panteleyev et al. 1998).

Morphologically catagen phase can be divided into 8 stages (Straile et al. 1961). During the first two early stages of catagen the hair matrix and DP are reduced in size (Straile et al. 1961). In the next three stages (mid), the DP becomes ball shaped and narrows; epithelial strand and club hair are formed (catagen V) (Botchkareva et al. 2006). Late stages (catagen V-VIII) are morphologically defined by a shortening of the HF.

Telogen was recognized as a resting stage where the HF is quiescent; however, a growing number of studies demonstrated the major changes in gene activity within the telogen skin (Geyfman et al. 2012a; Greco et al. 2009). Two

stages of telogen have recently been identified: refractory and competent stages (Paus and Cotsarelis 1999; Plikus et al. 2008). During the refractory period high levels of bone morphogenetic protein (BMP) signaling prevents anagen initiation (Plikus 2012; Plikus et al. 2008). In the competent telogen, the bulge stem cells become highly sensitive to anagen promoting signals; the BMP signaling activity is reduced and HFs are entering new anagen phase (Greco et al. 2009; Plikus 2012; Plikus et al. 2008).

Exogen is the hair shedding phase that was first characterized by the Stenn group as a highly regulated process (Milner et al. 2002). By examining the shed and plucked telogen hair shafts they observed distinctive morphological features in their bases. In shed hairs the base of hair fibers have sculpted edges and are bordered by cell membranes with deteriorating nuclei, whereas plucked telogen HS showed a smooth edge and rich in intact nucleated cells (Milner et al., 2002). This indicates that the exogen triggering event is the proteolytic separation of the mooring cells (Milner et al. 2002), suggesting that hair shedding is not a passive event (Higgins et al. 2011).

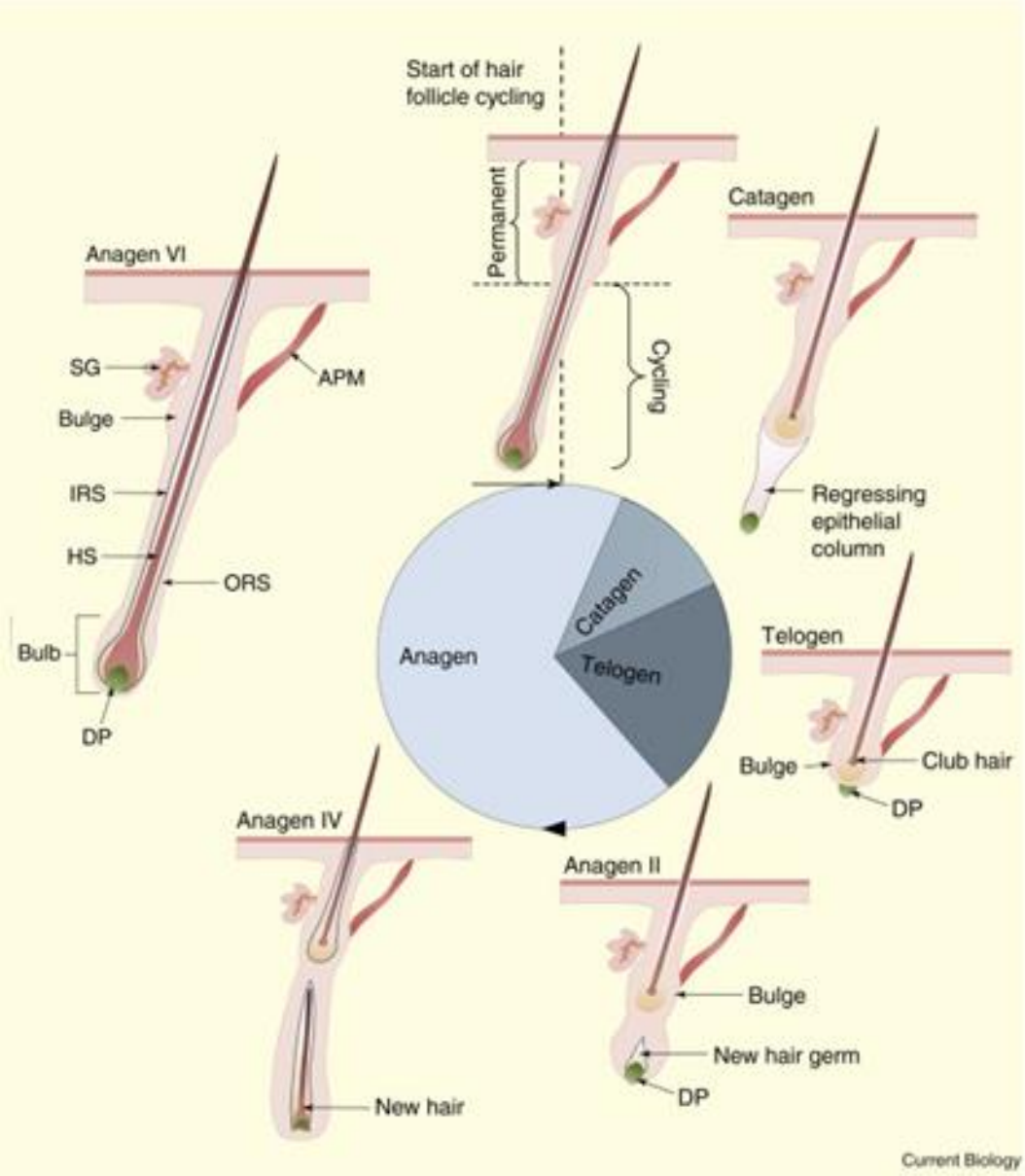

Figure 1-3 Key stages of the hair cycle

The hair cycle consists of three different phases: anagen (growth phase), catagen (regression phase) and telogen (quiescent phase). APM: arrector pili muscle; DC, dermal condensate (green); DP: dermal papilla (green); HS: hair shaft (brown); IRS: inner root sheath (blue); MC: melanocytes; ORS: outer root sheath; SC: sebocytes (yellow); SG: sebaceous gland. (Adapted from (Schneider et al. 2009)

1.1.3 Molecular mediators of hair cycle

Epithelial-mesenchymal interactions are fundamental drivers of the hair cycle. At least six major growth factor families are now recognized to be important in this context, including bone morphogenetic proteins (BMP), Sonic Hedgehog (SHH), Wingless (WNT), fibroblast growth factor (FGF), transforming growth factor TGF-beta, epidermal growth factor (EGF), tumor necrosis factor (TNFα) and neurotrophin families (reviewed in (Botchkarev and Kishimoto 2003; Millar 2002).

Refractory telogen is molecularly characterized by up-regulation and activation of BMP2/4 ligands produced by the HFs (Botchkarev et al. 2001; Greco et al. 2009) and the surrounding dermal microenvironment (Plikus et al. 2008). WNT signaling is very low, partly because of the WNT antagonists present in the dermal macro-environment (Plikus et al. 2011). Low levels of FGF7 in the DP also maintain the refractory phase (Greco et al. 2009). BMP4 functions by binding to the transmembrane serine/threonine kinase receptor BMPR1A, that is broadly expressed in the epidermis and HF (Botchkarev 2003), resulting in phosphorylation of SMADs 1,5 and 8. Phosphorylated SMADs bind to SMAD4 and translocate into the nucleus, where they form the complex with transcription factors and regulate transcription of target gene like Dkk1, an inhibitor of the Wnt-beta-catenin signaling pathway (Mishina 2003). Reduction in the BMP2/4 signaling is mediated by Noggin, the BMP antagonist that prevents binding of BMPs to BMPR1A, leading into the competent telogen, when WNT protein signaling is turned on (Botchkarev et al. 2001; Plikus et al. 2008).

The peak of activity of Wnt/β-catenin in early anagen is necessary for the initiation of a new hair cycle and HS differentiation: absence of β-catenin

induces hair loss and HFSC fail to differentiate into follicular keratinocytes, instead they adopt an epidermal fate (Huelsken et al. 2001). While not required for anagen onset, Shh is necessary for subsequent events, including proliferation of epithelial cells and down-growth of the HF into the dermis (Wang et al. 2000). The ectopic expression of Shh achieved by the administration of an E1(-) adenovirus vector, AdShh, into the mouse back skin causes significant acceleration of anagen onset (Sato et al. 1999).

The increase in TGF-β1 and FGF5 activities promotes catagen development in HFs (Hansen et al. 1997; Hebert et al. 1994; Oshimori and Fuchs 2012). Experimental deletion of TGF-β1 in mice prolongs anagen, whereas administration of TGF-β1 induces pre-mature anagen-catagen transition, suggesting its essential role in triggering catagen (Foitzik et al. 2003). FGF5-deficient mice exhibit a prolonged anagen phase resulting in an angora hair phenotype (Hebert et al. 1994). In human HF, FGF-5 expression was observed in the upper ORS and in small round cells surrounding the HF (Higgins et al. 2014). The same study demonstrated that mutations in the human FGF5 gene are associated with familial trichomegaly (or extreme eyelash growth), and that FGF5 inhibits hair growth in an organ culture model by initiating catagen (Higgins et al. 2014). The human counterpart to the mouse angora phenotype was disclosed, suggesting that in human FGF-5 could also induce catagen by binding to FGF-R1 expressed in the DP (Ota et al. 2002)

Other molecules worthy to be mentioned in controlling catagen entry are Vitamin D receptor (Bikle et al. 2006; Palmer et al. 2008), the transcriptional repressor *Hairless* (Panteleyev et al. 1998) and the retinoic acid receptor (Foitzik et al. 2005). A representation of mentioned key factors involved in the

hair cycle is given in Figure 1-4. Taken together, multiple elements need to be involved in the regulation of the hair cycle: spatio-temporal changes of signal transducers are needed for progression or maintenance of the HF during the distinct hair cycle phases, however none of these factors act as the pace-maker of the cycling by itself.

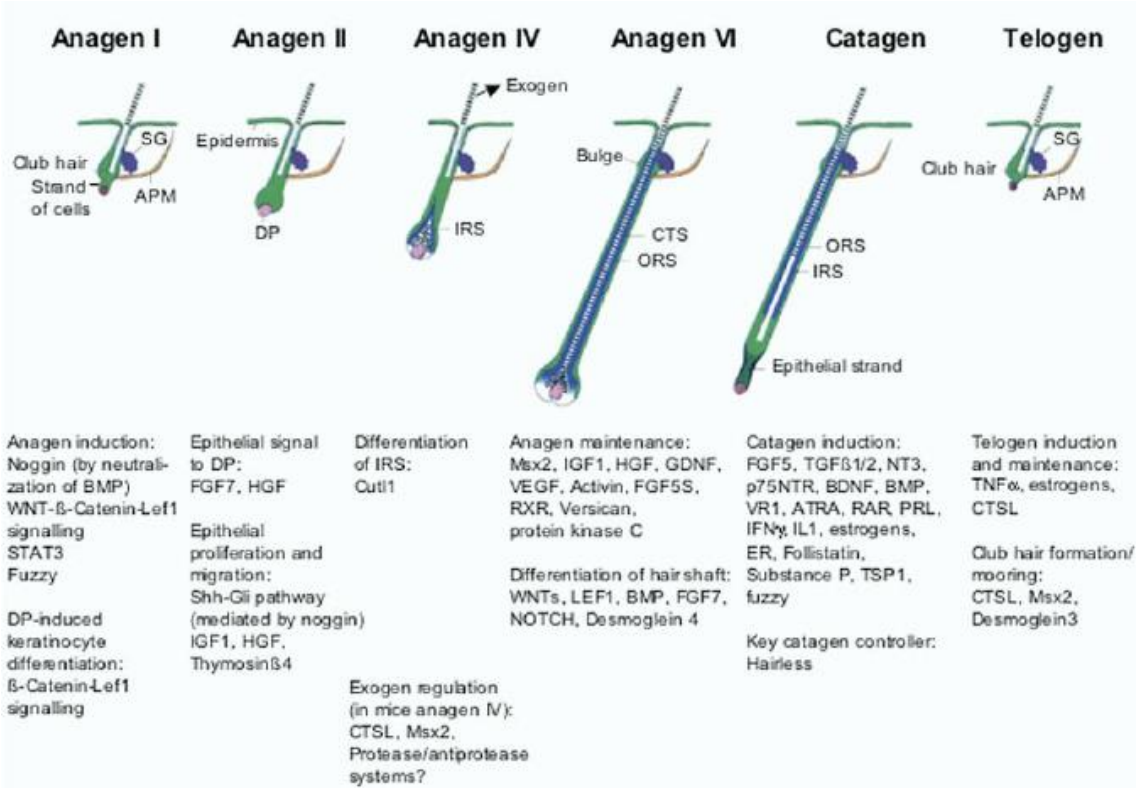

Figure 1-4 Molecular players in hair cycle control

The figure shows key factors that drive the HF through the hair cycle stages. BMP, bone morphogenetic protein; WNT, wingless; STAT3, signal transducer and activator of transcription 3; FGF7, fibroblast growth factor 7; HGF, hepatocyte growth factor; Shh, sonic hedgehog; IGF1, insulin like growth factor; CTSL, cathepsin L; cutl, transcriptional repressor; GDNF, glial cell line-derived neurotrophic factor; BDNF, brain-derived nerve growth factor; VEGF, vascular endothelial growth factor; ATRA, all-trans retinoid acid; RXR, retinoid x receptor; RAR, retinoid acid receptor; NGF, nerve growth factor; Lef1, lymphoid enhancer-binding protein; TGFβ, transforming growth factor β; p75NTR, low affinity neurotrophin receptor; PRL, prolactin; PRLR, prolactin receptor; IFN, interferon ; ER, estrogen receptor; IL1, interleukin 1; VR1, vanilloid receptor 1; TNF, tumor necrosis factor; TSP1, thrombospondin 1. (Krause and Foitzik 2006)

1.2 Essentials of Hair Health

Male and female pattern hair loss is a common disorder affecting 30 and 50% of women and men, respectively, by the age of 50 (Norwood 2001; Severi et al. 2003). The slow, relentless, involuntary loss of hair creates emotional stress for millions of men and women. Alopecia is a generic term for hair loss that results from a diminution of visible hair. Alopecia can be classified as cicatricial or scarring alopecia and non-cicatricial. Cicatricial alopecia refers to a group of rare disorders that destroy the HF replacing it with scar tissue causing the permanent hair loss (Templeton and Solomon 1994). The most common forms of non-cicatricial alopecia are androgenetic alopecia (AGA) and alopecia areata (AA) (Cotsarelis and Millar 2001).

1.2.1 Androgenetic Alopecia

AGA is the most common form of hair loss in men affecting almost 50% of the male population by the age of 50 (Norwood 1975; Severi et al. 2003). Estimates of its prevalence in women have varied widely, though recent studies claim that six percent of women aged under 50 years are affected, increasing to a proportion of 30–40% in women aged 70 years and over (Norwood 2001). AGA refers to hair loss in individuals with a genetic predisposition caused by effects of androgens such as testosterone and its derivative dihydrotestosterone (DHT) (Price 1999; Trueb 2002). It is assumed that the genetically predisposed HFs are the target for androgen-stimulated HF miniaturization, leading to gradual replacement of large, pigmented hairs (terminal hairs) by barely visible hairs

(vellus hairs) in affected areas (Paus and Cotsarelis 1999). This results in a progressive decline in visible scalp hair density.

Testosterone is a hormone that diffuses across the cell membrane. It's converted by the cytoplasmic enzyme 5-α-reductase to DHT, which is five-fold more potent than testosterone, based on its affinity for the androgen receptor (Trueb 2002). There are two types of 5-α-reductase: the type 1 isozyme represents the 'cutaneous type'; it is mainly located in sebocytes, but also can be expressed in epidermal and HF keratinocytes, DP cells and sweat glands as well as in the fibroblasts from genital and non-genital skin. The type 2 isozyme is expressed mainly in the prostate, in the fibroblasts of normal adult genital skin, in the IRS (Chen et al. 1998) and in the ORS of the HFs (Sawaya and Price 1997). People affected by AGA have higher levels of 5-α-reductase, more androgen receptors, and lower levels of cytochrome P-450 aromatase (Sawaya and Price 1997), suggesting that the observed clinical patterns of AGA may reflect quantitative differences in the levels of these enzymes.

All steroid hormones act by diffusing through the plasma membrane into the target cell and binding to specific intracellular receptors. The androgen receptor (AR) is believed to be responsible for determining the sensitivity of cells to androgens (Banka et al. 2013) (Quigley 1998): expression of the AR has been found to be increased in balding scalp (Sawaya and Price 1997) and polymorphism of the AR gene has been found to be associated with AGA (Ellis et al. 2001). While major progress has been done in the understanding of androgen metabolism, the genetic predisposition to AGA remains poorly understood. It has been hypothesized that AGA has polygenic inheritance that is dependent on a combination of mutations, e.g. in or around the AR gene

affecting the expression of the AR, and other genes controlling androgen levels (Trueb 2002).

While a genetic predisposition to an increased HF sensitivity to androgens is a prerequisite for AGA development, clinical practice has shown that simply blocking androgens does not results in the conversion of miniaturized HFs into terminal ones in advanced AGA. Interestingly, histologic examination of bald scalp biopsies shows that miniaturization of terminal HF is frequently associated with perifollicular lymphocytic infiltration, and eventually fibrosis (Jaworsky et al. 1992; Mahe et al. 2000; Whiting 1993). Therefore, it is conceivable that the role of this “microscopic follicular inflammation” causing fibrosis participates in preventing restoration of a terminal HF (Trueb 2002).

The role of stem cell differentiation in AGA should also be taken into account. In a recent work Garza et al (2011) compared HF stem cells obtained from bald versus non-bald scalp areas of AGA donors and quantified the expression of stem- and progenitor cell markers. They found that K15+ cells are present in the HFs obtained from both balding and non-balding scalp samples. However, they found the decrease in a well-demarcated population of cells $CD200^{high}/ITGA6^{high}$ in bald versus haired scalp. These cells were intermediate in size compared to $K15^{hi}$ cells, and localized in the bulge region and the secondary germ of telogen HF from haired scalp. Because of these features $CD200^{high}/ITGA6^{high}$ cells were classified as progenitor cells. In addition, 10-fold decrease in $CD34^{+}$ cells population was observed in bald versus haired scalp (Garza et al. 2011).

These findings suggest that AGA develops not as a result of loss of HFSC, but a diminished conversion of stem cells into the progenitor cells. The preservation

of stem cell population in AGA can be the key feature to improve the reversibility of this condition, while the loss of progenitor cell population can provide insights into possible mechanisms leading to HF miniaturization.

1.2.2 Alopecia areata

Alopecia Areata (AA) is one of the most prevalent autoimmune diseases, affecting approximately 5.3 million people in the United States alone, including males and females across all ethnic groups (Alkhalifah et al. 2010; Harries et al. 2010; Safavi 1992). The disease usually initiates as a hair loss patching normal-appearing skin, which can occur anywhere on the body, although the scalp is the most common site. AA develops due to the collapse of the “immune privilege” of the HF that is characterized by aberrant expression of major histocompatibility complexes (MHC class Ia) antigens and a reduced synthesis of important immunosuppressant, such as alpha-MSH and TGF-beta1(Safavi et al. 1995; Tan et al. 2002; Tosti and Duque-Estrada 2009; Tosti et al. 2008). AA is often associated with others autoimmune disorders such as vitiligo, celiac disease and diabetes (Goh et al. 2006; Kuchabal and Kuchabal 2010; Kurtev and Iliev 2005; Wang et al. 1994). The course of the disease is notoriously unpredictable: the initial patches can coalesce and progress to cover the entire scalp (alopecia totalis, AT) or eventually the entire body (alopecia universalis, AU) (Olsen et al. 2004; Sehgal and Jain 2003). The HFSC are generally not destroyed, therefore the HF retains its capacity to regenerate and continue cycling such that AA can spontaneously remits (Gilhar et al. 2012). AA preferentially affects pigmented anagen HF; when hair regrowth occurs within

the AA patches, it frequently grows back white or colorless (Cline 1988; Gilhar et al. 2012).

The early stage of AA is characterized by the attack of the anagen HF by T cells; they form peri- and intra-follicular inflammatory infiltrates leading to an abrupt conversion from anagen to catagen and ultimate HS shedding (Gilhar et al. 2012; Wasserman et al. 2007; Whiting 2003). The infiltrates are mainly composed of CD4+ and CD8+ T lymphocytes; in addition, the numbers of NK cells and mast cells are greatly increased in the perifollicular infiltrates (Bodemer et al. 2000; Cetin et al. 2009; Dressel et al. 1997).

The hypothesized pathogenesis of AA is a collapse of immune privilege of the HF, when pro-inflammatory signals upregulate MHC-Ia expression in the proximal HF epithelium (Paus et al. 2005). In this condition, follicular autoantigens (Gilhar et al. 2001) are not sequestered any longer and can be presented in the normally MHC Ia-negative epithelial hair bulb (Paus et al. 2005). In presence of appropriate co-stimulatory signals, autoreactive CD8+ T cells, CD4+ T cells and cytotoxic NK cells attack the hair bulb (Paus et al. 1993). This activates a vicious cycle of secondary follicle-damaging autoimmune phenomena, whose quality and magnitude largely determine the resulting degree of HF damage and, thus, the actual clinical manifestation, hair loss (Paus et al. 1993).

Genetic predisposition plays an important role in AA development. Recent genome wide association studies identified susceptibility loci for AA on chromosomes 6p (HLA), 6q (UL 16 binding protein, (ULBP), 10p (IL2RA), and 18p (PTPN22) (Martinez-Mir et al. 2007; Petukhova et al. 2010). Furthermore, a

number of genes were identified that may be associated with AA and other autoimmune diseases, such as *ULBP*, which encodes a class of ligands activating NKG2D receptors (Petukhova et al. 2010).

1.2.3 Overview of available treatments

For AGA the available pharmacological treatments consist of two drugs: Minoxidil (DeVillez et al. 1994; Jacobs et al. 1993) and Finasteride, which are approved by The Food and Drug Administration (FDA). Both drugs can increase coverage of the scalp by enlarging existing hairs and retard further thinning in both the vertex and the frontal regions. However, the response differs among patients and neither drug restores all the hair (Price 1999).

Minoxidil is a potassium channels opener and vasodilator (Buhl et al. 1993). Its mechanism of action with respect to the stimulation of hair growth is not known, but it appears to be independent of vasodilatation (Buhl 1991), and is probably linked to the stimulation of VEGF (Lachgar et al. 1998). It is administrated as topic solution that significantly increases hair count (Rietschel and Duncan 1987), although efficacy is variable and temporary. The adverse effects of topical Minoxidil are mainly dermatologic (Price 1999). Some beneficial effects of Minoxidil were also observed in AA patients.

Finasteride, a competitive inhibitor of type II 5-α-reductase that blocks the conversion of testosterone to its active metabolite, DHT (Rittmaster 1994). Finasteride treatment is safe and well tolerated: in male adverse effects of sexual functions were reversible (Rittmaster 1994).

Patients with AA are treated with either immune-modulating therapies, such as glucocorticoids (Sawaya and Hordinsky 1995) or topical immunotherapy (Shapiro and Price 1998). Both treatments exert several adverse effects, such as persistent dermatitis, painful cervical lymphadenopathy, generalized eczema, blistering, contact leukoderma, and urticarial reaction (Singh and Lavanya 2010). Notably, a recent work by the Christiano's laboratory reported a near-complete hair regrowth in three AA patients treated with oral ruxolitinib (Xing et al. 2014). This chemotherapeutic drug acts by inhibiting Janus kinase (JAK) family protein tyrosine kinases (JAK1 and 2), downstream effectors of the IFN-γ and γ-cytokine receptors that are expressed by infiltrative T cells. This successful experiment has opened the possibility for systematic clinical trials of JAK inhibitors for AA treatment (Jabbari et al. 2015; Kennedy Crispin et al. 2016).

Other available approaches for AGA treatment include hair transplant surgery (Rose 2015), often in combination with treatments that prevent hair loss, such as the use of growth factors present in the platelet-rich plasma fraction (Singh and Goldberg 2016) or prostaglandin E2 (PGE2) (Garza et al. 2012; Johnstone and Albert 2002). However, because of its high costs, such treatments are not affordable for many people.

Up to now the list of light-based devices for the management of hair regrowth with FDA 510k premarket notification clearance counts thirty two entries (Jimenez et al. 2014; Lanzafame et al. 2013; Lanzafame et al. 2014; Leavitt et al. 2009). The efficacy of light-based therapy is reported to be similar to that of existing FDA-approved drugs (Minoxidil and Finasteride) (Kim et al. 2013a; Leavitt et al. 2009; Munck et al. 2014) and more important free of potential side

effects (Mysore 2012). Nevertheless, observed effects are still not fully cosmetically acceptable. Moreover, the design of the reported clinical studies and the accuracy of the hair count has been contested (Mignon et al. 2016a).

The picture is further complicated by a virtual lack of proof about the exact molecular targets that mediate the physiological response of skin and HF to low levels of light. Unrevealing these targets is of primary importance to improve current technologies and deliver novel light-based solutions for hair loss. An introduction of the already known basic principles of light interactions with skin will be given below.

1.3 Basic principles of Photobiomodulation

Photobiomodulation (PBM) has clinically been reported to have a positive impact on hair growth (Jimenez et al. 2014; Lanzafame et al. 2013; Lanzafame et al. 2014; Leavitt et al. 2009), skin rejuvenation (Dierickx and Anderson 2005; Rinaldi 2008), wound healing (Gupta et al. 1998; Hopkins et al. 2004; Kajagar et al. 2012), psoriasis (Pfaff et al. 2015; Weinstabl et al. 2011) and eczema (Keemss et al. 2016). The lack of the risk of potential systemic side effects is well recognized as a benefit in the treatment of cutaneous disorders (Metelitsa and Green 2011; Mysore 2012). PBM defined the therapeutic use of visible to near infrared radiation (NIR) light absorbed by endogenous chromophores, triggering non-thermal, non-cytotoxic, biological reactions through photochemical events (Anders et al. 2015). In November 2015, the term ‘Photobiomodulation Therapy’ was formally adopted as an official NIH U.S. National Library of Medicine (MeSH) term: biostimulation, low-level laser (or

light) therapy (LLLT), low-intensity laser therapy, low-power laser therapy, cold laser, soft laser, photobiostimulation were the other names previously used for this therapy (Anders et al. 2015). Photobiomodulation therapy results in beneficial therapeutic outcomes, including, but not limited to, tissue regeneration (Hopkins et al. 2004), alleviation of inflammation (Weinstabl et al. 2011) and pain (Naeser 2006). Endre Mester introduced the phenomenon of using light for hair regeneration in 1967 (Mester et al. 1967). To test if laser radiation might cause cancer in mice, he irradiated mouse back skin with a low power ruby laser (694 nm). As a result, he didn't observed neoplastic formations in treated mice, while he noticed a quicker hair regrowth compared to the untreated mice (Mester et al. 1967). Since this observation, several clinical studies reported encouraging results demonstrating the increase in hair density and thickness in response to red and near infrared light-based therapy. However, the molecular mechanism underlying light-mediated hair regrowth remain largely unknown. To understand the various modalities of laser-tissue interaction, it is necessary to understand how photons penetrate biological tissues and their molecular triggers.

1.3.1 Optical properties of biological tissues

When photons strike the surface of the tissue, a portion (4–10%) of photons are reflected according to the angle of incidence due to the refractive index change (Steiner 2011). Photons penetrating the surface initially are refracted, obeying the law of Snellius. In biological tissues, like the skin, the photons may be scattered or absorbed, exciting the absorbing molecule by an electronic transition (Steiner 2011).

Blood, melanin and water are the main absorbing components in biological tissues (Jacques 2013). Others photosensitive molecules are porphyrin, flavin, retinol, nuclear acids, deoxyribonucleic acid (DNA)/ribonucleic acid (RNA), and reduced nicotinamide adenine dinucleotide (Bachmann et al. 2006). While peak of absorption for water is in the NIR range of the light spectrum, others molecules mainly absorb light in the visible range, between 400 nm and 700 nm (Jacques 2013).

The scattering behavior of biological tissues is also important, because it determines the volume distribution of light intensity in the tissue. Scattering is the primary step for tissue interaction, followed by absorption and heat generation (Steiner 2011). Scattering of a photon is accompanied by a change in the propagation direction without loss of energy that influences light penetration depth (Steiner 2011).

In correlation to scattering and absorption, skin penetration of light is maximized between 600 and 1200 nm, which is called an “optical window” (Huang et al. 2009).

1.3.2 Light-tissue interactions

Applying different light parameters such as irradiance (power density) and exposure time, it is possible to induce distinct reactions in tissues like the skin (Figure 1-5): 1) photoablation, where the damage is confined to the specific tissue structures and preconditions for tissue ablation are high absorption and very short laser pulse (Müller et al. 1991); 2) thermal reactions, where energy of laser irradiation is transferred into heat due to the absorption of the photons by

tissue components (such as melanin) (Steiner 1993); 3) photobiomodulation, a non-thermal-photochemical reactions induced by low light level stimulation of a photo-acceptor (Huang et al. 2009).

Many lines of evidence suggest that red/NIR light delivered at low doses can prevent cell apoptosis and improve cell proliferation, migration and adhesion *in vitro* (AlGhamdi et al. 2012; Gao and Xing 2009). A large number of animal and clinical studies demonstrated highly beneficial effects of LLLT on a variety of diseases. Gundogan et al (2004) reported two successful treatments of AA using a 308 nm xenon laser (Gundogan et al. 2004); different light treatments have been used to improve both acute (Hopkins et al. 2004) and chronic wound healing (Yu et al. 1997).

The light sources in use in PBM are lasers or light-emitting diodes (LEDs). Both light sources are used in clinical practice and demonstrate successful results (Karu 2011; Sazonov et al. 1985). A laser emits light through a process of amplification by stimulated emission of photons: characteristics of the laser emitted light are spatial and temporal coherence (Paschotta 2008). This property is intrinsic of the light emission process and is derived by the fact that emitted photons are in phase. Spatial coherence allows for a small beam divergence of a moderately sized beam, temporal coherence is expressed as a narrow optical spectrum or a quasi-monochromatic emission (Paschotta 2008). An LED is a semiconductor light source that emits non-coherent light across the visible, ultraviolet and infrared wavelengths (Chung et al. 2012).In PBM lasers and LEDs have been used with the following range of optical parameters: 1) wavelength, between 390-1100 nm that can be continuous wave or pulsed (Avci et al. 2013; Hamblin and Demidova 2006); 2) dose or radiant exposure in the

range of 1-100 J/cm^2 with variable wavelength (Avci et al. 2013; Mignon et al. 2016a); 3) irradiance covering two orders of magnitude (1-100 mW/cm^2) (Avci et al. 2013; Huang et al. 2009; Mignon et al. 2016a).

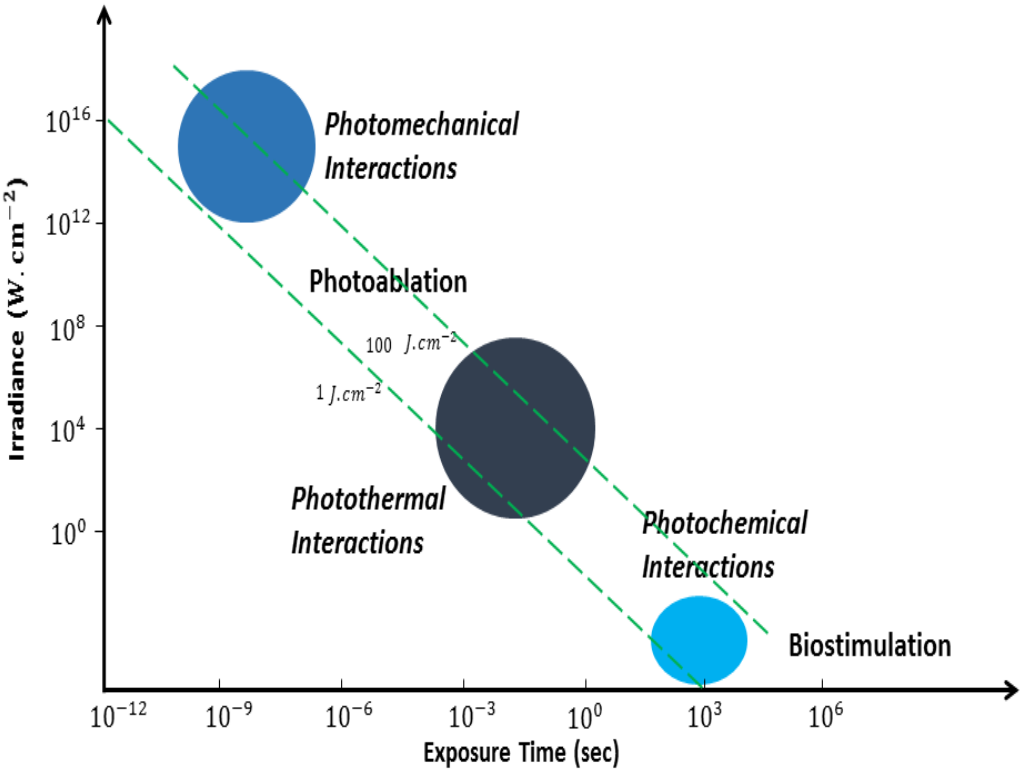

Figure 1-5 Light - biological tissue interactions defined by power density and exposure time

Modulation of irradiance (power density) and exposure time of the light source triggers different reactions in tissues: photomechanical, photothermal or photochemical. The two diagonals show constant radiant exposures at 1 J/cm2 (lower diagonal) and 100 J/cm2 (upper diagonal). Adapted from (Boulnois 1986).

1.3.3 Photobiomodulation: mechanisms of action

In PBM absorbed photons interact with organic molecules or endogenous chromophores present in the tissue to trigger biological reactions. The most commonly accepted cellular chromophore for photobiomodulation therapy is cytochrome c oxidase (COX) (Hamblin and Demidova 2006).

The pioneering work of Dr Tiina Karu suggested that cytochrome c oxidase plays a role of a light acceptor with absorption bands in red and near-infrared (NIR) range (650 – 980 nm) and even higher (about ten times) extinction coefficient around 400-500 nm (Karu 1989). Her theory was supported by biochemical studies conducted by Passarella and colleagues on the effects of HeNe laser treatments on isolated mitochondria (Pastore 2000): after discovering an increase in the rate of electron transfer and in H^+/e^- ratio for COX, as a result of irradiation in isolated mitochondria, they also demonstrated that changes in COX reactivity are modulated by laser treatment (Pastore et al. 1995; Pastore et al. 1994). Over the years a majority of the evidence for COX as photo-acceptor has come from experiments in neuronal and HeLa cells. Functionally inactivated respiratory chains in *in vitro* neuronal cells were partially rescued by light (Karu et al. 2004; Wong-Riley et al. 2005). In HeLa cells, absorption spectra obtained for COX in different oxidation states were very similar to the action spectra for DNA and RNA synthesis rate and for cell adhesion after light irradiation (Karu and Kolyakov 2005). Photons interacting with COX are thought to trigger the increase of ATP via a proton gradient (Karu 1999). The process involves the release of nitric oxide (NO) either via photo-dissociation from COX (Karu et al. 2005) or via reduction of nitrite to NO COX-mediated, as shown by Ball et all using a 590 nm LED light (Ball et al. 2011).

The end products of both processes are ATP and ROS, natural by-product of the respiration metabolism. Interestingly, ROS can affect the expression of genes related to proliferation, migration, cytokines production and growth factors, inducing a long lasting effect that is needed for tissue repair (Hawkins et al. 2005; Moore et al. 2005; Song et al. 2003).

Light mediated vasodilation triggered by NO release was first described in 1968 by Furchgott et al (Ehrreich and Furchgott 1968). Hemoglobin is considered the chromophore that supply NO leading to vasodilation (Mittermayr et al. 2007). Nevertheless, a recent work reported the presence of Opsin 4 (OPN4) in blood vessels and demonstrated that OPN4 mediates wavelength-specific, light-dependent vascular relaxation (Chaudhry et al. 1993).

Recent studies have also revealed the existence of a large group or family of ion channels called transient receptor potential (TRP) channels. TRP channels are ‘cellular sensors’: they respond to environmental stimuli due to changes in temperature, stretch/pressure, oxidation/reduction, osmolarity and pH (Kaneko and Szallasi 2014) . In insects, TRPV channels are involved in vision (Hardie 2014) and it has been shown that TRPV are able to respond to green (Gu et al. 2012) and infrared light (Albert et al. 2012).

Several aspects are to be taken into account when entering the field of PBM: the complexity of a large number of illumination parameters and the biochemical mechanisms that are likely to be triggered. A recent review by Mignon et al highlighted issues that arose from these uncertainties: reviewing 30 years of literature pertaining skin PBM, it was concluded that the range in wavelengths, irradiance and radiant exposures used for stimulating skin cells is too wide, and

that the presence of several potential photoreceptors in the skin requires further examination; finally neither of the mechanisms triggered by light provide a convincing explanation for all the physiological effects observed (Mignon et al. 2016a).

Thus, a pressing need remains to identify the potential molecular mediators of these processes, and subsequently their mode of action.

1.4 Light-sensitive receptors in skin

In recent years, several molecules have emerged as novel mediators of light activation in non-photosensitive tissues, such as nitrosated proteins regulating nitric oxide (NO) and the flavoprotein-containing cryptochromes that are also involved in the regulation of the circadian rhythm, as well as Opsin receptors.

1.4.1 Opsins and the visual functions

Opsins are 30- to 40-kDa proteins. They belong to the G-protein-coupled-receptors (GPCR) protein family, seven helix transmembrane receptors, which activate heterotrimeric GTP-binding proteins after photochemical activation of the retinaldehyde chromophore, covalently linked to the apoprotein. Opsins can be divided into two sub-families (Table 1): 1) visual Opsins, including Opsin 1 (short, middle and long wavelength), a colour vision mediator found in cone cells, and Opsin 2 (Rhodopsin), a dim-light vision mediator that is expressed in rod cells; 2) non-visual Opsins, including Opsin 3 (Panopsin or Encephalopsin), Opsin 4 (Melanopsin) and Opsin 5 (Neuropsin) (Terakita 2005). Peak of

absorption for each of mentioned Opsins is reported in Table 1. However, it must be noted that the exact range of the absorption band for both, OPN 2 and OPN 3, depends on the amino-acid sequence, the type of retinal bound (7- 9-cis, 11-cis, 13-cis) (Sekharan and Morokuma 2011), and also on dark versus light conditions (Menon et al. 2001). The respective spectral sensitivity of OPN2 through animal kingdom covers an extremely broad range of the sunlight spectrum from 358 nm (near ultraviolet, UVA) to 630 nm (red) (Luck et al. 2012). OPN3 is a bi-stable pigment absorbing in the region of 400-530 nm, generating a stable photoproduct and reverting to its original state upon subsequent light absorption rather than undergoing photobleaching (Koyanagi et al. 2013).

Table 1. Summary table of Opsin family receptors. Colors represent the wavelength of absorption peaks for each member of the Opsin family in the visible spectrum.

Photoreceptors (λ max)	Functions	Site of Expression
OPN5 Neuropsin (380 nm)	Non visual opsin; G protein coupled receptor; putative photoisomerase activity (convert all-trans-retinal into 11-cis isomer in a light-dependent manner)	Brain, spinal cord, retina (Terakita 2005) Melanocyte and keratinocyte (Haltaufderhyde et al. 2015)
OPN1 Short wavelenght (420 nm)	Visual opsin; G protein coupled receptor, trigger Gt pathway; bind chromophore 11-cis-retinal; induce phototransduction in color vision	Cones from the outer human retina (Terakita 2005) Melanocyte and keratinocyte (Haltaufderhyde et al. 2015) Epidermis upper layer (Tsutsumi et al. 2009)
OPN4	Non visual opsin; G protein	Ganglion and amacrine

Melanopsin (470 nm)	coupled receptor, Trigger Gq pathway	cell layers of the retina (Terakita 2005) Melanocyte (Haltaufderhyde et al. 2015)
OPN3 Encephalopsin (480/500 nm)	Non visual opsin; G protein coupled receptor	Brain, testis, liver, placenta, heart, lung, skeletal muscle, kidney, and pancreas (Terakita 2005) Melanocyte and keratinocyte (Haltaufderhyde et al. 2015)
OPN2 Rhodopsin	Visual opsin for dim-light G protein coupled receptor, trigger Gt pathway; bind chromophore 11-cis-retinal via K296 aa; induce phototransduction.	Disc membranes in the outer segment of rod photoreceptor cells (Terakita 2005) Melanocyte and keratinocyte (Haltaufderhyde et al.

(500 nm)		2015) Epidermis upper layer (Tsutsumi et al. 2009)
OPN1 Middle wavelenght (530 nm)	Visual opsin, induce phototransduction in color vision; G protein coupled receptor, trigger Gt pathway; bind chromophore 11-cis-retinal.	Cones from the outer human retina (Terakita 2005) Epidermis basal layer (Tsutsumi et al. 2009)
OPN1 Long wavelenght (560 nm)	Visual opsin, induce phototransduction in color vision; G protein coupled receptor, trigger Gt pathway; bind chromophore 11-cis-retinal.	Cones from the outer human retina (Terakita 2005) Epidermis basal layer (Tsutsumi et al. 2009)

OPN2 has been the most extensively studied Opsin: bovine OPN2 was the first to be crystallized (Okada et al. 2000) allowing accurate structure-function studies. Similar to others GPCR OPN2 is characterized by phosphorylation sites at Ser and Thr residues in the carboxy-terminal tail, although its special feature, as visual pigment, is the presence of a retinal chromophore covalently linked (Rando 1996). 11-cis-retinal (11-cis-RAL) is the chromophore linked via a protonated Schiff base bond to a specific Lysine residue in the membrane embedded domain of OPN 2 apoprotein (Menon et al. 2001). Photon capture leading to photoisomerization of the 11-cis- to all-trans-form of the RAL chromophore is the primary event in visual signal transduction, and it is the only light-dependent step (Menon et al. 2001). After photoisomerization, OPN2 decays thermally to metarhodopsin II (meta-II), the active form of the receptor, which catalyzes guanine nucleotide exchange by the rod cell heterotrimeric G protein transducin (Gt) (Menon et al. 2001). In the case of the vertebrate visual system, Gt activation leads to the activation of a cGMP phosphodiesterase and the closing of cGMP-gated cation channels in the plasma membrane of the rod cell. The cascade causes a graded hyperpolarization of the rod cell (Menon et al. 2001).

Restoration of the photosensitive receptor conformation in the eye requires the formation of the 11-cis-RAL chromophore from the all-trans-retinal (at-RAL) via the retinoid cycle that mainly occurs within the specialized retinal pigment epithelial cells (RPE) (Blomhoff and Blomhoff 2006). The entire cycle in humans occurs on a time scale of minutes for OPN 2. After photon-induced isomerization of 11-cis-RAL to at-RAL, the reduction to all-trans retinol (at-ROH)

takes place in rod cells outer segments. All other reactions that leads to restoration of 11-cis-RAL occur within RPE (Baehr et al. 2003).

Relevant reactions of the visual cycle are represented in Figure 1-6. All-trans retinyl esters (at-RE) are mobilized by the retinoid isomerohydrolase (RPE65): interestingly high doses of 13-cis retinoic acid, that are used in the treatment of cancer and acne, can inhibit the visual cycle function, due to competition of the retinoic acid with at-RE to RPE65 (Gollapalli and Rando 2004). Also retinol dehydrogenase 5 (RDH5) and 11 (RDH11) knock-out mice show minor modifications in dark adaptation (Kasus-Jacobi et al. 2005; Kim et al. 2005). These evidences are consistent with a role for those enzymes in the visual cycle.

Figure 1-6 The visual cycle in human.

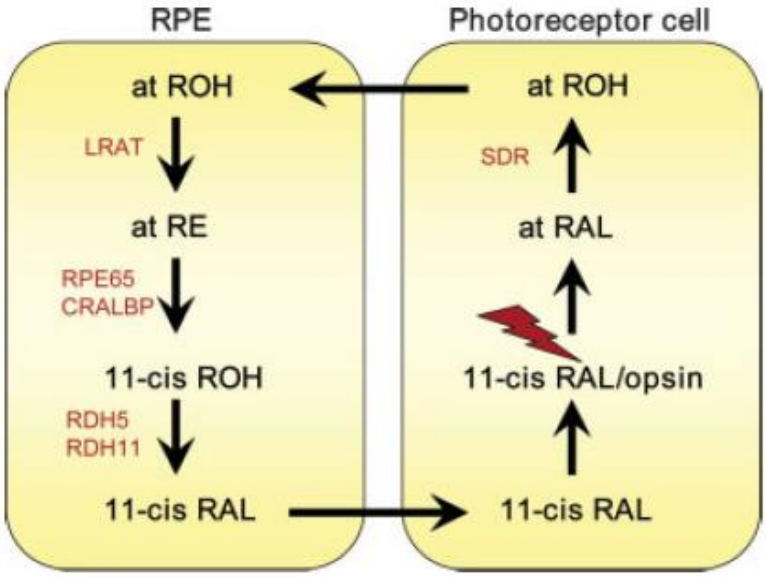

The figure shows main reactions within the visual cycle in human retina. All-trans-retinal (at-RAL), all-trans-retinol (at ROH), short-chain dehydrogenase/reductase (SDR). lecithin:retinol acyl transferase (LRAT), isomer-hydrolase (RPE65), 11-cis retinol (11-cis ROH), interstitial retinoid-binding protein (IRBP) (Blomhoff and Blomhoff 2006).

1.4.1.1 Opsin alternative pathways in the skin

Recent studies have revealed that the distinct members of the Opsin family are present in human skin and could contribute to skin homeostasis (Tsutsumi et al. 2009). For example, OPN2 expression was found in both human epidermal keratinocytes and melanocytes (Wicks et al. 2011). A single exposure to violet light (380 – 410 nm) activated OPN2 and suppressed keratinocyte differentiation (Kim et al. 2013b). In human melanocytes, OPN 2 was found to contribute to photo-transduction of ultraviolet A radiation (UVA) to increase melanin synthesis (Wicks et al. 2011). OPN 3 expression was found in the retina, as well as in the cells outside of visual system, which suggests that OPN 3 might function as a photoreceptor in various tissues (Halford et al. 2001; White et al. 2008). Interestingly, a homolog of the vertebrate OPN 3 maintained photosensitive properties *in vitro* after transfection in mammalian cells, suggesting that OPN3 homologs might have the same ability to bind the non-conventional isomer 13-cis retinal to form an active photopigment (Koyanagi et al. 2013; Sugihara et al. 2016).

1.4.2 Cryptochrome and clock genes

Cryptochromes belong to the photolyases family of photoreceptors that respond to blue light. Photolyases are enzymes that utilize light energy to repair UV-damaged DNA, while Cryptochromes lack this enzymatic activity and function as signaling molecules that respond to blue light in plants (Chaves et al. 2011). Structurally, Photolyases and Cryptochromes are very similar; they both share two chromophores at the N-terminal region, a pterin and a flavin domain, while the C-terminal domains are variable in length and poorly conserved (Chaves et

al. 2011). Blue-light dependent photoactivation is a common reaction, also to human Cryptochromes, involving electron transfer and flavin reduction (Cashmore et al. 1999; Hoang et al. 2008). It has recently been demonstrated in plants that Cryptochrome activation via flavin photoreduction is a reversible mechanism novel to blue light photoreceptors: Cryptochromes activation by blue light (420-480 nm) was inhibited by green-yellow light (550-600 nm). This photocycle may have adaptive significance for sensing the quality of the light environment in multiple organisms (Bouly et al. 2007; Giovani et al. 2003).

The accepted definition of Cryptochrome is a protein with similarity to photolyases that has lost or has a reduced DNA repair activity and has gained a novel role in signaling (Chaves et al. 2011). Two human genes with high degree of sequence homology to the blue light photoreceptors present in plants were discovered in 1996 (Hsu et al. 1996). The two human Cryptochrome 1(CRY1) and Cryptochrome 2 (CRY2) are 73% homologous to each other, but exhibit no sequence homology within the C-terminal 75 amino acids (Lin and Todo 2005). It is thought that this domain may bind to effector molecules (Lin and Todo 2005). The hCRY1 protein is 586 amino acids in length and encodes a protein of 66 kDa. The hCRY2 protein is 593 amino acids in length and has a mass of 67 kDa (Hsu et al. 1996).

Mammalian Cryptochromes are integral components of the circadian clock, an endogenous timekeeper that generates rhythms in behavior, physiology, and metabolism with a periodicity of approximately 24 hours; the rhythm generated by the molecular machinery will be discussed later. The suprachiasmatic nucleus (SCN) of the hypothalamus is considered as the master clock: the SCN receives external cues (or zeitgeber, from German zeit = time and geber =

giver) such as light and dark cycles, detected by eye, and synchronises the circadian activity of the molecular clock found in peripheral tissues, which consist in auto-regulatory feed-back loops. This synchronization is directed by the SCN by rhythmic expression of hormones (prolactin, cortisol) that influences activity of multiple organs (Golombek and Rosenstein 2010; Sancar 2000). However, the role of the central clock has been challenged in recent years by the discovery of self-sustained oscillations in several tissues throughout the body, which might be particularly relevant for local rhythmic events (Golombek and Rosenstein 2010; Kowalska and Brown 2007).

Mammalian Cryptochromes participate in the regulation of the molecular clock at cellular levels. A first classification identified two types of Cryptochromes. Type I Cryptochrome is light responsive and acts as circadian photoreceptor, as in Drosophila and other insects. Type II was considered to be light-irresponsive, with a transcription-repressing activity, as in mouse, human, and other vertebrates (Chaves et al. 2011). However, several studies demonstrated the light-dependent functions of mammalian CRY proteins: knockout mice lacking one or both *Cry* genes have a reduced or abolished ability to induce expression of genes such as *Period* (*Per*) and the proto-oncogene *c-fos* in response to light (Selby et al. 2000; Thresher et al. 1998). Moreover, the pupils of mutant mice lacking both Cry1 and Cry2 have reduced reflex responses to light (Van Gelder et al. 2003), and even if *Cry1/Cry2* double mutant mice show an apparently normal rhythmicity in light-dark cycling conditions, they lose rhythmicity instantaneously and completely in “always dark” conditions (Van Der Horst et al. 1999). Interestingly, mice with retinal degeneration preserve the ability to respond to light-dark cycles, unless not only Opsins receptors but also

Cryptochromes are ablated, suggesting that Opsins and Cryptochromes photoreceptors may share functionally redundant roles in the transduction of light information (Selby et al. 2000). In particular, Cryptochromes may play both roles: acts as photoreceptors and mediate the activity of circadian clock.

1.4.2.1 Molecular mechanisms of the circadian clock

Circadian rhythms produce oscillations at the molecular, physiological and behavioral levels in organisms with periodicity of 24 hours, as a consequence of exposure to daily light-dark cyclic variation. Circadian rhythms are observed in all animal species and are synchronized with the environment by light. In mammals light is absorbed by Opsins located in the outer retina of eye for vision. In mice has been described a specific localization of Cryptochromes in the ganglion cells and the inner nuclear layer of the retina, leading to the hypothesis that these molecules can be the photo-acceptors of light for synchronizing the circadian clock (Sancar 2000). The mammalian circadian system is organized in a hierarchy of oscillators: at the top of the master "synchronizer" is the SCN, anatomically localized in neuron clusters in the anterior hypothalamus (Yamazaki et al. 2000). For long time it was commonly thought that peripheral circadian regulation was only governed by neuroendocrine mediators released by the SCN, as emerged by arrhythmic behavior and abolished *Per2* expression in rats having SNC lesions (Sakamoto et al. 1998). In recent years it has been not only well established that molecular oscillators are present in every tissue and cell types, including the skin (Brown et al. 2005; Zanello et al. 2000), but also that organs like the liver, heart and

kidney have peripheral molecular clock activity that oscillate irrespective of the central pacemaker (Sato et al. 2014; Schmutz et al. 2012; Yoo et al. 2004).

In mammals, the circadian molecular machinery is cell autonomous and consists of a network of transcriptional and translational feedback loops that drive expression of clock components (Buhr and Takahashi 2013; Ko and Takahashi 2006). The transcriptional activators Clock Circadian Regulator (CLOCK) and the Brain and Muscle ARNT-Like (BMAL) proteins are at the core of the oscillator: the two transcription factors heterodimerize and bind to E-box elements to induce transcription of CRY and PER genes. Once the products accumulate in the cytoplasm, PER and CRY can dimerize and translocate into the nucleus where they inhibit their own expression, acting on the CLOCK-BMAL complex (Buhr and Takahashi 2013; Ko and Takahashi 2006). Once CLOCK-BMAL1 complex is formed, the second feedback loop is initiated, inducing the transcription of the Retinoic Acid-Related Nuclear Orphan Receptor, *Rev-Erbα* and *Rorα* genes: the two proteins compete for the retinoic acid-related Orphan receptor Response Element (RORE) binding sites within the promoter of BMAL1, where RORα and REV-ERBα proteins initiate and inhibit Bmal1 transcription respectively (Ko and Takahashi 2006). The auto-regulatory feedback loops described takes almost 24 hours to complete a cycle and constitute the circadian molecular clock (Figure 1-7) (Ko and Takahashi 2006).

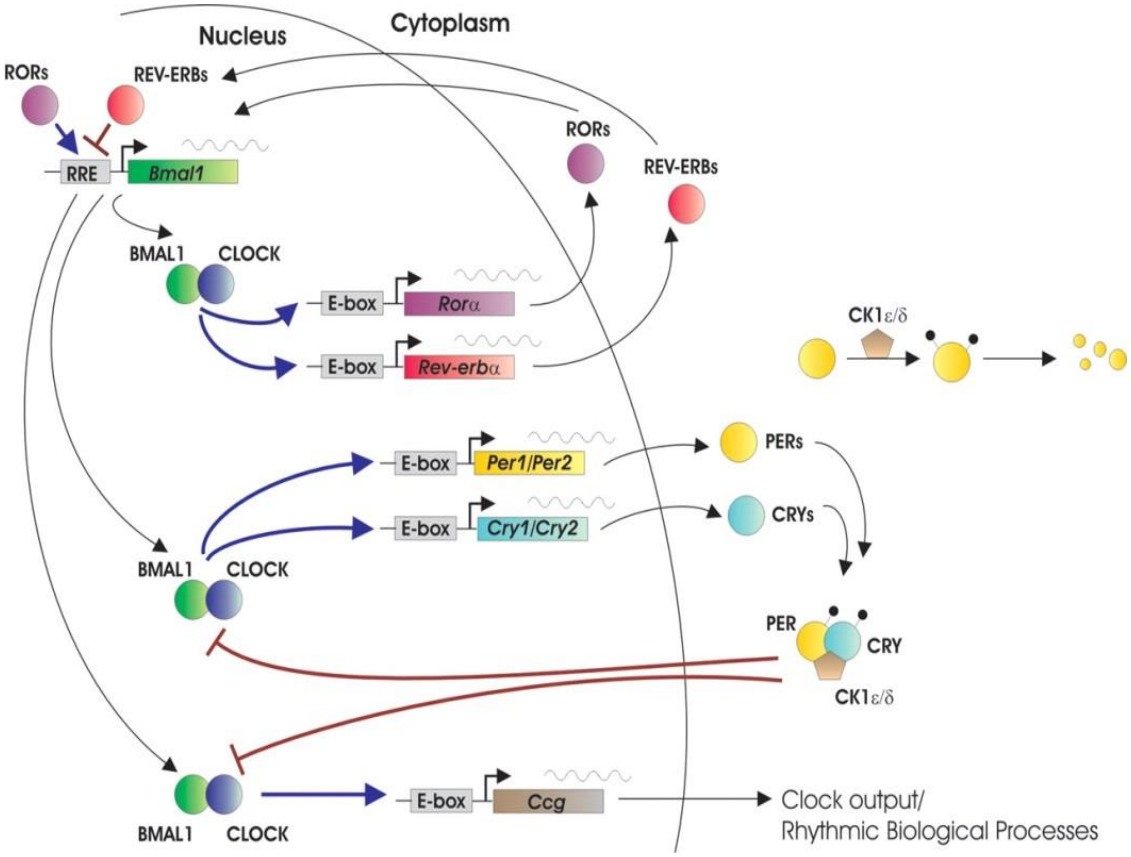

Figure 1-7 Network of the mammalian molecular clock

Autoregulatory feedback loops: Generation of the 24 hours molecular clock is governed by post-translational modifications such as phosphorylation and ubiquitination of clock proteins. These processes affect the stability and nuclear translocation of core clock proteins as PER and CRY. Casein kinase 1 epsilon and Casein kinase 1 delta (CK11 and CK1d) mediates the critical aspect of protein phosphorylation (Ko and Takahashi 2006)

1.4.2.2 Role of the molecular clock in hair follicles

Genes whose expression is regulated by clock transcription factors are largely tissue and cell specific (Balsalobre et al. 1998; Storch et al. 2002). It has recently emerged that the peripheral clock machinery can regulate physiological functions in the skin (Al-Nuaimi et al. 2014; Plikus et al. 2013). In vivo (Plikus et al. 2013; Tanioka et al. 2009) and *in vitro* (Al-Nuaimi et al. 2014) studies demonstrated that HFs present a robust molecular clock that play a role in hair cycle regulation.

An important aspect emerging from studies on mice is the compartmentalization of clock activity over time: circadian genes are robustly expressed in hair germ progenitors during telogen and the telogen-to-anagen transition (Lin et al. 2009). In contrast, CLOCK (Al-Nuaimi et al. 2014; Plikus et al. 2013) and clock output genes (Lin et al. 2009) are most highly expressed in the matrix and DP cells during anagen phase (Plikus et al. 2013). Furthermore, although all of the core clock genes are expressed in telogen and anagen skin, only about 6% of clock-regulated genes overlap between these two phases of the hair growth cycle (Geyfman et al. 2012a). It is possible that the peculiar distribution of clock genes during different phases of the cell cycle leads to differential expression of circadian regulated genes. In mice deletion of *Bmal1* leads to a delay in anagen initiation (Lin et al. 2009). Double *Cry1/Cry2* deletion alters the daily mitotic rhythm of hair matrix cells (Plikus et al. 2013), suggesting a role for the circadian clock machinery in regulation of hair cycle in mice.

Recent studies has confirmed that clock activity in human HF is similar to that of mice and that clock elements are present in all compartments of the HF (Al-Nuaimi et al. 2014; Hardman et al. 2015). Robust circadian activity in human

HFs is maintained *in vitro* in the absence of synchronizing inputs from the CNS. Furthermore, downregulation of BMAL1 or PER1 leads to the prolonged growth of HF in culture and their hyperpigmentation (Al-Nuaimi et al. 2014; Hardman et al. 2015).

Taken together, the circadian clock plays the important role in mediating cell proliferation and in hair growth control. However, if Cryptochromes could directly mediate effects of light in the HF is largely unknown.

1.5 Aims and Objectives

Though devices for hair growth based on low levels of light have shown encouraging results, further improvements of their efficacy is impeded by a lack of knowledge on the exact molecular targets that mediate physiological response in skin and hair follicle. The objective of this study was to identify the expression of light-sensitive receptors in the human hair follicle that could mediate the positive effect of UV-free blue light on hair growth.

The following specific aims will be addressed:

1) To determine the presence of light-sensitive receptors and define their localization in specific hair follicle compartments: the expression of Cryptochromes and Opsins will be evaluated in human full-thickness skin and micro-dissected anagen hair follicles by employing qPCR and immunofluorescence analysis

2) To determine the functional significance of the identified receptors in hair growth control; the effects of gain- or loss-of function of the selected receptors on hair growth ex-vivo and on the activity of primary hair follicle cells will be assessed using chemical or RNA interference approach

3) Light treatment will be performed on hair follicle ex-vivo and on primary hair follicle cells to evaluate effect on hair growth and proliferation: UV-free blue light is selected because highly absorbed by investigated light receptors.

4) To assess if positive effect of light on hair growth could be mediated by the selected light-sensitive receptors the hair follicles ex vivo and hair follicle cells will be co-treated with light and corresponding siRNAs.

2 Material and Methods

2.1 Human skin and hair follicle collection

The present project was run in two countries UK and Netherlands. Tissue supply was arranged as follow: in Bradford (UK) human scalp skin was obtained from the occipital regions from female or male donors undergoing elective cosmetic surgery from the Farjo medical centre (Manchester, UK).Tissue was obtained with full written consent adhering to the Declaration of Helsinki principles and following institutional approval from the University of Bradford, under human tissue act guidelines. For the work performed at Philips Research (Eindhoven, Netherlands) HFs were isolated from the temporal or beard region of fresh surplus residual facial skin within 8 hours of surgery. Human skin was obtained after facelift surgery from healthy donors adhering to the Declaration of Helsinki principles under Human Tissue Transfer Agreement, between Philips Electronics Nederland B.V. acting through Philips Research and corresponding clinics, where clinics were responsible for obtaining written informed consent from all patients. All experimental protocols were approved by the Philips Internal Committee of Biomedical Experiments (ICBE), DocSet ID ICBE-2-6171. Philips Electronics Nederland B.V., acting through Philips Research Eindhoven, confirms that it was its responsibility to ensure that approvals by appropriate local and/or national Ethics Committees and relevant authorizations were obtained whenever such approvals were required for the experiments. In the Netherlands, collection and use of human tissue for scientific research is regulated via Article 467 of the Medical Treatment Contracts Act (Wet op de geneeskundige behandelingsovereenkomst, WGBO).

A list of donor samples employed for the experiments is reported in the Table 2.

Table 2: A list of donor samples employed for the experiments in the project

Subject ID	Age	Sex	Body location	Model	Experiment	Country
1	42	M	occipital	HFs	KL001 treatment	UK
2	46	F	temporal	HFs	KL001 treatment	Netherland
3	51	M	occipital	HFs	KL001 treatment	UK
4	65	F	temporal	HFs	KL001 treatment	Netherland
5	41	M	occipital	HFs	CRY1 silencing in HFs	UK
6	55	F	temporal	HFs	CRY1 silencing in HFs	Netherland
7	46	M	occipital	HFs	CRY1 silencing in HFs	UK
8	43	F	occipital	HFSC	cell sorting	UK
9	70	F	occipital	HFSC	cell sorting	UK
10	66	F	occipital	HFSC	cell sorting	UK
11	55	F	temporal	ORS	RNA and IF	Netherland
12	58	F	temporal	ORS	RNA and IF	Netherland
13	68	F	temporal	ORS	RNA and IF	Netherland
14	53	F	temporal	ORS	siCRY1	Netherland
15	54	F	temporal	ORS	light tx,siOPN3	Netherland
16	55	F	temporal	ORS	light tx,microarray, siOPN3	Netherland
17	56	F	temporal	ORS	light tx, siOPN3	Netherland
18	65	F	temporal	ORS	siCRY1	Netherland
19	69	F	temporal	ORS	light tx, microarray, siCRY1	Netherland
20	-	F	temporal	HFs	HFs and light	Netherland
21	55	F	temporal	HFs	HFs and light	Netherland
22	-	F	temporal	HFs	HFs and light	Netherland
23	-	F	temporal	HFs	HFs and light	Netherland
24	-	F	temporal	HFs	HFs and light	Netherland
25	-	F	temporal	HFs	HFs and light	Netherland
26	-	F	temporal	HFs	HFs and light	Netherland
27	53	F	temporal	HFs	HFs and light	Netherland
28	67	F	occipital	full thickness skin	IF	UK
29	46	F	occipital	full thickness	IF	Netherland

				skin		
30	60	F	occipital	full thickness skin	IF	UK
31	46	M	beard	full thickness skin	IF	UK
32	-	M	beard	full thickness skin	IF	Netherland

2.2 RNA extraction and cDNA synthesis

Total RNA was isolated from either microdissected HFs or primary HF keratinocytes. Microdissected HFs were collected in 1 ml of TRIzol® (Life Technologies), mechanically homogenised with a pestle and optionally stored at -80°C. Primary ORS cells lysate was collected in 300 µl TRIzol® (Life Technologies), vortexed for few seconds and optionally stored at -80°C. RNA isolation was performed using the spin column kit Direct-zol™ RNA MiniPrep (Zymo research) following manufacturer's protocol.

Briefly, an equal volume of 100% ethanol was added to a sample lysed in TRIzol® (Life technologies) and mixed thoroughly. The mixture was transferred into a Zymo-Spin™ Column. All centrifugations were performed at room temperature (RT) at 13000 x g for 30 seconds using a bench centrifuge (Eppendorf), except were indicated differently. 400 µl of RNA Wash Buffer solution were added to the column and centrifuged. DNase I treatment was performed in column by incubating with the digestion mix, prepared as follow: 5 µl DNase I (6 U/µl) and 75 µl DNA Digestion Buffer (15 minutes, RT). Next, 400 µl of Direct-zol™ RNA PreWash buffer were added to the column and

centrifuged followed by adding 700 µl of RNA Wash Buffer to the column and centrifugation for 2 minutes. Finally, the column was carefully transferred into an RNase-free tube. To elute RNA 50 µl of DNase/RNase-Free Water was added directly to the column and centrifuged at maximum speed for 30 seconds. Extracted total RNA was either stored at ≤-80°C or used for further analysis. First strand cDNA synthesis was performed using the High-Capacity cDNA Reverse Transcription Kit (Applied Biosystems™). Random primers were used; manufacturers' protocol was followed for 2X master-mix preparation. 100 ng of RNA were added to 10 µl of 2X master-mix in each tube. cDNA was synthesized using a Master Cycler gradient machine (Eppendorf) under the following cycling conditions: 25°C for 10 minutes, followed by 37°C for 120 minutes and 85°C for 5 minutes.

2.3 RT-PCR

Primers listed in Table 3 were used for PCR amplification of the region corresponding to the retinal-binding site of human Opsins 1,3,4 and 5 (Haltaufderhyde et al. 2015). OPN2 and CRY1 primers targeting the 3'UTR region of the transcript were employed.

Table 3 RT-PCR primer sequences

Accession Number	Gene	Sense/anti-sense primers	Source
NM_001708	Opsin 1 short wavelength (OPN1sw)	F:GTGGGGCCGTGGGATGGGCCTCAGTACCAC R:CCTCAGTTGGGGCCAACTTGGGTAGACGAGACAG	(Haltaufderhyde et al. 2015)

NM_020061	Opsin 1 middle-long wavelength (OPN1)	F:GGARGTGASSCGCATGG TGGTKGTGATG R:TCATGCAGGCGATACCG AGGACACAGATGAGAC	(Haltaufderhyd e et al. 2015)
NM_000539	Rhodopsin (OPN2)	F:TATAGAATGGGGCACACA GTAGG R:TATAGTCTGATGACTGCA TTCTGC	New Design
NM_014322	Encephalopsin (OPN3)	F:GGTCATGGTCACCTGGTC ACTCCAACAATATC R:CCTGTCCCCATCTT TCTGTGACATCACAATGG	(Haltaufderhyd e et al. 2015)
NM_001030 015	Melanopsin (OPN4)	F:ACTCAGGATGAACCCTCC TTC R:TGAACATGTTGGCAGGTG TC	(Haltaufderhyd e et al. 2015)
NM_181744	Neuropsin (OPN5)	F: TTCAGATCCCTCGTGGTTC GAGAACAGA R:GCAAGCCGTTCACCATCA TCTCTTGCTTTTGTCAC	(Haltaufderhyd e et al. 2015)
NM_004075	Cryptochrome 1 (CRY1)	F:ATATGGGTCAACAAGTTT GGGATC R: ATATGCTTCCAAGAGAATTG CCTC	New Design

For the amplification reaction GoTaq® DNA Polymerase 1,25 u (Promega) has been mixed with 0,2 µM each dNTPs, 1µM of forward and reverse primers in 1x Reaction buffer, water up to 20 µl final volume. The amount of cDNA required for the amplification reaction was optimized for each primer set. Amplification was performed using the touchdown PCR protocol for OPN1, 3, 4 and 5 primers as described by Haltaufderhyde et al, (Haltaufderhyde et al. 2015). For OPN2

amplification, standard PCR conditions were employed: 95°C for 2 min, followed by 34 cycles of denaturation (95°C for 20 s), annealing (51°C for 20 s), and elongation (72°C for 30 s). Total RNA from the human eye (Amsbio) and from HaCaT cell lines was used as positive control.

For DNA detection agarose gel was prepared mixing 1.2% (w/v) Agarose (Gene Flow) in 1x TBA Buffer in a Erlenmeyer flask. The agarose/buffer mix was heated in a microwave for 30 seconds or until agarose has completely dissolved. After cooling the gel mixture Ethidium Bromide at a concentration of 10 µg/ml (Invitrogen) was added to the solution. Samples and High Ranger Plus 100bp DNA ladder (Norgen) were loaded in the gel solidified in electrophoresis chambers (Fisher brand). The PCR products were run under 90V (Bio-Rad's PowerPac™ power supplies) for 40 minutes; products size have been evaluated under a UV lamp (Ingenius Sungene BioImaging). Images were acquired using Gene Snap (SynGene) software.

2.4 RT-qPCR

RT-qPCR was performed using Applied Biosystems Fast PCR mix, using 10ng cDNA and 1µM primers. PCR primers used for qPCR are listed in Table 4.

Table 4 RT-qPCR primer sequences

Accession Number	Gene	Sense/anti-sense primers	Ann. T (°C)
NM_004075	CRY1	F:AGGAGAACCACGACGAGA R:TCCGCTTCACCTTTTTATAC	61
NM_001127457	CRY2	F:TGGTGGTTGTGATGGTAGGA R:ATGCAAGTTGGAACTGCTT	61

NM_014322	OPN3	F:AGGAACACGAGGATTCTTGC R:GCGAGGGTCTGAGAGGATAG	61
NM_000539	OPN2	F:ACCCCACTCAGCATCATCGT R:CCAGCAGAAGCAGAATGCCAGGAC	62.2
NM_002616	PER1	F:TGGCTATCCACAAGAAGATTC R:GGTCAAAGGGCTGGCCCG	61
NM_022817	PER2	F:TCCAGATACCTTTAGCCTGATGA R:TTTGTGTGTGTCCACTTTCGA	61
NM_001289861	PER3	F:CCCCTCTCTGTCCTCTGTTG R:ACTGCCATTGTTGCCTGTAA	61
NM_001267843.1	CLOCK	F:TTGTAAGCTGCCTGGGTTTC R:CTCAGTGTTTGCTGGTGGTG	61
NM_001030272.2	BMAL1	F:AAACCAACTTTTCTATCAGACGATGAA R:TCGGTCACATCCTACGACAAAC	61
NM_000526	K14	F:GCCTGTCTGTCTCATCCTC R:CTGAAGCCACCGCCATAG	62
NP_002266.2	K15	F:AAAGAAGTGGCCTCCAACACA R: TCTCGGCCAGTGAGTTCTCC	62
NP_001004196	CD200	F:TGTTACATGTGTCTCTTCA R: AGTGGCAGAGCAAGTGATAT	59.8
NP_001020280	CD34	F: CTACAACACCTAGTACCCTTGGA R: GGTGAACACTGTGCTGATTACA	62
NM_025218	ULBP1	F:AAGGCCTGGTGGATGAAAGG R: CAGGGTGAGGGGCTCAATG	62,5
NM_007085	FSTL1	F:GAGCAATGCAAACCTCACAAG R:CAGTGTCCATCGTAATCAACCTG	62,5
NM_022754	SFXN1	F:TTCAATGCCGTCGTCAATTACA R:CGTAAGCTGTTCCCAACTCAT	62,5
NM_001206747	CAV2	F:AAGACCTGCCTAATGGTTCTGC	62,5

		R:CTCGTACACAATGGAGCAATGAT	
NM_002577	PAK2	F:CACCCGCAGTAGTGACAGAG R:GGGTCAATTACAGACCGTGTG	62,5
NM_015902	UBR5	F:GTCCATCCATTTCGTGGTTCA R:CCAATTCCAATCTGTCTGGCTG	62,5
NM_001001342	BLOC1S2	F:CAAGTGGAGGGATGTCGGAA R:GTCTTCACTGGTGGCCGT	62,5
NM_001008895	CUL4A	F:AGCAGCACCTCCATCAGGTA R:TCCTGCCAGCACGTGTTAAT	62,5
NP_003208	TMBIM6	F:CATATAACCCCGTCAACGCAG R:GCAGCCGCCACAAACATAC	60,1
NP_002799	PSMD2	F:TGCTCGTGGAACGACTAGG R:CAGTTTGCCATAGTGTGGACG	60,1
NP_006792	KDELR1	F:TCAAAGCTACTTACGATGGGAAC R:ATTGACCAGGAACGCCAGAAT	60,1
NP_001138778	CDK6	F:TCTTCATTCACACCGAGTAGTGC R:TGAGGTTAGAGCCATCTGGAAA	60,1
NP_057529	PLEK2	F:CCGAAGCATGGGAGCCATT R:AGTGCTCAGGCTAATTTCTTCC	62,5

All primers were optimised using Human Universal reference cDNA (Clontech) at different temperatures: 58°C, 61°C, 62°C and 64°C. Analysis of melting curves was used to determine optimum annealing temperature.

Amplification was performed using StepOnePlus™ real-time PCR system (Applied Biosystems) and following conditions:

Stage	Temperature	Time	Cycles

Initial Denaturation	95°C	20 seconds	
Amplification cycles : Denaturation	95°C	3 seconds	40
Annealing	Table 4 RT-qPCR primer sequences	30 seconds	
Elongation	95°C	15 seconds	

After amplification, a melting curve was created by gradually heating the PCR products from 65°C to 90°C. For each gene of interest, RT-qPCR was performed in duplicates. The differences between samples and controls were calculated using the Genex™ software (Bio-Rad) based on the Ct ($C_t^{\Delta\Delta}$) equitation method and normalized to the housekeeping GAPDH gene.

2.5 Tissue processing

Depending on the experimental design either microdissected HFs or full thickness skin were placed in OCT embedding medium (Thermo-scientific), snap frozen in liquid nitrogen and stored at -80ºC. Subsequently, 6 µm thickness cryosections of OCT embedded HFs or full thickness skin were cut using a cryostat (Cryotome™ FSE Cryostats, Thermo Scientific) and mounted on glass microscope slides (Superfrost+, Thermo-scientific).

2.6 Immunofluorescence

HF or skin cryosections were briefly air-dried followed by fixation step in acetone (10 minutes, -20°C) or in 4% paraformaldehyde (PFA) (10 minutes, RT) (Thermo-Fisher Scientific) depending on primary antibodies used (Table 5). An additional permeabilization step in 0.1% Triton X100 for the detection of nuclear antigens was performed. The tissue sections were incubated in 5% BSA (Sigma) for blocking of non-specific binding of antibodies. Optimal dilutions for primary antibodies were used (Table 5); incubation was performed overnight at 4°C. Subsequently, sections were incubated with corresponding secondary antibodies, Alexa-488 or Alexa-555 or Alexa-647 (Invitrogen) for 1 hour at 37°C. Cell nuclei were labelled using VECTASHIELD® mounting medium containing DAPI (4', 6-diamidino-2-phenylindole) (Vector Labs).

TUNEL assay was performed by employing the ApopTag® Fluorescein Direct In Situ Apoptosis Detection Kit (Millipore) following manufacturer's instruction.

Image acquisition was performed using a confocal microscope (Leica) and a fluorescent microscope Nikon Eclipse 501 in combination with DS-C1 digital camera and ACT-2U image analysis software (Nikon).

Table 5 Primary antibodies and dilutions.

Antigen	Host	Manufacturer	Diluition
Cryptochrome 1	Mouse	Abcam	1:400
Encephalopsin (OPN3)	Rabbit	Abcam	1:100
Rhodopsin, RETP1 clone	Mouse	SIGMA	1:50
Keratin-15	Mouse	Abcam	1:100

CD200	Goat	R&D system	1:100
Hair cortex keratin (AE13)	Mouse	Abcam	1:100
Trichohyalin (AE15)	Mouse	Abcam	1:500
Keratin 10	Rabbit	Abcam	1:200
Keratin 14	Rabbit	Abcam	1:100
CDK6	Rabbit	Abcam	1:500

2.6.1 Image analysis

Image acquisition was performed using a fluorescent microscope (Nikon Eclipse 501) and Image Analysis software (ImageJ). For density measurement of the immunoreactivity of CRY1 and CDK6 in HFs, images were taken at x20 magnification and same exposure time in the experimental and control groups. Background correction was performed for every image using the “rolling ball” algorithm (ImageJ software) by setting the radius to a size that correspond to the largest object that is not part of the background. Intensity of immunoreactivity in the bulb region was measured by selecting an area of a defined size. Means±SD were calculated from pooled data (2-3 donors, 4 HFs from each donor) and statistical analysis was performed using Mann-Whitney test.

2.6.2 Quantitative analysis of proliferation and apoptosis (Ki-67/TUNEL staining)

The number of Ki-67 and TUNEL positive cells was counted below Auber’s line (the widest part of the DP). The percentage of proliferative and apoptotic cells was calculated against the total number of DAPI+ nuclei below this line.

Means±SD were calculated from pooled data (2-3 donors, 4 HFs from each donor) and statistical analysis performed using Mann-Whitney test.

2.7 Human hair follicle organ culture

Anagen HFs isolated from the full-thickness skin were microdissected with forceps and a scalpel using a stereo microscope. If HFs were collected as pilosebaceus units they were trimmed to remove the epidermis, dermis, fat, and sebaceous glands. Microdissected HFs we cultured at 37°C in a humidified atmosphere of 5% CO2 under serum-free conditions in William's E medium (Thermo Fisher Scientific) supplemented with hydrocortisone 10 ng/ml (Sigma-Aldrich), L-glutamin 2mM (Sigma-Aldrich), and Penicillin 1000 U/ml / Streptomycin 1mg/ml (Sigma-Aldrich), with or without insulin 10 µg/ml (Sigma-Aldrich), depending on experimental conditions. Under complete conditions anagen HF continue to produce a pigmented hair shaft up to 10 days (Philpott et al. 1994b).

2.8 CRY1 stabilization with KL001 treatment

To enhance CRY1 activity in the HF a small molecule, KL001 (N-[3-(9H-carbazol-9-yl)-2-hydroxypropyl]-N-(2-furanylmethyl)-methanesulfonamide) (Sigma) diluted in DMSO (20 mg/ml) was used. In brief, HFs from 4 donors (42-65 y.o) were micro-dissected and grown in 24 multi-well culture plate, one HF in each well. HFs were grown in supplemented William's E media but without insulin, in order to mimic hair growing under impaired conditions. 2,7 and 8 µM

KL001 was added to the HF culture media on days 1 and 3. HFs were cultured up to 7 days. In the control group 0.01% DMSO was used. Images of the HFs were taken at day 0, day 3 and 7 under a stereoscopic microscope at x20 magnification and a Nikon Coolpix digital camera using the Visicam image analysis software to assess HF morphology.

2.9 Silencing of CRY1

Microdissected cultured anagen HFs (three donors, 41-55 y.o.) were grown in a 24 multi-well plate, one HF per well in William's E complete media and transfected with a mixture of small interference RNA (siRNA) against *Cry1* gene (Accell SMARTpool - Human, Dharmacon) and with non-targeting scrambled siRNA as a negative control (Accell Non-targeting siRNA- Human, Dharmacon) after the 24h equilibration period. Only growing HFs were selected for transfection. Accel- modified siRNAs are used without additional transfection reagents, virus or instruments, in serum free conditions. siRNA were re-suspended in complete William E medium at a final concentration of 1 μM for the pool of siRNA (siCRY1) or scrambled siRNA and the mixtures were added to the cultured HFs. Ninety-six hours after transfection half of the HFs (5-12) from each group were collected for RNA extraction to evaluate silencing efficiency. The rest of the HFs was embedded in cryomatrix and snap frozen for immunohistochemical analysis. Images were taken at day 0, 3 and 4 of the experiment using a stereoscopic microscope at x20 magnification equipped with a Nikon Coolpix digital camera for morphological evaluation. Images were analyzed using the Visicam image software.

2.10 Light treatment of HF *ex vivo*

Microdissected HFs from 7 donors (53-55 year old) were cultured in phenol red-free supplemented Williams E medium (Life Technology). Williams E medium contains traces of retinol, as specified in the media formulation. Because HF cells are known to possess a system for synthesis and metabolism of retinoids (McDowall et al. 2008), no cis-retinal was added to the culture medium. HFs were cultured at 37°C in a humidified atmosphere of 5% CO2 up to 14 days. Light treatment was performed using two proprietary LED-based devices with flat homogeneous illumination over the area of the 24-well plate. Each device was emitting one discrete wavelength: 453 nm central wavelength,16 nm full width half maximum (PHILIPS, The Netherlands) previously used for the experiments on in vitro human cells study and in human clinical trials (Kleinpenning et al. 2010; Liebmann et al. 2010), and 689 nm central wavelength, 24 nm full width half maximum (PHILIPS, The Netherlands). Separate groups of HFs were treated daily using 453 nm or 689 nm wavelengths, 16mW/cm2 irradiance, 3.2 J/cm2 radiant exposures during 10 consecutive days. Irradiance and radiant exposure were set to low levels to assure initiation of only photobiological effects, avoiding photothermal reactions. 450 nm wavelength was selected based on absorption spectra of investigated receptors, Opsin and Cryptochorme; impact of red light was also evaluated because often use for devices for *in vivo* hair growth stimulation (Lanzafame et al. 2013; Lanzafame et al. 2014) .Optical power was measured before each experiment using the Nova II power meter (Ophir Optronics Solutions Ltd) at the plane of HFs, assuring delivery of the correct irradiance (watts per area). No

increase in temperature above 37°C was observed as monitored using FLIR A655sc Infrared Camera, (FLIR® Systems, Inc). Culture medium was refreshed every other day over the period of light treatment, adapting the protocol of Mignon et al (Mignon et al. 2016b). The images were taken with wide-field microscope (Leica) for morphological evaluation. For statistical analysis, the effects of medium, donor, and light treatments on mean survival time with standard errors, were based on a random-effects interval-data regression model. A commercial software package was used: StataCorp. 2015. Stata Statistical Software: Release 14. College Station, TX: StataCorp LP.

2.11 Cell culture and transfection

Primary human outer root sheath (ORS) keratinocytes were isolated from microdissected anagen HFs as described previously (Inoue and Yoshimura 2013). Briefly, total skin was washed with 1x PBS, hair shafts were shaved and subcutaneous fat was removed. The skin was cut into several stripes of 1 mm width and incubated with Dispase I (Roche) overnight at 4°C, which allowed separating epidermis and the HFs from the dermis using forceps. After removal of sebaceous glands HFs were incubated with 0.05% trypsin- 0.02% EDTA at 37°C for 5 min. Following enzymatic digestion HFs were transferred into a solution with 10% FBS in DMEM to neutralize trypsin. Cells were filtered through a 40 um nylon mesh filter, pelleted by centrifuging at 170 g for 5 minutes and re-suspended in Keratinocyte Growth Medium 2 supplemented with Bovine Pituitary Extract 0.004 ml / ml, Epidermal Growth Factor (recombinant human) 0.125 ng/ml, Insulin (recombinant human) 5 µg/ml,

Hydrocortisone 0.33 µg/ml, Epinephrine 0.39 µg/ml, Transferrin-holo (human) 10 µg/ml, and CaCl2 0.06 mM (Promocell), 100 Units/ml penicillin and 100 µg/ml streptomycin (Pen/Strep) (GIBCO) and 2.48 µg/ml fungizone (GIBCO).

Primary ORS keratinocytes at early passages (p3-4) were seeded into 24 well-plate at a density of 10000 cells per well, and cultured in fully supplemented phenol-red free Keratinocyte Growth Medium 2 (Promocell).

For CRY1 or OPN3 knockdown, ORS cells that were 70% confluent were transfected with 50 nM of the corresponding smartpool siRNAs (ON-Targetplus) and a non-targeting control (Dharmacon) using Lipofectamine (RNAiMax, Invitrogen) according to the manufacturers' protocol.

To study CRY1 functions, experiments were initiated with inducing clock machinery synchronization with Dexamethasone (Sigma) as a pre-treatment (Balsalobre et al. 2000): cells were incubated for 30 minutes with 100 nM of Dexamethasone before transfection followed by a washing step in sterile 1x PBS (Sigma).

2.12 Alamar Blue® metabolic activity assay

Primary ORS keratinocytes at early passages (p3-4) were seeded into 24 well-plate with a black frame (Porvair) at a density of 60000 cells per well, and cultured in fully supplemented phenol red free Keratinocyte Growth Medium 2 (Promocell). The cell mono-layers were treated with 3.2 J/cm^2 light (453 nm) using a proprietary LED-based device as described above. The changes in metabolic activity were assessed 24 hours after irradiation, using the Alamar Blue® assay (Thermofisher) following the manufacturer protocol. The

fluorescence intensity of the supernatant was measured using a temperature controlled plate reader (FLUOstar OPTIMA, BMG Labtech).

2.13 EdU incorporation assay

Primary ORS keratinocytes at early passages (p3-4) were seeded into 12 well-plate on coverslips coated with 0.5% gelatin, at a density of 100000 cells per well, and cultured in fully supplemented phenol red free Keratinocyte Growth Medium 2 (Promocell), until 80% confluent. Single light treatment with 3.2 J/cm2 light (453 nm) was performed as described above. After the light treatment, cells were incubated with fresh media containing 10 uM of the thymidine analogue EdU that incorporates into newly synthesized DNA (Click-iT® EdU Imaging Kits, Invitrogen). To investigate if OPN3 is involved in mediating the effects of blue light, cells were transfected with either scrambled siRNA (control) or siRNA against OPN3 followed by the exposure to 3.2 J/cm^2 light (453 nm). 4 hours and 8 hours after light irradiation the cells were fixed in 4% PFA (10 minutes, room temperature). EdU detection was assessed following the manufacturer protocol. Cell nuclei were counterstained using VECTASHIELD® mounting medium containing DAPI (Vector Labs). Image acquisition was performed using a fluorescence microscope in combination with DS-C1 digital camera and ACT-2U image analysis software (Nikon): 10 to 15 fields of view (FOV) from each coverslip were randomly acquired for every condition.

2.13.1 Image analysis for EdU positive cells and CDK6 immunofluorescence in vitro

Image acquisition was performed using a fluorescent microscope (Nikon Eclipse 501) and Image Analysis software (Image J) for counting of the number of EdU+ cells and cell nuclei visualized using DAPI (Vector Labs) each image. A threshold method was used to identify objects in every image; threshold values were the same for control and experimental groups. The ratio of proliferative EdU+ cells was calculated against the total number of DAPI+ nuclei in every FOV. Means±SD was calculated from pooled data (n=10) and statistical analysis performed using ANOVA.

To quantify CDK6 nuclear intensity the Integrated Intensity value of the nuclear compartment in each cell was analyzed. The average CDK6 nuclear intensity for every image was used for statistical purposes.

2.14 Microarray and bioinformatic analysis

Total RNA was extracted from the ORS cells 48 hours post OPN3 or 24 hours post CRY1 siRNA transfection as described above. Quality of total RNA was tested by capillary electrophoresis on an Agilent 2100 bioanalyzer (Agilent). Gene expression profiling was performed using arrays of human HTA-2_0-st-type from Affymetrix. Biotinylated antisense cRNA was then prepared according to the Affymetrix standard labelling protocol with the GeneChip® WT Plus Reagent Kit and the GeneChip® Hybridization, Wash and Stain Kit (both from

Affymetrix, Santa Clara, USA). Afterwards, the hybridization on the chip was performed on a GeneChip Hybridization oven 640, then dyed in the GeneChip Fluidics Station 450 and thereafter scanned with a GeneChip Scanner 3000. All of the equipment used was from the Affymetrix-Company (Affymetrix, High Wycombe, UK). A Custom CDF Version 20 with ENTREZ based gene definitions was used to annotate the arrays (38). The Raw fluorescence intensity values were normalized applying quantile normalization and RMA background correction. ANOVA was performed to identify differential expressed genes using a commercial software package SAS JMP10 Genomics, version 6, from SAS (SAS Institute, Cary, NC, USA). A false positive rate of a=0.05 with false discovery rate (FDR) correction was taken as the level of significance.

2.15 Sorting of hair follicle stem cells

HF stem cells were isolated from scalp skin of 3 female donors (44-, 66 - and 70-years-old) as published before (Inoue and Yoshimura 2013). Briefly, skin was washed with 1x PBS, hairs were shaved and subcutaneous fat was removed using a scalpel. The skin was cut into several stripes of 1 mm width and incubated with Dispase I (Roche) overnight at 4°C that allowed separating epidermis and the HFs from the dermis using forceps. At least 50 HFs, were incubated with 0.05% trypsin- 0.02% EDTA at 37°C for 30 min. After enzymatic digestion HFs were transferred into a solution with 10% FBS in 1x PBS to neutralize trypsin. Cells were filtered through a 40 um nylon mesh filter, pelleted by centrifuging at 170 g for 5 minutes and re-suspended in PBS with 0.5% BSA.

Cells were labelled with a mix of anti-human PE- conjugated CD200 (eBioscience), APC-CD34 (eBioscience) and FITC-CD49f integrin (eBioscience)

antibodies for 30 min at 4°C in the dark followed by 15 minutes incubation with 7-AAD (BD Pharmingen) on ice to identify living cells. Two stem cell populations, CD200+/CD49f+ and CD34+/CD49f+, were sorted using Moflo XDP cell sorter (Beckman Coulter). Cell populations were sorted based on the standard FSC/SSC profile, as well as each fluorochrome and collected in TRIzol® LS Reagent for isolation of total RNA.

2.16 Statistical analysis

Statistical analysis was performed in Graphpad Prism® (La Jolla, CA, USA). Data were assessed for a normal distribution before statistical analysis using a D'Agostino-Pearson omnibus normality test. For normally distributed data a Student's T test was used. Where the data did not follow a normal distribution a Mann-Whitney test was used. The ANOVA test was used for multiple comparisons.

For the analysis of HF survival rate ex vivo, the effects of medium, donor, and light treatments on mean survival time with standard errors, were based on a random-effects interval-data regression model. A commercial software package was used: StataCorp. 2015. Stata Statistical Software: Release 14. College Station, TX: StataCorp LP.

3 Results

3.1 Analysis of the expression of light-sensitive receptors in human hair follicle

To investigate the expression of putative molecular targets for light therapy in human anagen HFs, a screening of Cryptochrome transcription factors and Opsins was performed in microdissected HFs by RT-PCR. Primers encompassing the Lysine residue, that is required for the photo-activation of Opsin receptors, were employed for amplification of OPN1SW (Opsin 1 short wavelength), OPN1MW (Opsin 1 middle-long wavelength), OPN2 (Rhodopsin), OPN3 (Panopsin or Encephalopsin), OPN4 (Melanopsin), and OPN5 (Neuropsin) (Haltaufderhyde et al. 2015). To amplify CRY1 (Cryptochrome 1) primers annealing to the 5'-UTR region were used. Total RNA isolated from human retina and HaCaT cells were used as a positive control.

Specific PCR products corresponding only to CRY1, OPN2 and OPN3 were detected in the HFs, whilst the expression of OPN1 short and middle wavelength, OPN4 and OPN5 was not observed (Figure 3-1 A).

To compare the relative levels of detected Opsins and Cryptochromes in anagen microdissected HF, semi-quantitative PCR analysis was performed that revealed the higher CRY1 expression levels followed by OPN2 and OPN3 and CRY2 in the samples obtained from 6 donors; such expression pattern was sex and age independent (Figure 3-1 B).

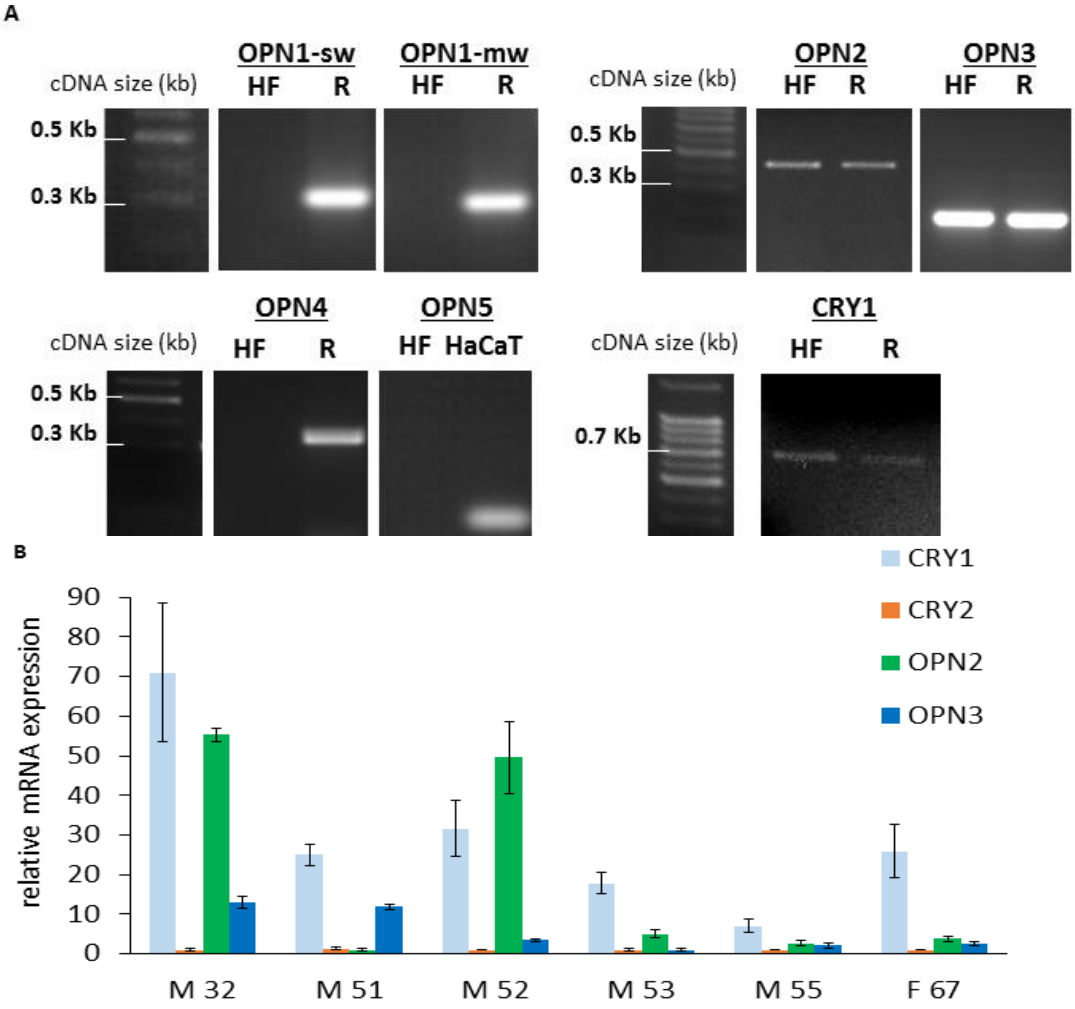

Figure 3-1 Detection of light sensitive receptors in human hair follicles.

(A) RT-PCR: only OPN2, OPN3 and CRY1 were amplified from HFs cDNA, whilst OPN1sw and OPN1mw, OPN4 and OPN5 amplicons were not detected. Human retina (R) or HaCaT cell line cDNA were used as positive controls. (B) qPCR: relative expression of CRY1, CRY2, OPN2 and OPN3 were measured in micro-dissected anagen HFs. CRY1 transcript was highly expressed, followed by OPN2 and OPN3, while CRY2 was very low in expression; this pattern was sex and age independent in 5 out of 6 patients. Sex and age of each donor are below bars clusters (mean ±SD of duplicates). Analysis was performed with Genex software (Bio-Rad) using ΔΔCt equitation method. Abbreviations: M - male; F – female (6 donors, 32-67 y.o.).

Next, immuno-fluorescence analysis was performed to characterize the localization of detected light-sensitive receptors in skin.

CRY1 is ubiquitously expressed in the epidermis as well as in the dermis (Figure 3-2 A). The double staining of CRY1 with cytokeratin 14 (CK14) and 10 (CK10), markers of the basal and supra-basal layers respectively, showed that CRY1 is expressed in undifferentiated and more differentiated keratinocytes (Figure 3-2 B-C). In anagen HFs, the expression of CRY1 was detected in the dermal papilla, the connective tissue sheath, in the epithelial outer and inner root sheaths (Figure 3-2 D) and in the bulge area, known to harbor the stem cells of the HFs (Figure 3-2 E). In order to validate that CRY1 is present in the HF stem cells, a double immunostaining using CRY1 and CD200, a marker of HF stem cells, was performed. The co-expression of CRY1 and CD200 confirmed the presence of CRY1 in follicular stem cells (Figure 3-2 F). CRY1 subcellular localization can be nuclear or cytoplasmic, depending on its activation state: nuclear CRY1 actively represses transcription of itself and other clock genes, inducing rhythmic gene expression (Sancar 2000). In human skin and HFs only nuclear expression of CRY1 was observed. However, in primary unsynchronized cells isolated from the ORS of anagen HFs CRY1 protein was detected in both cytoplasmic and nuclear compartments (Figure 3-2 G).

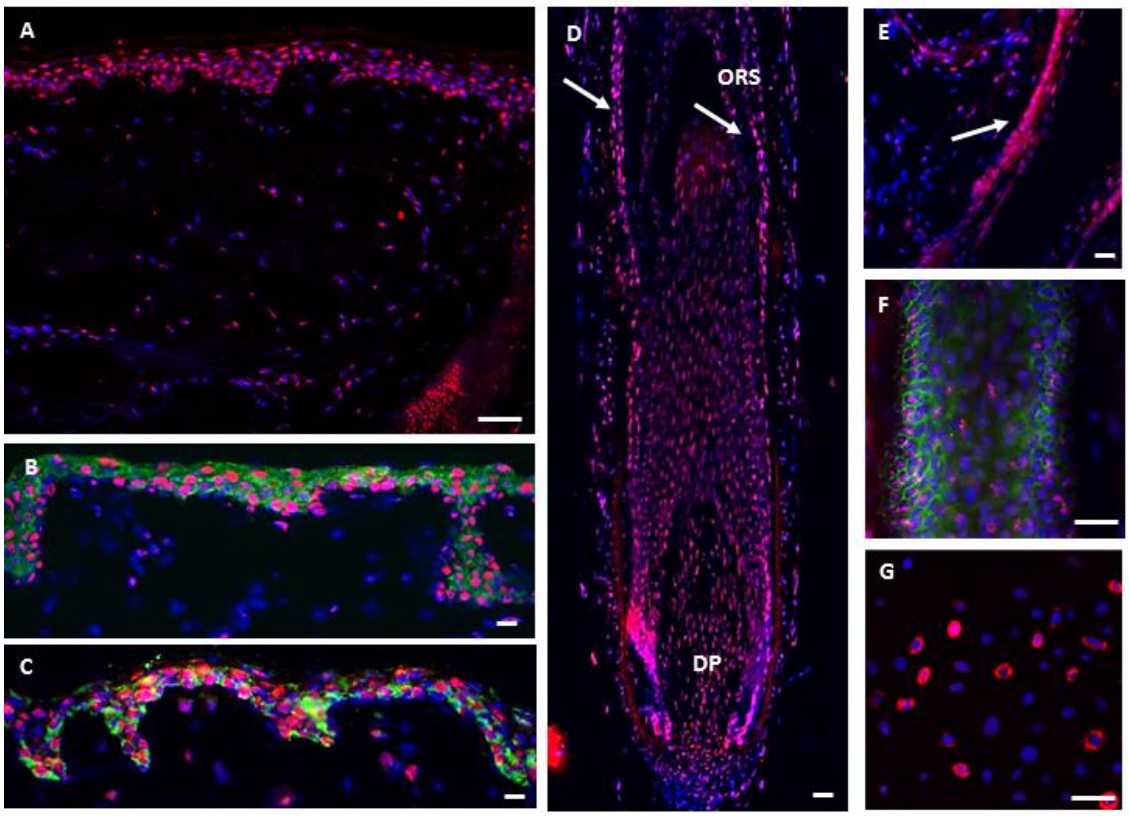

Figure 3-2 Localization of CRY1 in human skin

Immunofluorescence: (A) CRY1 is expressed in the epidermis and dermal fibroblasts. (B) CRY1 (red) is co-localised with CK10 (green), (C) CRY1 (red) is co-localised with CK14 (green). (D) In anagen HFs CRY1 expression was detected in DP, matrix cells, in the IRS and ORS (arrows). (E) CRY1 expression in the bulge area of the ORS (arrow). (F) Co-localization of CRY1 (red) and CD200 (green) in the bulge area. (G) CRY1 expression in unsynchronized primary ORS cells in both nuclear and cellular compartments. Abbreviations: DP - dermal papilla, ORS – outer root sheath. Scale bar 50 µm, nuclear staining: DAPI (blue)

Prominent expression of OPN2 was seen in the epidermis and in dermal fibroblasts in skin obtained from either male beard or female scalp regions (Figure 3-3 A-B). OPN2 expression was co-localized with cytokeratin 14 (CK14), suggesting the presence of OPN2 in the basal epidermal layer (Figure 3-3 B). In the HF, the expression of OPN2 was restricted to the lower and upper ORS (Figure 3-3 C-D-E). Similar pattern of OPN2 expression was detected in terminal (Figure 3-3 C-D) and vellus HFs (Figure 3-3 E). In addition, OPN2 expression was seen in the HF compartment harboring the stem cells (bulge) as demonstrated by the double staining of OPN2 with a stem cell marker CD200 (Figure 3-3F-G).

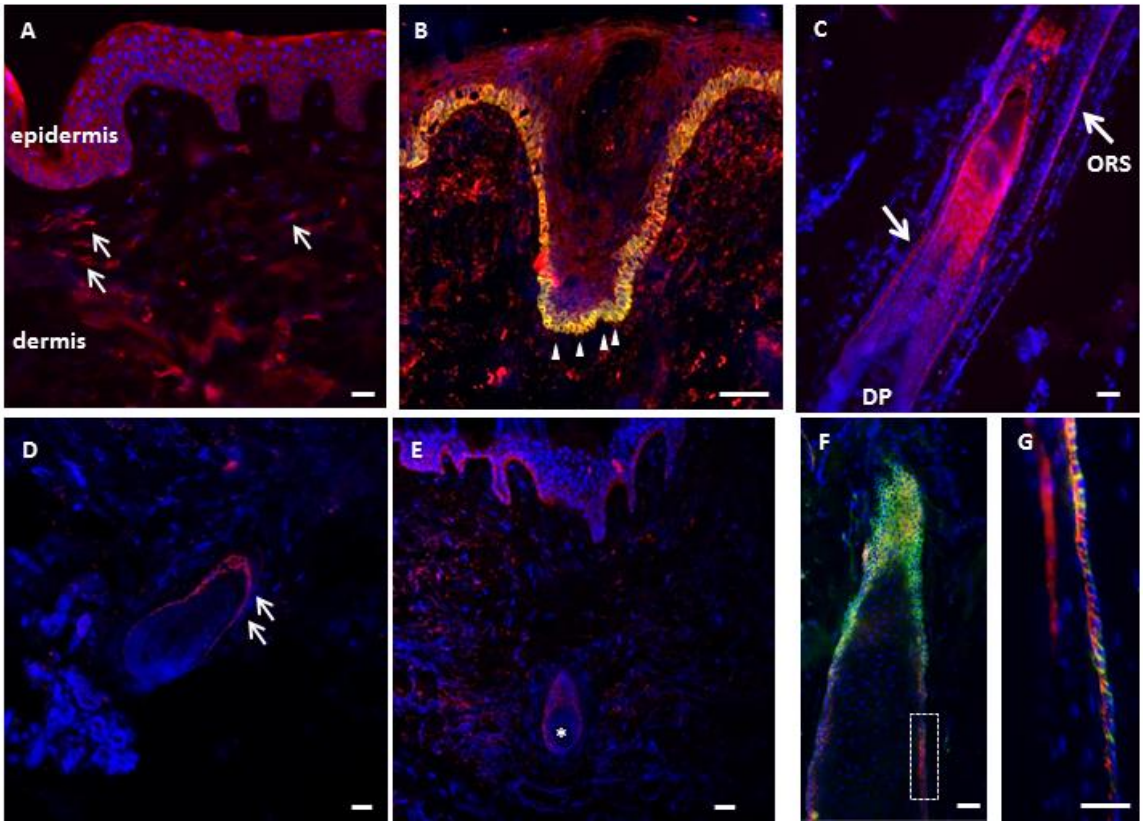

Figure 3-3 Expression of OPN2 in human skin.

Immunofluorescence: (A) OPN2 is expressed in the epidermis and dermal fibroblasts (arrows). (B) OPN2 (red) expression in the basal layer of epidermis (arrowheads), which is co-localized with CK14 (green) (C). Expression of OPN2 (red) in anagen HFs along the ORS (arrows). (D-E) OPN2 expression in the lower ORS in terminal (D, arrows) and vellus (E, asterisk) HFs. (F-G) Co-expression of OPN2 (red) with CD200 (green), a marker of stem cells in human HFs. (F-G). Scale bar 50 µm. Nuclear staining: DAPI (blue). Abbreviations: ORS – outer root sheath, DP – dermal papilla.

Analysis of OPN3 expression revealed its presence in the epidermis, as well as in the dermis (Figure 3-4 A). In the HFs, OPN3 expression was predominantly seen in IRS and in the lateral hair matrix (Figure 3-4 B). Similar pattern of OPN3 expression was seen in the scalp terminal (Figure 3-4 B) and vellus HFs (Figure 3-4 C). The IRS specific OPN3 expression was further confirmed by double-immunolabelling with AE15 that detects trichohyalin, an intermediate filament-associated protein involved in the IRS differentiation (Figure 3-4 D). Expression of OPN3 was not detected in the hair cortex as it was not co-localized with anti-hair cortex Cytokeratin AE13 (Figure 3-4 E). Also, co-localization of OPN3 and ORS specific Keratin 15 was not observed. (Figure 3-4 F).

Taken together, our data assert that light –sensitive receptors, such as CRY1, OPN2 and OPN3 are expressed in anagen HFs; their specific localization can suggest their different roles in hair physiology.

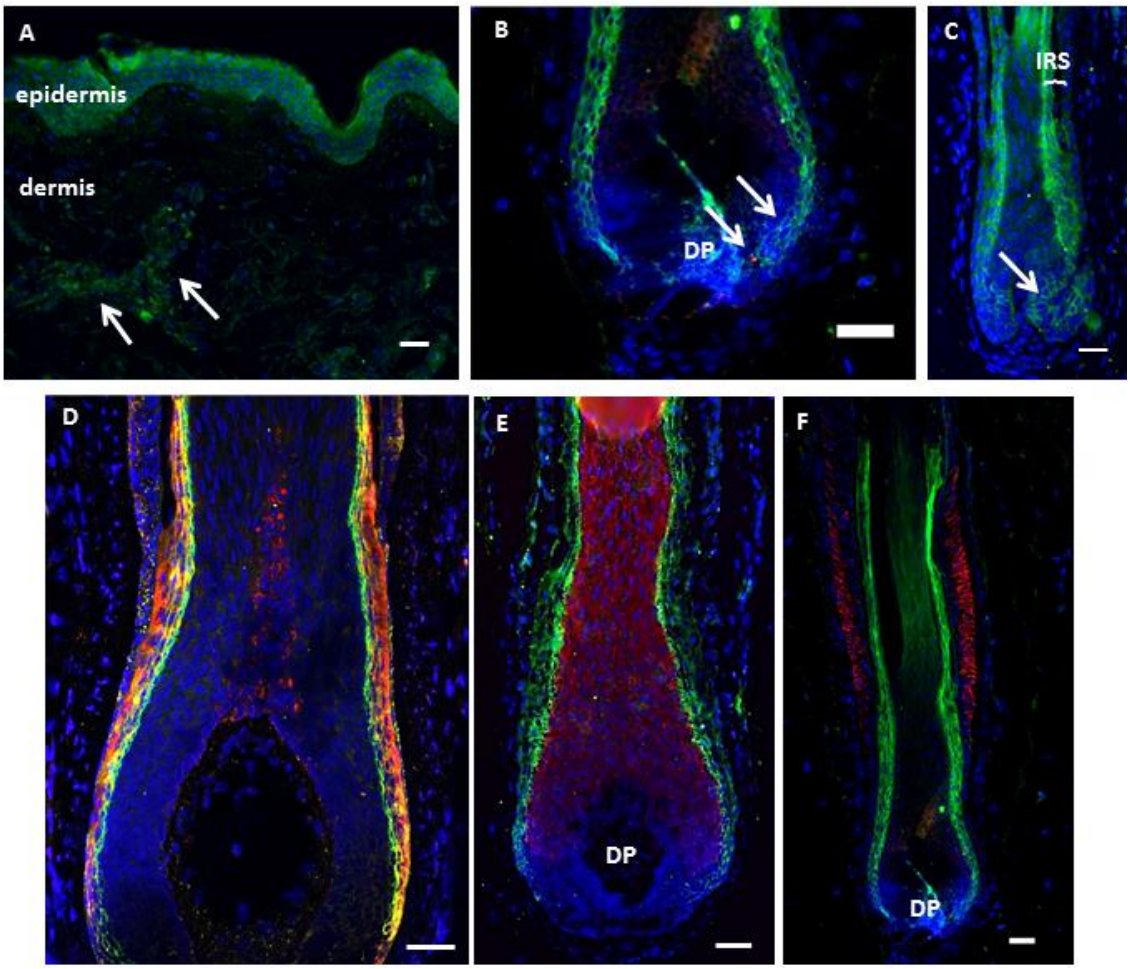

Figure 3-4 Expression of OPN3 in human skin.

(A) OPN3 is expressed in the epidermis and in the dermal fibroblast (arrows); (B-C) OPN3 is expressed in the hair matrix (arrows) and in the IRS of terminal anagen scalp HF (B) and facial vellus HF (C). (D) Double immunostaining of OPN3 (green) with trichohyalin (AE15, red): OPN3 is co-localized with AE15; (E) Double immunostaining of OPN3 (green) with hair cortex cytokeratin (AE13, red): lack of co-localisation. (F) OPN3 (green) is not expressed in the central ORS, as confirmed by double immunostaining with keratin 15 (K15, red). Scale bar 50 µm. Abbreviations: DP – dermal papilla, IRS – inner root sheath, ORS – outer root sheath. Nuclear staining: DAPI (blue)

3.2 Expression of light-sensitive receptors in HF stem cells

To confirm the preliminary in-situ observations that selected light-sensitive receptors are expressed in the HF stem cells (Figure 3-2 Figure 3-3 G), HF stem cells have been sorted from micro-dissected HFs isolated from fresh human scalp skin, using a combination of antibodies CD200, CD34 and CD49 f-integrin markers, as described previously (Ohyama et al. 2006). CD200 is a cell-surface marker of the epithelial HFSC found in the bulge region, while CD34 is expressed in the HF stem cells of the supra-bulbar ORS (Inoue et al. 2009; Kloepper et al. 2008; Ohyama et al. 2006; Purba et al. 2014). A representative dot plot of the cell populations sorted by FACS is shown in Figure 3-5 A: as expected cells from the bulge region, CD200+/CD49+ correspond to the 10% of total number of sorted cells, while CD34+/CD200- cell population represented 40% of isolated cells. Enrichment in stem cells markers was evaluated by RT-qPCR: the bulge CD200+/CD49f+ stem cell population was enriched in *CD200* and *K15* expression; CD34+/CD200- progenitor cells exhibited high level of *CD34* expression, while expression of *K15* and *CD200* was decreased comparing to the bulge stem cells population. Furthermore, the expression of *K14*, a marker of the basal layer of the epidermis, was undetectable in sorted stem cells (Figure 3-5 B).

By qPCR, *CRY1, CRY2, OPN2* and *OPN3* transcripts were detected in both CD200+ and CD34+ cell populations (Figure 3-5 C-D). This analysis confirmed that light-sensitive receptors CRY1 - 2 and OPN2 - OPN3 are expressed in the HF stem cells- enriched cell population, suggesting a putative light sensitivity of HF stem cells.

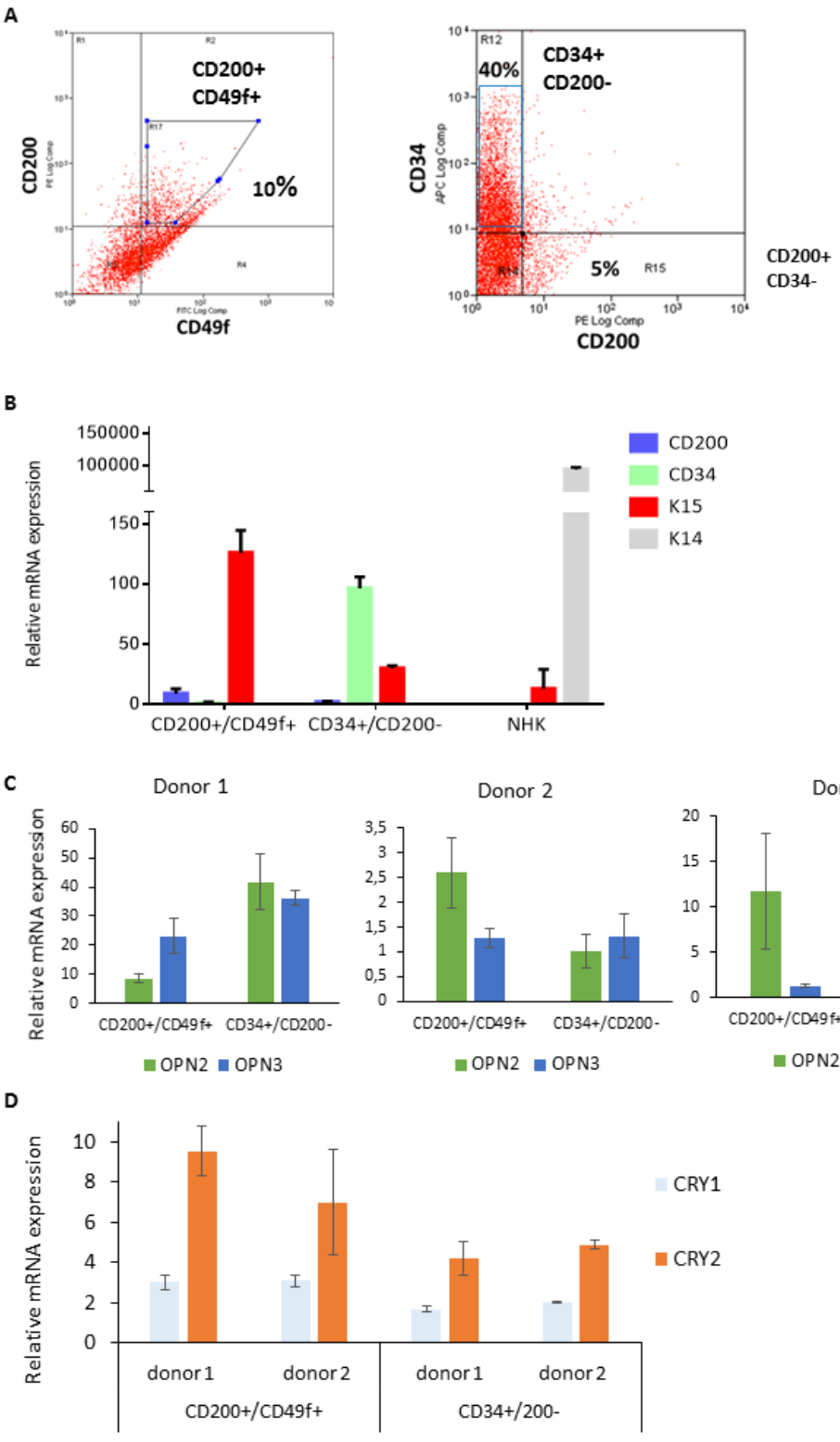
A
CD200+
CD49f+
10%
CD200
CD49f
CD34+
CD200-
40%
5%
CD200+
CD34-
CD34
CD200
B
Relative mRNA expression
150000
100000
150
100
50
0
CD200
CD34
K15
K14
CD200+/CD49f+
CD34+/CD200-
NHK
C
Donor 1
Donor 2
Donor 3
Relative mRNA expression
CD200+/CD49f+
CD34+/CD200-
OPN2
OPN3
D
Relative mRNA expression
10
8
6
4
2
0
CRY1
CRY2
donor 1
donor 2
donor 1
donor 2
CD200+/CD49f+
CD34+/200-

Figure 3-5 mRNA expression of light-sensitive receptors in the hair follicle stem cells.

HF stem cells were sorted from micro-dissected HF (3 donors' 43-70-y.o.). (A) Representative dot-plots showing 2 populations of sorted cells: CD200+/CD49f+ bulge stem cells and CD34+/CD200- progenitor cells. (B) Enrichment in stem cells markers was evaluated by RT-qPCR: the bulge CD200+/CD49f+ stem cell population was enriched in *CD200* and *K15* stem cells markers. CD34+/CD200- progenitor cells expressed high levels of *CD34* and low levels of *K15* and *CD200* transcripts; both the CD200+/CD49f+ and CD34+/CD200- cell populations had significantly decrease levels of *K14* comparing to human epidermal keratinocytes (NHK) (n=2, 3 donors in duplicates; mean ±SD). (C) *OPN2* and *OPN3* mRNA expression was detected in both CD200+ and CD34+ enriched stem cell populations (n=2; mean ±SD). (D) *CRY2* mRNA was highly expressed compared to *CRY1* mRNA in both CD200+ and CD34+ populations (n=2; mean ±SD). Analysis was performed with Genex software (Bio-Rad) using $\Delta\Delta$Ct equitation method.

3.3 Cry1 is a positive regulator of hair growth

To explore the functional significance of the identified light-sensitive receptors in the HFs, CRY1 activity was modulated in the HF organ culture using either chemical or RNA interference approaches. To stabilize CRY1, the small molecule KL001 that prevents CRY 1 and 2 degradation and induces lengthening of the circadian rhythm was used (Figure 3-6 A). To knock-down CRY1 expression in the HF siRNA against *CRY1* was employed in the HF *ex vivo* model.

In a first pilot experiment two concentrations of KL001 (2.7 µM and 8 µM) were tested in the ex-vivo HF organ culture to determine the efficacy of CRY1 stabilization. KL001 prevents CRY1 degradation and induces its translocation into the nucleus, where CRY1 activates the negative feedback loop for circadian clock regulation, inhibiting its own transcript expression and Period genes (Hirota et al. 2012; Oshima et al. 2015). KL001 treatment of HFs resulted in the decreased mRNA levels of CRY1 and 2, PER1 and 2 compared to the control HFs (Figure 3-6 B). More prominent nuclear expression of CRY1 protein was seen in the bulb region (Figure 3-6 C) of the HF treated with 8µM KL001, comparing to the control HF (Figure 3-6 D). These observations, consistent in three donors, indicate stabilization of CRY1 in the HFs cells upon KL001 treatment ex vivo (Figure 3-6 D).

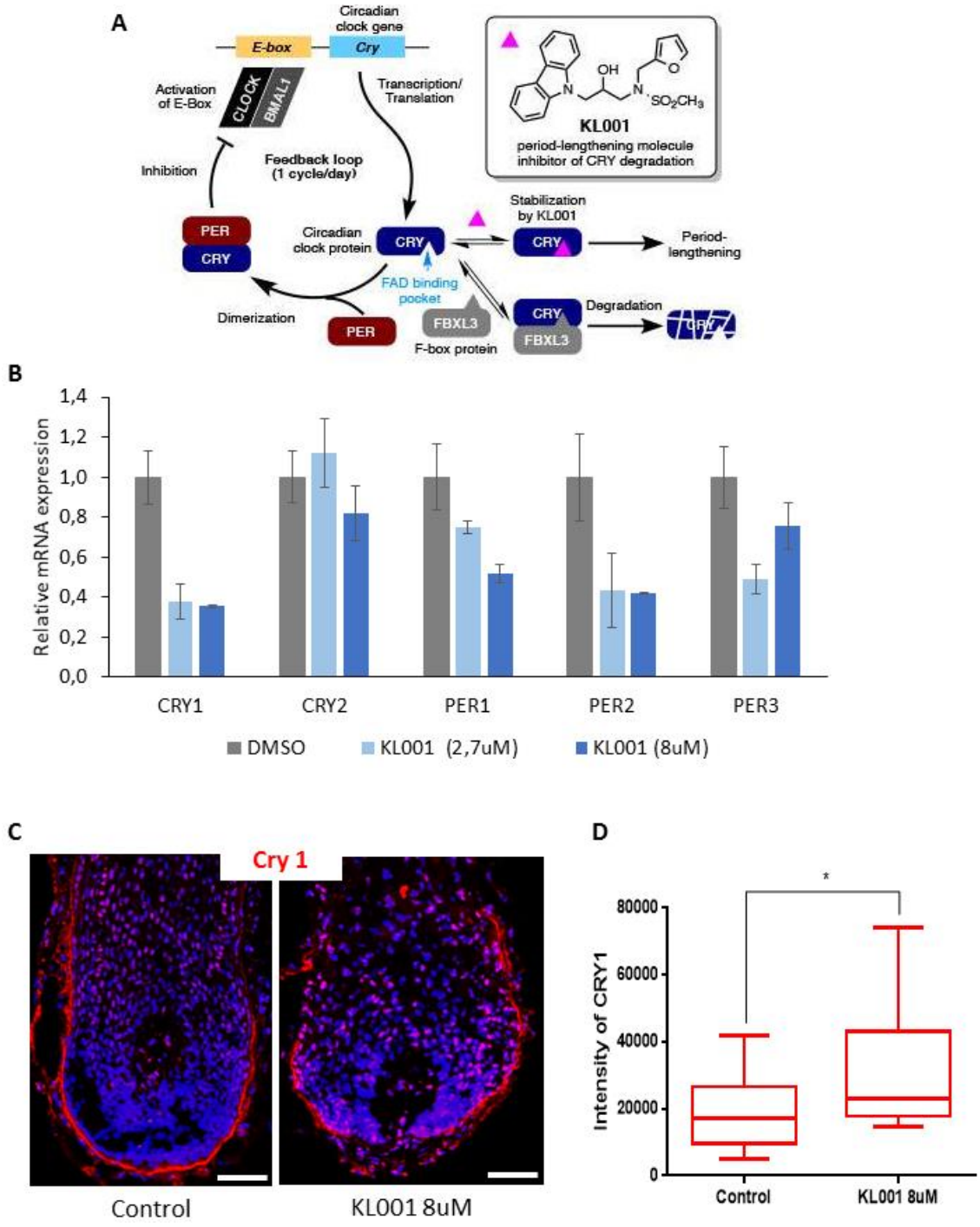
A
Circadian clock gene
E-box
Cry
Activation of E-Box
CLOCK
BMAL1
Transcription/ Translation
Inhibition
Feedback loop (1 cycle/day)
KL001
period-lengthening molecule
inhibitor of CRY degradation
Stabilization by KL001
PER
CRY
Circadian clock protein
CRY
CRY
Period-lengthening
FAD binding pocket
Dimerization
PER
FBXL3
F-box protein
CRY
FBXL3
Degradation
B
Relative mRNA expression
1,4
1,2
1,0
0,8
0,6
0,4
0,2
0,0
CRY1
CRY2
PER1
PER2
PER3
DMSO
KL001 (2,7uM)
KL001 (8uM)
C
Cry 1
Control
KL001 8uM
D
Intensity of CRY1
80000
60000
40000
20000
0
*
Control
KL001 8uM

Figure 3-6 Evaluation of CRY1 stabilization upon KL001 treatment in human HF organ culture.

(A) Schematic representation of KL001 mechanism of action: KL001 prevents CRY1 and 2 degradation and induces lengthening of the circadian rhythm (Oshima et al. 2015). (B) RT-qPCR: relative expression of *CRY1* and *2, PER 1,2* and *3* were measured in HFs at day 7 post treatment with 2µM and 8 µM KL001. *CRY1* and *CRY2* transcripts were reduced after treatment with 8 µM KL001 compared to the control group (DMSO); *Period* genes expression was downregulated with both concentrations of KL001 (n=2; mean ±SEM). Analysis was performed with Genex software (Bio-Rad) using ΔΔCt equitation method. (C-D) Prominent nuclear expression of CRY1 protein in the bulb region of the HF treated with 8 µM KL001, comparing to the control HF (n=12 from 3 donors, Student-t test, *p=0,03). Scale bar: 50 µm. Nuclear staining: DAPI (blue).

To determine if stabilization of CRY 1 can affect hair cycle progression, HFs were treated with KL001 8 µM every three days. The treatment was performed in the insulin depleted medium: insulin is an important growth factor that maintains HFs in anagen phase up to 10 days in culture (Philpott et al. 1994a). In control HF group, insulin deprivation resulted in the development of premature anagen-catagen transition: on day 4, 40% of the HFs entered catagen phase. In contrast, in KL001 treated group, the majority of the HFs (83%) remained in anagen-like phase ($p<0.05$, Fisher's exact test); this observation was confirmed in experiments from 4 different individuals (Figure 3-7 A). Assessment of proliferation and apoptosis was performed using immunofluorescence analysis: the number of proliferating Ki-67 positive cells was increased in KL001 treated HFs comparing to the control, nevertheless the difference was not statistically significant (Figure 3-7 B-C); no differences were observed in apoptosis, as the number of TUNEL positive cells was similar in KL001 treated and untreated HFs (Figure 3-7 B-C). RT-qPCR analysis revealed a significant downregulation of *CRY1, PER1,PER2* and *PER3* expression after KL001 treatment, suggesting that CRY1 is involved in anagen maintenance by exerting positive effect on cell proliferation and suppressing the expression of *PER1* that has been shown to promote pre-mature catagen development (Al-Nuaimi et al. 2014) (Figure 3-7D).

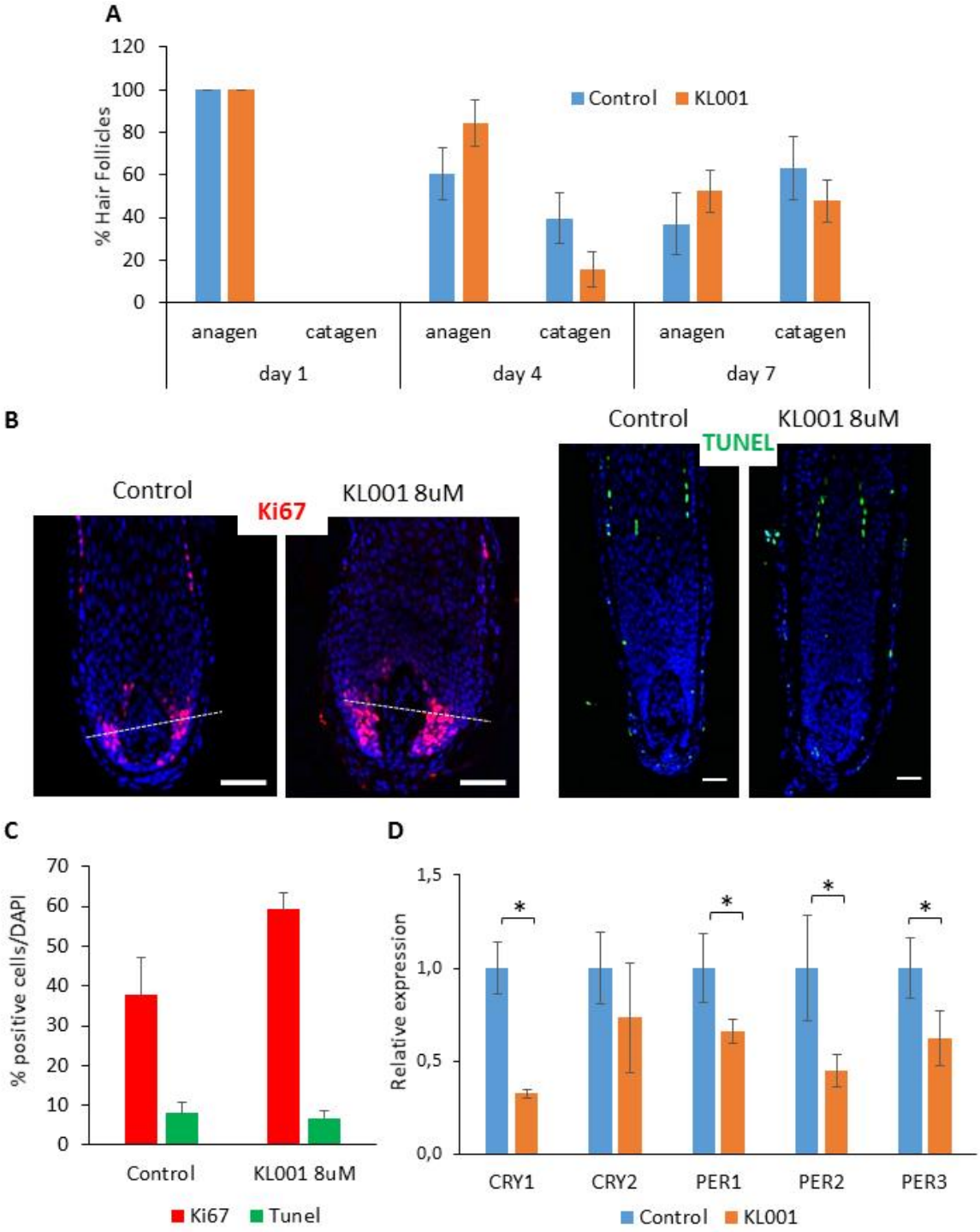
A
% Hair Follicles
120
100
80
60
40
20
0
Control
KL001
anagen
catagen
anagen
catagen
anagen
catagen
day 1
day 4
day 7
B
Control
Ki67
KL001 8uM
Control
TUNEL
KL001 8uM
C
% positive cells/DAPI
70
60
50
40
30
20
10
0
Control
KL001 8uM
Ki67
Tunel
D
Relative expression
1,5
1,0
0,5
0,0
*
*
*
*
CRY1
CRY2
PER1
PER2
PER3
Control
KL001

Figure 3-7 Effects of CRY1 stabilization by KL001 on hair growth *ex vivo*

(A) Effects of KL001, an activator of CRY1, on HF anagen-catagen transition *ex vivo* were analyzed by monitoring HF gross morphology. Day 4: 84% vs 60% of anagen HFs treated with KL001 and the control, respectively (p=0,016, Fisher's exact test). (B) Immunofluorescence: detection of proliferative Ki-67+ cells (red) in the hair matrix and apoptotic TUNEL+ cells (green). Scale bar 50 µm. Nuclear staining: DAPI (blue). (C) Quantitative analysis revealed the increased number of Ki-67+ cells in the HF treated with KL001, that however was not statistically significant (Mann-Whitney, p=0,11). No differences in the number of TUNEL+ cells. (D) RT-qPCR: down-regulation of *CRY1, PER1, PER 2 and PER3* transcripts was significant in KL001 treated HFs (n=3, 2 donors in triplicates, mean ±SD; One way ANOVA, *p<0.05).

To further confirm the positive effects of CRY1 on hair growth, CRY1 siRNA was used to knockdown CRY1 expression in HFs. The efficiency of silencing was evaluated 96 hours after HF transfection with CRY1 siRNA: more than 60% of *CRY1* transcript downregulation was achieved that was statistically significant (p=0,001, Student T-Test) (Figure 3-8 A). CRY1 protein down-regulation has also been confirmed by immunofluorescence (Figure 3-8 B). Intensity for CRY1 protein staining was substantially reduced in CRY1 siRNA transfected HFs (Figure 3-8 B). Effect of CRY1 siRNA on anagen - catagen transition was evaluated by morphological analysis and assessment of proliferation and apoptosis. At day 4, almost 50% of the HFs in the *CRY1* silenced group entered catagen, while 80% of the HFs in control group were still in anagen (Figure 3-8C), which was statistically significant (p=0.002, Fisher's exact test). Assessment of proliferation by quantitative analysis of Ki-67 revealed a significant (p=0.028, Mann-Whitney) decrease in the number of proliferating cells in the hair matrix and ORS of *CRY1* silenced HFs compared to the control group (Figure 3-8 D): 75% of Ki-67+ cells were detected in the hair matrix of control group, while only 46% of Ki-67+ cells was seen in the hair matrix in the HF transfected with siCRY1 (Figure 3-8D). Similar to the KL001 treatment, no differences were observed in the number of apoptotic TUNEL+ cells between siCRY1 treated and control HFs (Figure 3-8 D).

Altogether, these results suggest CRY1 has a positive impact on hair growth by sustaining proliferation in anagen phase and protecting HF from pre-mature entrance into catagen phase.

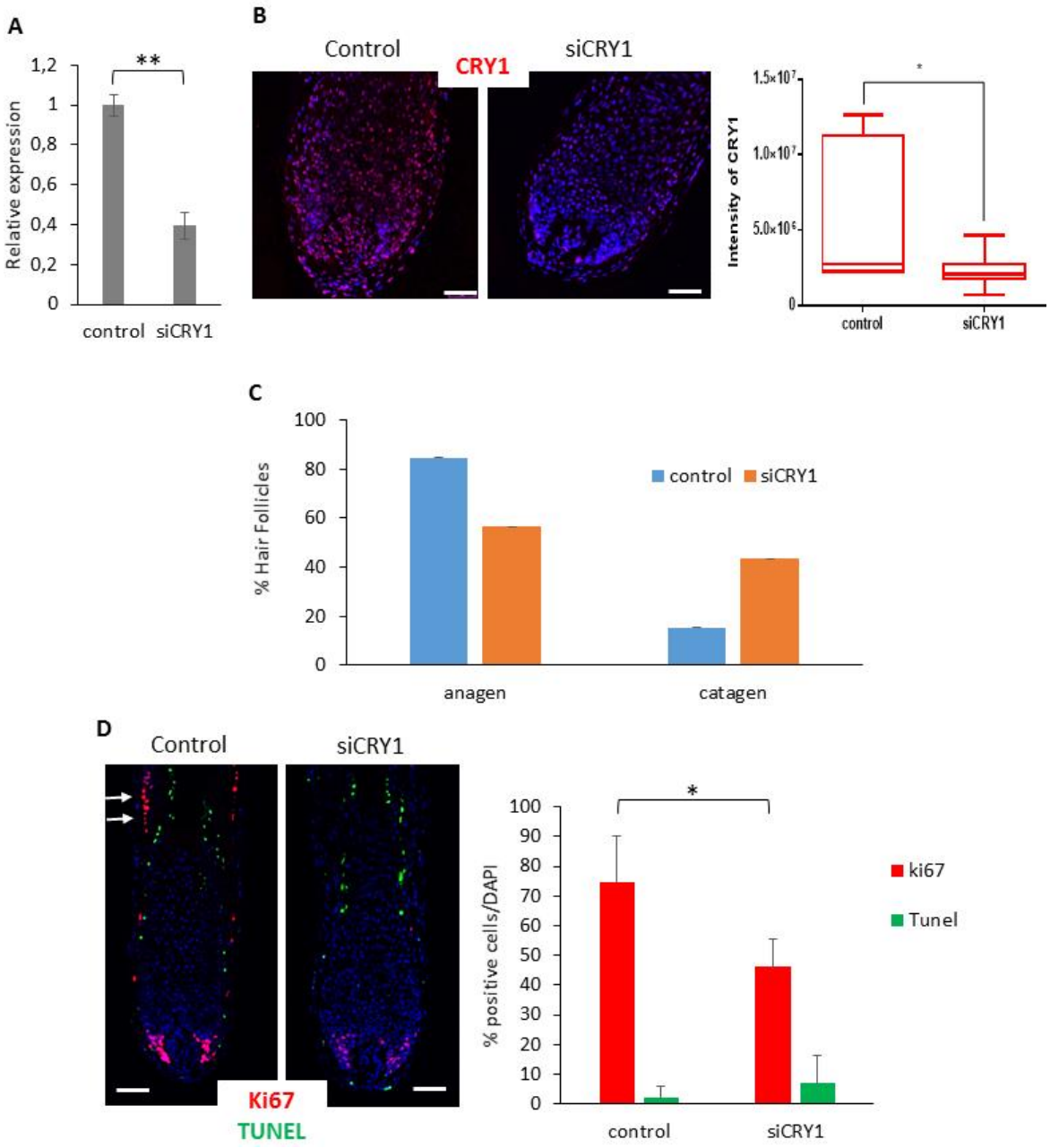
A
Relative expression
1,2
1
0,8
0,6
0,4
0,2
0
**
control
siCRY1
B
Control
CRY1
siCRY1
Intensity of CRY1
1.5×10⁷
1.0×10⁷
5.0×10⁶
0
*
control
siCRY1
C
% Hair Follicles
100
80
60
40
20
0
control
siCRY1
anagen
catagen
D
Control
siCRY1
Ki67
TUNEL
% positive cells/DAPI
100
90
80
70
60
50
40
30
20
10
0
*
control
siCRY1
ki67
Tunel

Figure 3-8 Effects of CRY1 silencing on hair growth *ex vivo*

Silencing efficacy was evaluated 96 hours after transfection with CRY1 siRNA (siCRY1) compared to scrambled control: (A) almost 100% downregulation of *CRY1* transcript was detected in HFs after Cry1 siRNA transfection (n=9 from 3 donors, mean ±SD;** p=0,001, Student T-Test). (B) Immunofluorescence analysis of CRY1 expression in HFs collected at day 4: statistically significant decrease in CRY1 protein expression (red) in siCRY1 transfected HFs compared to the scrambled control (n=9 from 3 donors; Mann-Whitney, *p=0.0185). (C) In siCRY1 group 43% of HFs entered catagen, while 85% HFs remained in anagen in the control (3 donors, mean ±SEM; p=0.002, Fisher's exact test). (D) In control HFs, numerous proliferating Ki-67+ cells (red) were detected in the hair matrix and in the ORS (arrows); a significant decrease in the number of proliferative Ki-67+ cells (red) was caused by CRY1 silencing (n=4, 2 donors; mean ±SEM; Mann-Whitney ,*p=0.028). Difference in TUNEL+ cells (green) was not significant between experimental and control groups. Scale bar 50 µm. Nuclear staining: DAPI (blue).

3.4 Molecular mechanism of action for CRY1 on cell proliferation

To further evaluate the effects of CRY1 on HF keratinocyte proliferation, primary synchronized ORS cells were transfected with CRY1 siRNA followed by analysis of proliferation using 5-ethynyl-2′-deoxyuridine (EdU) assay that is based on incorporation of EdU into newly synthesized DNA of replicating cells.

Macroscopic analysis of cell morphology did not reveal any difference between the cells transfected with either siCRY1 or scrambled RNA for 24 hours (Figure 3-9 A). Silencing efficiency was confirmed by RT-qPCR: a dramatic decrease in *CRY1* transcript levels (82%) was detected in siCRY1 transfected cells versus the control that was statistically significant (p=0,002), while the expression of *CRY2* was not affected by CRY1 silencing (Figure 3-9C). PER1, a clock gene with similar functions in circadian regulation, was also not affected at transcript levels by siCRY1.

Inhibition of CRY1 in the ORS cells resulted in the significant (p=0,01) decline in the number of EdU+ cells compared to the corresponding control (Figure 3-9 D). Therefore, similar to the HF *ex vivo* experiments, CRY1 silencing negatively affects proliferation in primary ORS. Thus, CRY1 is required for sustaining of keratinocyte proliferation in the HF.

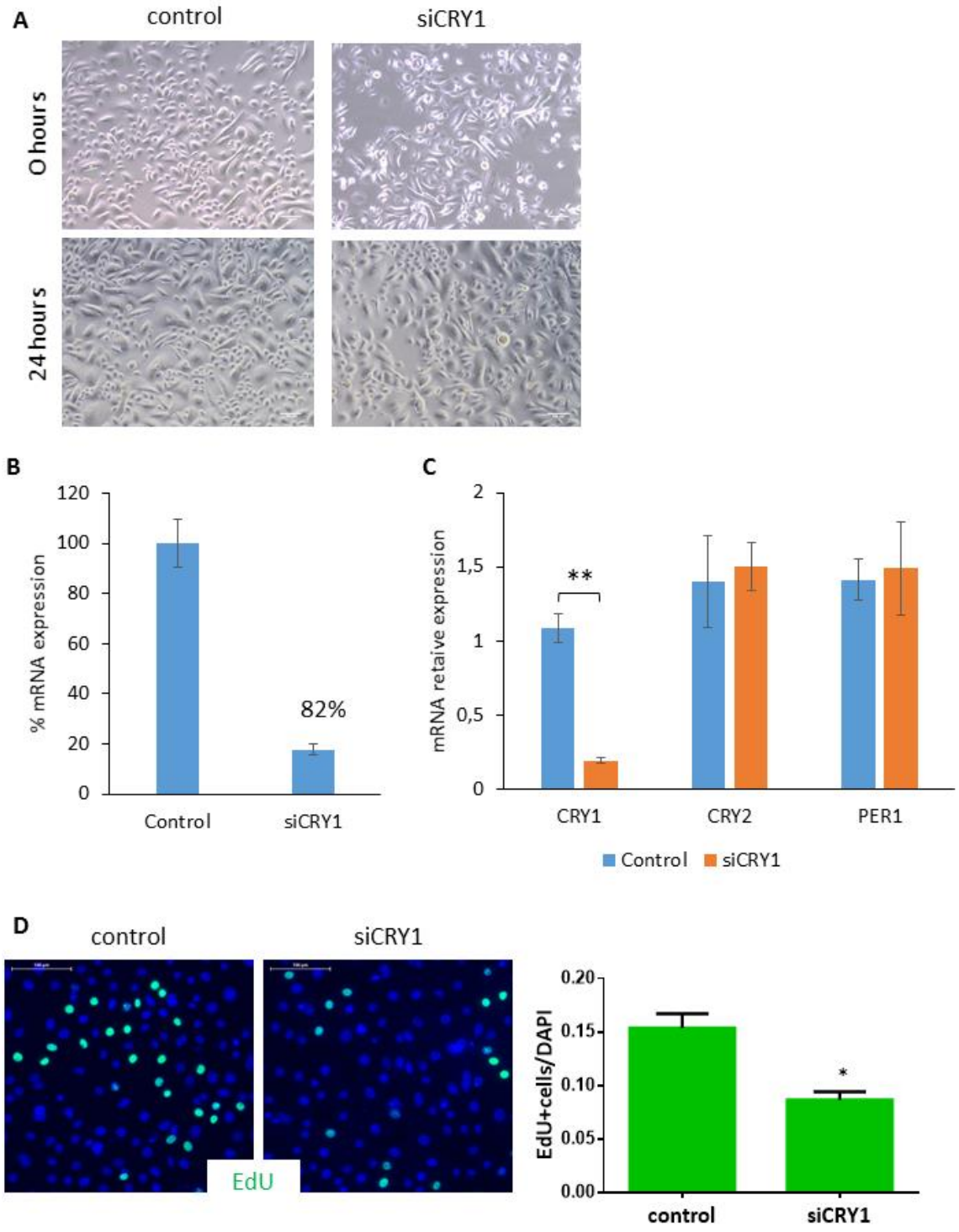
A
control
siCRY1
0 hours
24 hours
B
% mRNA expression
120
100
80
60
40
20
0
82%
Control
siCRY1
C
mRNA retaive expression
2
1,5
1
0,5
0
**
CRY1
CRY2
PER1
Control
siCRY1
D
control
siCRY1
EdU
EdU+cells/DAPI
0.20
0.15
0.10
0.05
0.00
*
control
siCRY1

Figure 3-9 CRY1 silencing inhibits proliferation of outer root sheath cells *in vitro*

(A) No morphological changes were observed in the ORS cells after 48 h of *CRY1* silencing (siCRY1). (B) RT-qPCR: dramatic decrease in CRY1 expression (82%) in the ORS cells due to CRY1 siRNA transfection (n=6 from 2 donors, mean ±SD). (C) *CRY2* and *PER1* transcripts were not affected by *CRY1* silencing (n=3, 2 donors in triplicates, mean ± SD; **p=0,002, Mann-Whitney). (D) Representative image of EdU assay: the number of proliferating ORS cells, assessed with EdU staining (green) significantly decreased 48 after silencing of *CRY1* (n=10,3 donors, 10 replicates, mean ±SEM, * p= 0.01, Student's t-test). Scale bar 100 µm. Nuclear staining: DAPI (blue).

To identify the possible downstream targets of CRY1, the transcriptomic profiling of the ORS cells transfected with CRY1 vs control cells was performed. Microarray analysis has identified significant changes in the expression of genes that are involved in the control of cell proliferation (Figure 3-10 A), including Pleckstrin 2 (PLEK2), cyclin-dependent kinase 6 (CDK6), proteasome 26S subunit non-ATPase 2 (PSMD2), transmembrane BAX inhibitor motif containing 6 (TMBIM6), KDEL Endoplasmic Reticulum Protein Retention Receptor 1 (KDELR1). The validation of microarray by RT-qPCR in 2 individuals confirmed the significant downregulation of *CDK6* (p=0,0009)*, PSMD2* (p=0,05)*, TMBIM 6* (p=0,05)*, PLEK2* (p=0,0009) and *KLER2* (p=0,05) expression in the ORS cells due to silencing of CRY 1 (Figure 3-10 B). Because CDK6 is a key protein involved in the G1 to S-phase transition, its protein expression was further evaluated in the ORS *in vitro*, using immunofluorescence approach. Nuclear staining intensity of CDK6 was measured in each cell and revealed that CRY1 silencing caused significant ($p<0.05$) 56% downregulation of CDK6 in ORS cells compared to the control (Figure 3-10 C). Notably, the cells expressing CDK6 were EdU negative: this is consistent with the fact that EdU binds to actively synthesized DNA (S phase), while CDK6 kinase catalyze G1 phase progression (Figure 3-10 C).

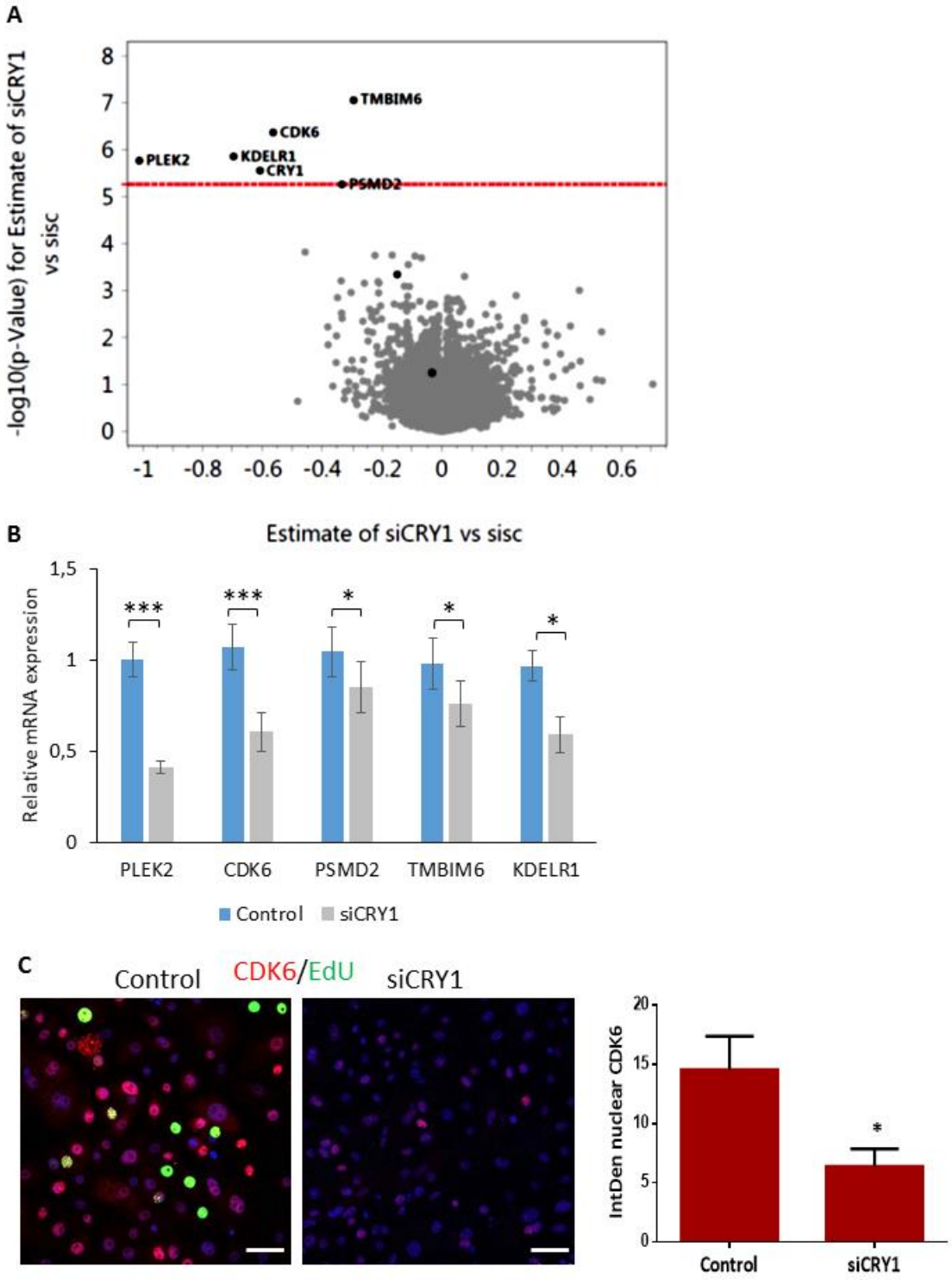
A
-log10(p-Value) for Estimate of siCRY1 vs sisc
TMBIM6
CDK6
PLEK2
KDELR1
CRY1
PSMD2
B
Estimate of siCRY1 vs sisc
Relative mRNA expression
PLEK2
CDK6
PSMD2
TMBIM6
KDELR1
Control
siCRY1
C
Control
CDK6/EdU
siCRY1
IntDen nuclear CDK6
Control
siCRY1

Figure 3-10 Gene expression profiling in ORS keratinocytes transfected with siCRY1 identified CDK6 as a downstream target controlling keratinocytes proliferation.

(A) Dot plot of differential gene expression between siCRY1 and control groups based on fold-change; the red line demarcates the threshold level of significance of the adjusted p-value (p<0,05): *PLEK2, CDK6, PSMD2, TMBIM6, KDELR1* are significantly downregulated, as emerged by microarray analysis . Experiment was performed in triplicates. (B) Validation of microarray by RT-qPCR (n=6 from 2 donors; mean ±SD; *** p=0.0009, *p=0.05, one way ANOVA). (C) Immunofluorescence: decreased CDK6 expression and number of EdU+ cells after CRY1 silencing; nuclear staining intensity of CDK6 was measured with ImageJ software (n=3, 2 donors in triplicates; mean ±SD; *p<0.05, Student's t-test). Scale bar 50µm. Nuclear staining: DAPI (blue).

To investigate if CDK6 is also regulated by CRY1 in HFs, CDK6 expression was examined in HFs either transfected with CRY1 siRNA or treated with CRY1 stabilizer KL001.

In total human skin, CDK6 expression was found to be restricted to the IRS of anagen terminal HFs (Figure 3-11 B). No CDK6 positive cells were observed in the epidermis or dermis of human skin (Figure 3-11 A). Similar pattern of CDK6 expression was seen in the control HF grown *ex vivo*. However, less prominent expression of CDK6 was seen in the proximal IRS of the HF transfected with CRY1 siRNA (Figure 3-11 C). In contrast, significant upregulation in the expression of CDK6 was detected in the HFs treated with KL001 compared to the control (Figure 3-11 D).

These data provide additional evidence that CRY1 is involved in regulation of HF proliferation that is likely mediated by CDK6.

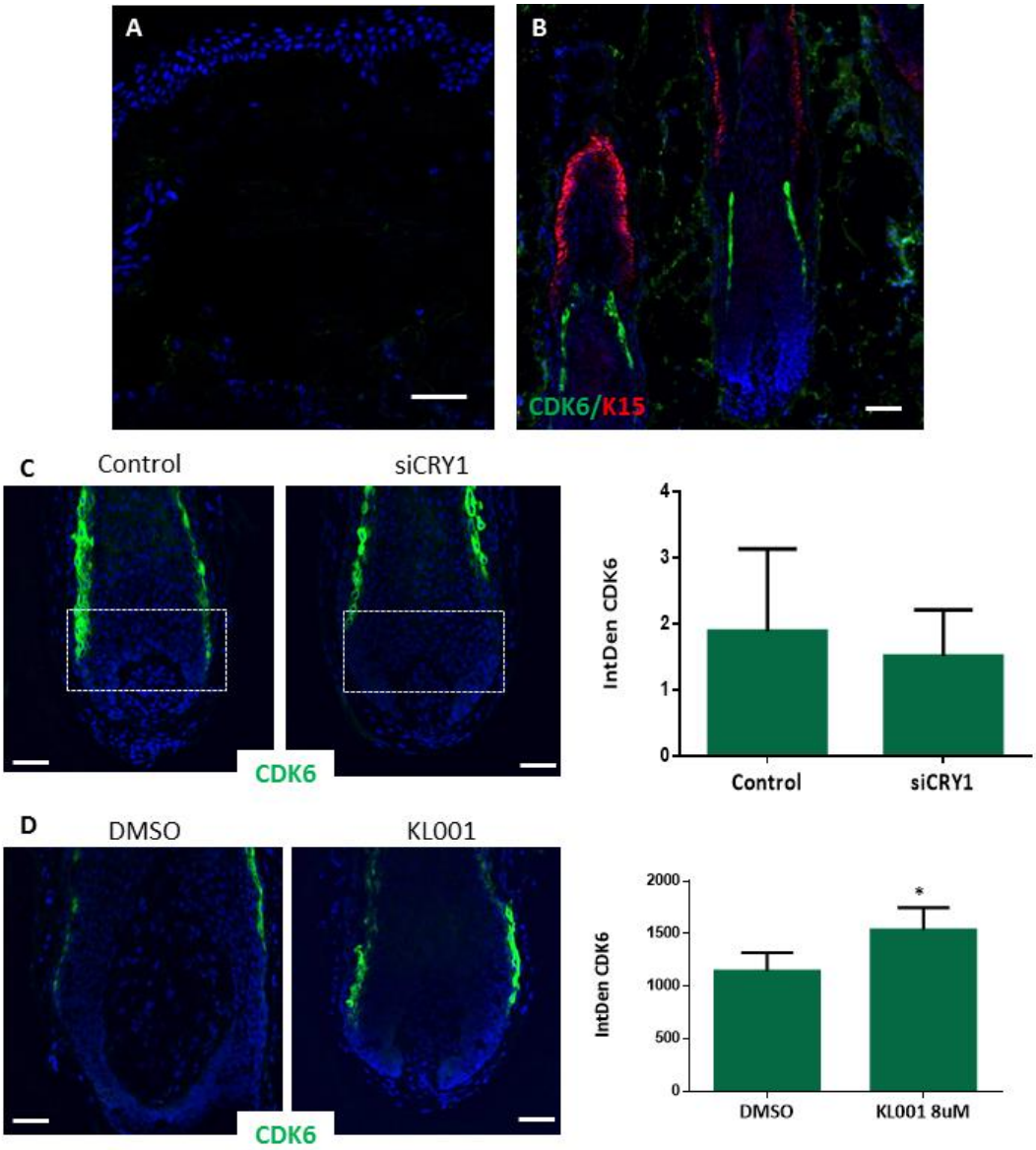

Figure 3-11 CDK6 is a putative mediator of CRY1 activity on cell proliferation in the hair follicle.

(A) Lack of CDK6 expression in the epidermis and dermis of hairless skin (B) CDK6 (green) is localized in the IRS of terminal anagen HF. Double immunostaining with K15 (red) confirmed absence of CDK6 (green) in the ORS. (C) CRY1 silencing results in the reduction of CDK6 expression in lower IRS (not significant). (D) KL001 treatment significantly increases CDK6 staining intensity in cultured HFs, compared to control (n=6, from 2 donors; mean ±SD; *p=0.03, Student's t-test). Scale bar 50 µm. Nuclear staining: DAPI (blue)

3.5 Opsins and hair growth

As it was shown above OPN2 and OPN3 expression was detected in the different compartments of the HF: OPN2 was detected in the ORS (Figure 3-3), while OPN3 was expressed in the IRS and lateral hair matrix (Figure 3-4). Because expression of OPN3 was detected in the keratinocytes of the IRS that do not undergo proliferation, the effect of OPN3 silencing was evaluated in highly proliferative cultured ORS cells. Both OPN2 and OPN3 are expressed in the primary ORS keratinocytes *in vitro,* as confirmed by RT-PCR and qPCR in three female donors of different age (Figure 3-12 A). The protein expression of OPN2 and OPN3 in the ORS cells was seen in their cytoplasm as was confirmed by immunofluorescence analysis (Figure 3-12 B).

OPN3 silencing was performed to investigate the effects of this photoreceptor on HF keratinocyte proliferation. Forty-eight hours after silencing of OPN3 no gross changes in cell morphology were detected at wide field microscope (Figure 3-12 C). Efficiency of OPN3 silencing was confirmed by real-time PCR analysis: over 80% decline in *OPN3* transcript level was observed in siRNA OPN3 treated cells comparing to the control (Figure 3-12 D). Effects on proliferation was evaluated employing the EdU assay 48h after siOPN3 transfection: significant ($p<0.0001$) decrease in the number of EdU+ cells was observed after OPN3 silencing, compared to the scrambled control (Figure 3-12 E).

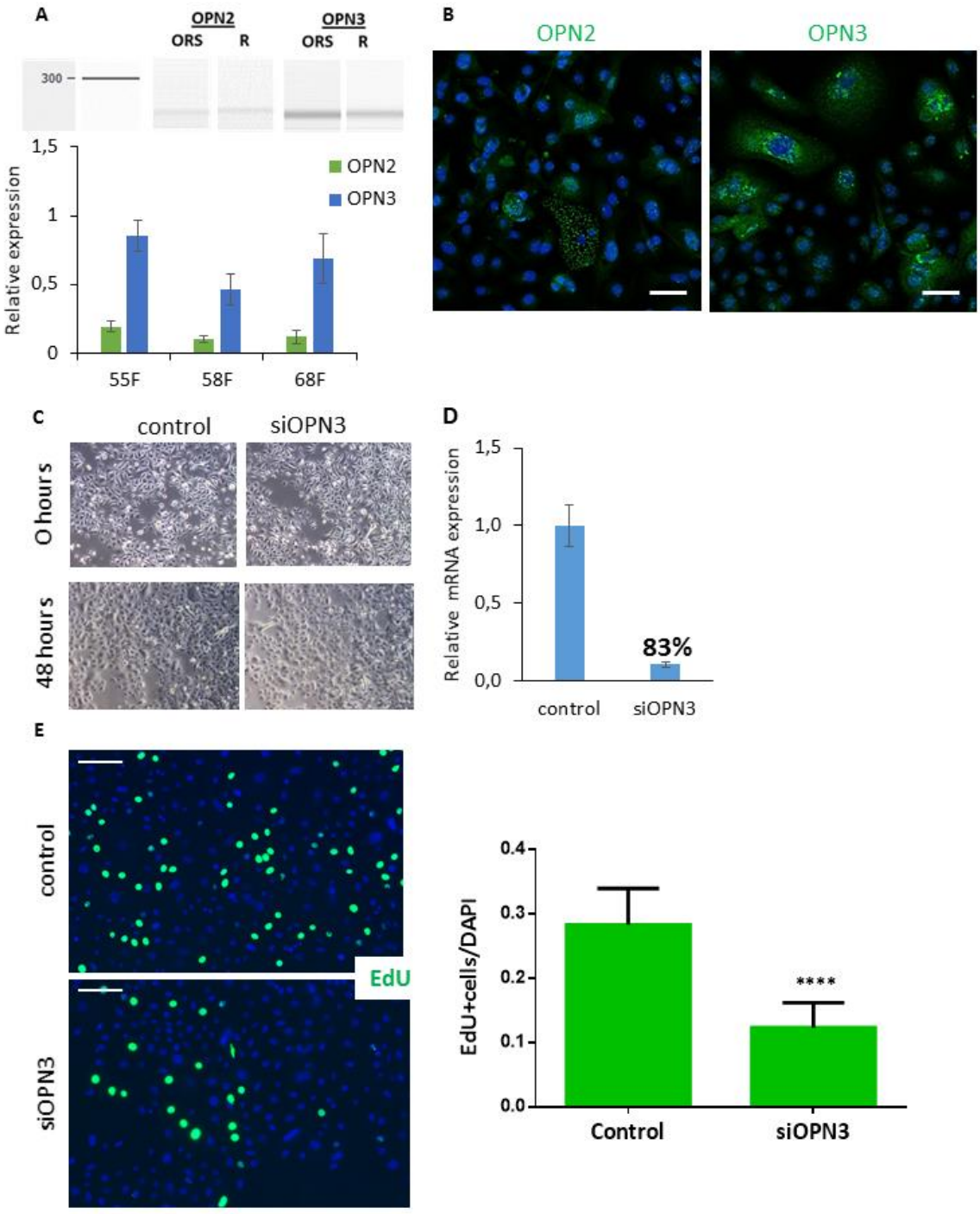
A
OPN2
ORS R
OPN3
ORS R
300
1,5
1
0,5
0
Relative expression
OPN2
OPN3
55F
58F
68F
B
OPN2
OPN3
C
control
siOPN3
O hours
48 hours
D
Relative mRNA expression
1,5
1,0
0,5
0,0
83%
control
siOPN3
E
control
siOPN3
EdU
EdU+cells/DAPI
0.4
0.3
0.2
0.1
0.0
****
Control
siOPN3

Figure 3-12 Effects of OPN3 on the outer root sheath cells *in vitro*.

(A) RT-PCR: OPN2 and OPN3 transcripts were detected in the ORS keratinocytes *in vitro*; qPCR confirmed expression of both OPN2 and OPN3 in primary ORS keratinocytes from 3 female donors of different age (age and sex below bars cluster; mean±SD of triplicates) (B) Immunofluorescence: OPN2 and OPN3 protein expression was detected in the cytoplasm of the primary ORS cells. Scale bar 50 µm. Nuclear staining: DAPI (blue). (C) No morphological changes were observed in the ORS cells after 48 hours of OPN3 silencing (siOPN3). (D) RT-qPCR: dramatic decrease in *OPN3* expression (83%) in the ORS cells due to OPN3 siRNA transfection (n=3, triplicates; mean ±SD). (E) Representative image of EdU assay: the number of proliferating ORS cells is significantly decrease 48 after silencing of OPN3 (n=10, 2 donors, 10 replicates; mean ±SD; **** $p<0.0001$; Student's t-test). Scale bar 100 µm. Nuclear staining: DAPI (blue).

Microarray analysis of the global gene expression in the ORS keratinocytes treated with OPN3 siRNA or corresponding control revealed the significantly (adjusted p-value <0,05) altered expression of 41 genes: 37 were downregulated, while only 4 were upregulated due to OPN3 knockdown (Table 6). Microarray validation by qPCR confirmed that the expression of UL16 binding protein 1 (ULBP1), p21 protein (Cdc42/Rac)-activated kinase (PAK2), follistatin-like 1 (FSTL1) and ubiquitin protein ligase E3 component N-recognin 5 (UBR5) was downregulated in the ORS cells after OPN3 silencing (Figure 3-13). In contrast, the expression of sideroflexin 1 (SFNX1), caveolin 2 (CAV2) and biogenesis of lysosomal organelles complex 1 subunit 2 (BLOC1S2) was increased due to OPN3 silencing in the ORS cells (Figure 3-13).

Taken together, these data demonstrate that OPN3 downregulation reduces proliferation in ORS *in vitro* and impact the expression of genes that are involved in the control of proliferation and apoptosis.

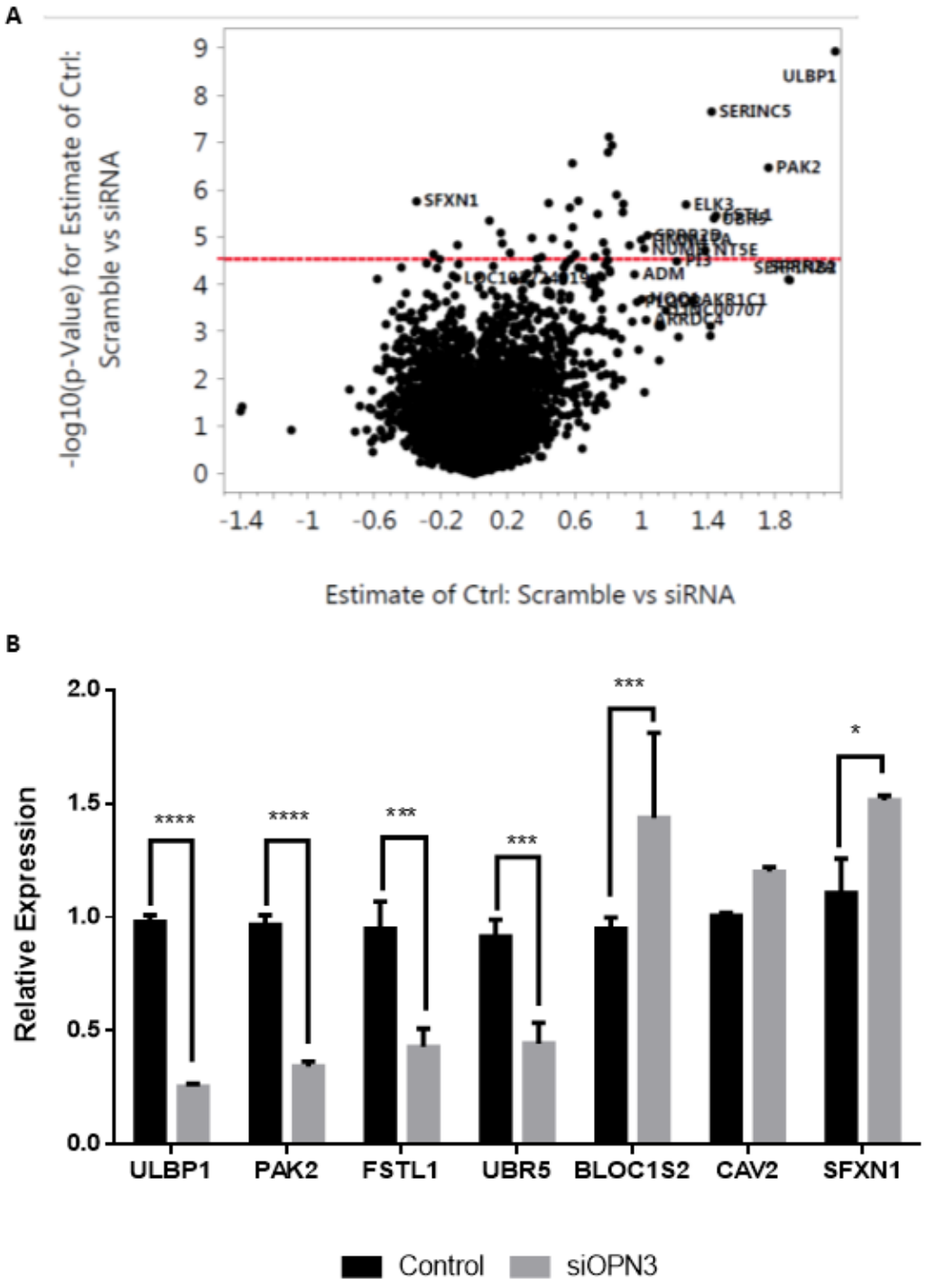
A
-log10(p-Value) for Estimate of Ctrl: Scramble vs siRNA
Estimate of Ctrl: Scramble vs siRNA
ULBP1
SERINC5
PAK2
SFXN1
ELK3
ADM
B
Relative Expression
ULBP1
PAK2
FSTL1
UBR5
BLOC1S2
CAV2
SFXN1
Control
siOPN3

Figure 3-13 Effects of OPN3 on the gene expression in outer root sheath cells in vitro.

(A) Microarray: dot plot of the changes in gene expression in primary ORS cells after silencing of OPN3, the cut-off line of significant p-value ($p<0,05$) is highlighted in red. Experiment performed in triplicates; (B) Validation of microarray by RT-qPCR: knock-down of OPN3 induced downregulation of *ULBP1, PAK 2, FSTL1, UBR5*, and upregulation of *BLOC1S2, CAV2, SFXN1* expression (n=3; mean ± SD; ****$p< 0,0001$, ***$p<0,001$, *$p<0,05$ two-way ANOVA).

Table 6 List of significantly differentially expressed genes in the outer root sheath cells transfected with OPN3 siRNA

GeneSymbol	Full gene name	Fold change: Scrambled vs OPN3 siRNA		Adjusted p-Value:
ULBP1	UL16 binding protein 1	-	4,481	0,000
PAK2	p21 protein (Cdc42/Rac)-activated kinase	-	3,395	0,004
FSTL1	follistatin-like 1	-	2,730	0,014
UBR5	ubiquitin protein ligase E3 component n-Recognin 5	-	2,707	0,015
SERINC5	serine incorporator 5	-	2,681	0,001
NT5E	5'-nucleotidase, ecto (CD73)	-	2,612	0,040
ELK3	ELK3, ETS-domain protein (SRF accessory protein 2)	-	2,410	0,011
SPRR2D	small proline-rich protein 2D	-	2,054	0,028
NUMB	numb homolog (Drosophila)	-	2,025	0,037
TIMM17A	translocase of inner mitochondrial member	-	2,001	0,030
GPRC5A	G protein-coupled receptor, class C, Group 5 Member A	-	1,906	0,033
VAMP3	vesicle-associated membrane protein 3	-	1,857	0,011
NCKAP1	NCK-associated protein 1	-	1,854	0,013
RCC2	regulator of chromosome condensation 2	-	1,806	0,010
F11R	F11 receptor	-	1,772	0,002
MSN	moesin	-	1,751	0,002
GRB2	growth factor receptor-bound protein 2	-	1,744	0,003
H1F0	H1 histone family, member 0	-	1,731	0,041
SCRN1	secernin 1	-	1,709	0,032
ARF4	ADP-ribosylation factor 4	-	1,670	0,013
ZMYND11	zinc finger, MYND-type containing 11	-	1,650	0,047
MINK1	misshapen-like kinase 1	-	1,541	0,011
SLC39A9	solute carrier family 39, member 9	-	1,523	0,043
TMEM38B	transmembrane protein 38B	-	1,505	0,020
ZDHHC5	zinc finger, DHHC-type containing 5	-	1,503	0,004
MAPRE1	microtubule associated protein rp/eb family member 1	-	1,491	0,050
DSC2	desmocollin 2	-	1,487	0,012
CERS2	ceramide synthase 2	-	1,478	0,033
FLNB	filamin B, beta	-	1,383	0,030

CAST	calpastatin	-	1,362	0,011
CORO1C	coronin, actin binding protein, 1C	-	1,323	0,047
SNX30	sorting nexin family member 30	-	1,298	0,050
PRMT8	protein arginine methyltransferase 8	-	1,270	0,030
ENC1	ectodermal-neural cortex 1	-	1,161	0,042
MITF	microphthalmia-associated transcription	-	1,123	0,032
RNLS	renalase, FAD-dependent amine oxidase	-	1,117	0,026
MIR543	microRNA 543	-	1,065	0,016
RFX2	regulatory factor X, 2	+	0,933	0,033
BLOC1S2	biogenesis of lysosomal organelles complex 1 subunit 2	+	0,867	0,050
CAV2	caveolin 2	+	0,844	0,043
SFXN1	sideroflexin 1	+	0,787	0,011

3.6 Blue light prolongs anagen phase in hair follicle *ex vivo*

As Cryptochromes and Opsins have absorption bands in the blue-to-green region (Koyanagi et al. 2013; Sancar 2000; Sugihara et al. 2016) the impact of 453 nm wavelength light on hair growth was tested by performing daily irradiation of HFs *ex vivo* during 10 consecutive days.

It has recently been demonstrated that low radiant exposure, 2 J/cm^2 of blue 450 nm light exerts stimulatory effect on reticular and papillary dermal fibroblasts (Mignon et al. 2016b). Therefore, irradiance and radiant exposure were set to low levels (16 mW/cm^2 irradiance, 200 sec illumination duration, 3.2 J/cm^2 radiant exposures) to assure initiation of purely photobiological effects and to avoid any photothermal reactions. The impact of low levels of red light (689 nm, 16 mW/cm^2 and 3.2 J/cm^2) has also been evaluated. While this frequency mostly lies outside of the absorption band of discovered Opsins, it was included in the experiments as red wavelength at low radiant exposure is most often used in *in vitro* and animal experiments and in the devices for *in vivo* hair growth stimulation (Lanzafame et al. 2013; Lanzafame et al. 2014).

HFs were divided into three groups: a control group was kept in the dark, while treated groups were exposed daily to 3.2 J/cm^2 of either 689 nm or 453 nm light during 10 days. Culture medium was refreshed every other day after light irradiation to prevent accumulation of ROS species that can have toxic effects on HF. HF gross morphology was monitored daily, using a wide-field microscope to distinguish anagen and catagen phases (Figure 3-14 A). An interval regression with random intercept model was applied to analyze anagen to catagen transition, where mean survival time of a HF in culture (anagen

maintenance) was selected as a measure. Effects of medium, donor and light treatments on mean survival time from 7 independent experiments are shown in Figure 3-14 B. HF growth in the media without insulin was used as a positive control for this study. Insulin depletion caused significant premature catagen development (p=0) that is consistent with previously published data (Philpott et al. 1994b). A donor effect was also statistically significant (p=0.012). This has confirmed the applicability and quality of the statistical model. A radiant exposure of 3.2 J/cm2 of blue light has little impact increasing mean survival time of HF *ex vivo*, improving anagen maintenance (pairwise comparison control versus blue light significant at 10% level, p=0.066) (Figure 3-14 B). In contrast, HF treatment with 3.2 J/cm^2 of 689 nm light (red light) did not affect hair growth compared to the untreated control (pairwise comparison control versus red light, p=0.7) (Figure 3-14 B). Positive effects of blue light on hair growth was further confirmed by the assessment of proliferation in HFs: the number of proliferative Ki-67+ cells was significantly increased at day 2 post treatment with low level of blue light compared to the control (p=0.04) (Figure 3-14 C).

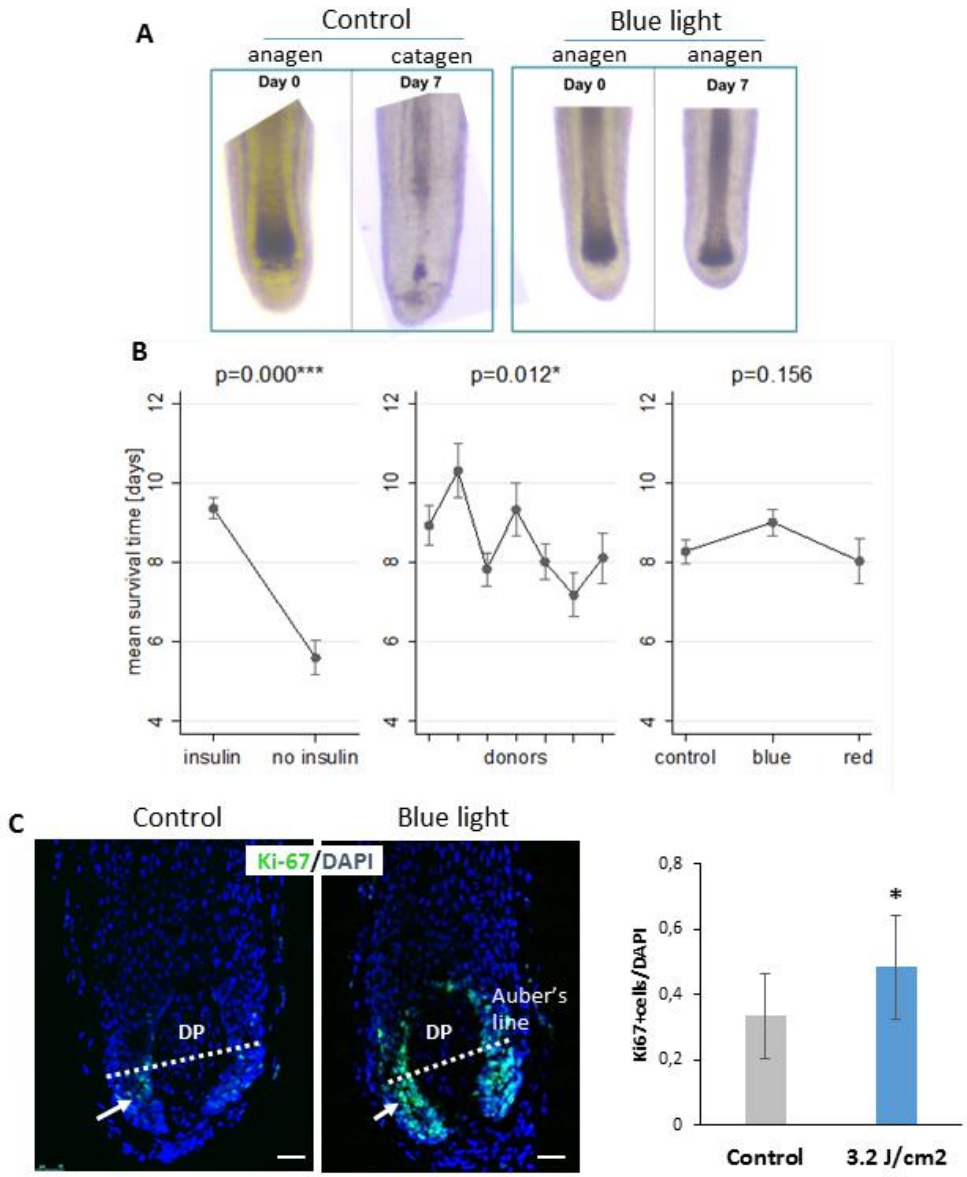
A
Control
Blue light
anagen
catagen
anagen
anagen
Day 0
Day 7
Day 0
Day 7
B
p=0.000***
p=0.012*
p=0.156
mean survival time [days]
4
6
8
10
12
insulin
no insulin
donors
control
blue
red
C
Control
Blue light
Ki-67/DAPI
DP
DP
Auber's line
Ki67+cells/DAPI
0
0,2
0,4
0,6
0,8
*
Control
3.2 J/cm2

Figure 3-14 Effects of 3.2 J/cm2 of blue light with 453 nm central wavelength on hair follicle growth *ex vivo*

(A) Representative microphotographs of anagen and catagen HFs at day 0 and day 7 of the experiment. (B) Effects of medium conditions (with insulin versus no insulin), donors and light treatment (blue and red light) on anagen to catagen transition expressed as mean survival time with 95% confidence intervals: insulin depletion caused premature catagen development as expected; donor effect was statistically significant (p=0.012), low levels of blue light increased mean survival time, improving anagen maintenance (pairwise comparison control vs blue light, significant at 10% level, mean ±SE, p=0.066); red light effect was not statistically significant (p=0.7). (C) Immunofluorescence: detection of proliferative Ki-67+ cells (green) in the hair matrix. Scale bar 50 µm. Nuclear staining: DAPI (blue); quantitative analysis revealed the statistically increased number of Ki-67+ cells in the HF treated with blue light (n=8 from 2 donors; mean ±SD; p=0.04, Student’s t-test).

3.7 Opsin 3 silencing abrogates positive impact of low levels of blue light on keratinocytes proliferation

The stimulatory effect of low levels of blue light was further assessed in primary ORS keratinocytes. 3,2 J/cm^2 of radiant exposure of blue light was tested. Stimulation of metabolic activity was assessed with Alamar assay after a single treatment with blue light that was significant compared with control group ($p<0,05$) (Figure 3-15 A). To confirm that an improvement in metabolic activity was correlated with an increase in cell proliferation EdU incorporation assay was performed: significant ($p<0.01$) increase in proliferation rate was detected in ORS cells 8 hours after treatment with 3.2 J/cm^2 of 450 nm light, compared to the control cells (Figure 3-15 B).

Evaluation of OPN3 silencing effects after irradiation with 3.2 J/cm^2 of blue light was assessed to investigate if OPN3 may mediate blue light stimulatory effect. Silencing of OPN3 abrogated the positive effect of blue light (3.2 J/cm2, 453 nm) on proliferation in the ORS cells (Figure 3-15 C). Significant inhibition ($p<0.0001$) in proliferation rate was observed in the ORS cells treated with blue light and transfected with OPN3 siRNA compared to the cells treated with blue light and transfected with control (scrambled) siRNA (Figure 3-15 C).

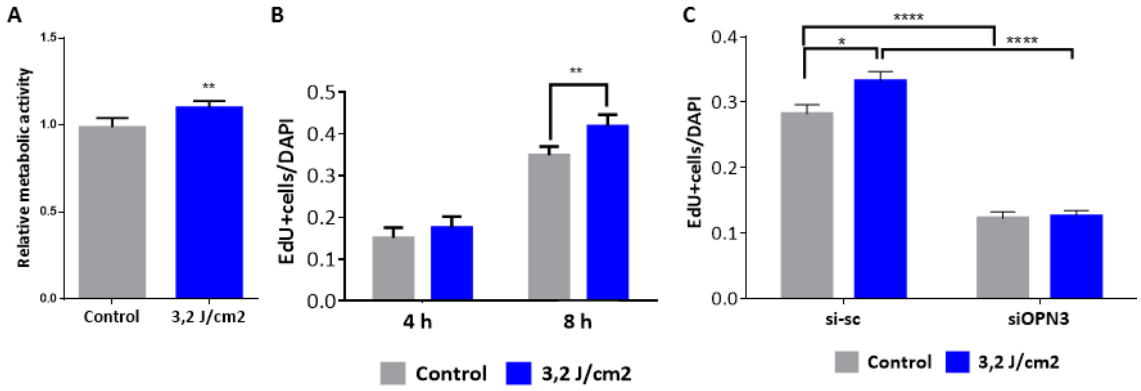

Figure 3-15 OPN3 silencing abrogates blue light stimulatory effect in primary outer root sheath keratinocytes.

(A) Alamar assay: increase in metabolic activity in the ORS keratinocytes *in vitro* after 3.2 J/cm^2 of blue light (Student T-test, p=0,0027, n=10; mean ± SEM). (B) EdU assay: the number of proliferating ORS cells is significantly increased 8 hours after blue light irradiation (n=10, 4 donors, 10 replicates; mean ± SEM, p<0.01, one-way ANOVA). C) Silencing of OPN3 in the ORS cells by siRNA significantly decreases proliferation rate compared to the control (scrambled) RNA and significantly represses proliferation induced by 3.2 J/cm^2 of blue light (n=15, 2 donors, 15 replicates; mean ± SEM; *p<0,05 , ****p<0,0001, two-way ANOVA test). Abbreviations: siSc - siRNA scrambled (negative RNA control); siOPN3 - siRNA against OPN3.

4 Discussion

4.1 Cryptochrome and Opsin receptors are expressed in human skin and anagen hair follicles

Over the last decades, PBM has been suggested as an alternative approach for hair loss treatment to drugs. Several clinical studies reported encouraging results demonstrating the increase in hair density and thickness in response to red and near infrared light-based therapy (Avci et al. 2014). However, the exact molecular mechanism underlying light-mediated hair regrowth remains largely unknown (Jimenez et al. 2014; Leavitt et al. 2009). The effect of PBM is triggered by the interaction of low levels of light with endogenous chromophores and photoreceptors in the skin (Mignon et al. 2016a; Vladimirov Iu et al. 2004). There is a rich spectrum of molecules absorbing optical radiation over the whole visible and near-infrared range (Mignon et al. 2016a; Vladimirov Iu et al. 2004). The effects of blue light could be mediated by photolytic generation of NO from nitrozated proteins (Liebmann et al. 2010; Oplander et al. 2013), radical oxygen species (ROS) formation as a result of enzymatic reactions of e.g. NADPH oxidase (Khan and Arany 2015), and COX (Karu 2014). Alternatively, it could be mediated by photoactive pigments or chromophores (including the flavin and retinal) bound to CRY (Hoang et al. 2008) and Opsin family members respectively (Kim et al. 2013b; Wicks et al. 2011), or intracellular calcium and light-gated ion channels (Wang et al. 2016). Light interaction with all these potential molecular targets could lead to multiple downstream reactions, such as changes in pH, [Ca2+], cAMP, ATP, NO (Mignon et al. 2016a; Wang et al. 2016).

In this study, we showed for the first time that CRY1 and 2, OPN2 and OPN3, the photoreceptors absorbing light in the visible blue-green wavelength range, are expressed in human skin, epithelial and mesenchymal components, and in the distinct compartments of the anagen HFs. Our data are in consistence with the study of Denda et al who demonstrated the expression of OPN2 in the human epidermal keratinocytes (Tsutsumi et al. 2009). In addition, we observed specific OPN2 expression in the basal layer keratinocytes expressing Keratin 14 (Figure 3-3 B). The Oancea group characterized the expression of OPN 1 short wavelength, OPN 2, 3 and 5 in human keratinocytes and melanocytes (Haltaufderhyde et al. 2015): we confirmed expression of OPN2 and OPN3 in epidermal keratinocytes (Figure 3-3 and Figure 3-4 respectively) and also in primary ORS cells (Figure 3-12). Intriguingly, the expression of both OPN2 and OPN3 was detected also in the HF stem cells (Figure 3-3 F-G, Figure 3-5). These findings suggest that the activity of HF and HF stem cells might be modulated by blue-green visible light.

Wavelength falling within the absorption band of discovered Opsins, could trigger G protein-related pathways or more complex reaction cascades, involving additional chromophores or photoreceptors, for example, cytochrome *c* oxidase, nitrosated proteins, and others (Wang et al. 2016). A similar hypothesis was investigated in human orbital fat stem cells: here green-light-induced directional migration, mediated by ERK signaling pathway, was also activated by overexpression of OPN3 (Ong et al. 2013). It has also been shown that melanin synthesis induced by UVA in melanocytes is triggered by OPN2 activation (Wicks et al. 2011). This work demonstrated that G-protein and phospholipase C (PLC) activation induced by OPN2 light-mediated stimulation

causes calcium (Ca2+) mobilization from intracellular stores in primary melanocytes, resulting in early melanin synthesis (Wicks et al. 2011). These studies suggest that Opsin receptors could indeed mediate important light dependent activities in non-visual tissues.

CRY1 is a component of the circadian clock machinery that is involved in a regulatory negative feed-back loop that determines rhythmicity of the circadian cycle (Baggs et al. 2009). CRY1 protein is widely expressed in all tissues of human body and plays a fundamental role in defining length of the circadian period (Baggs et al. 2009). In mice, expression of clock core proteins (PER2, CLOCK and NPAS2) is highly compartmentalized in anagen HF and follows circadian rhythmicity: hair matrix and DP are key sites of circadian activity (Plikus et al. 2013). Systemic knock-out of either *Cry1* or *Cry2* in mice abolishes synchronization of matrix cell mitosis in the different times of the day in both pelage and vibrissae follicles, whilst it does not have effects on hair length or hair shaft thickening (Plikus et al. 2013). However, peripheral circadian clock in the matrix cells creates daily mitotic rhythm that results in the faster hair growth in the morning than in the evening (Plikus et al. 2013). These results support the role of CRY1 in enforcing coordinated cell cycle checkpoint (Gaddameedhi et al. 2011; Geyfman et al. 2012b). For this reason and because CRY1 was suggested to act as a putative light-sensitive receptor (Sancar 2000; Thresher et al. 1998), the significance of the CRY family members in the regulation of human hair cycle was investigated in this project.

RT-PCR confirmed the presence of *CRY1* transcript in anagen HF **(**Figure 3-1 A) and quantitative PCR showed that both *CRY1* and *CRY2* mRNA are expressed in anagen HF (Figure 3-1 B) and in sorted HF stem cells (Figure 3-5

D). It has previously been shown that nuclear ratio of CRY1/CRY2 proteins controls the circadian length in a bidirectional manner: more CRY1 causes lengthening of the periods, while more CRY2 causes shortening of the periods (Anand et al. 2013; Hirota et al. 2012; Zhang et al. 2009). Therefore, a quantitative evaluation of differences in CRY1/2 ratio in HF stem cells and more differentiated HF cells would give indirect information regarding differences in the circadian length in the different cell types. How this balance could influence proliferation and differentiation processes in the HF, and how it affects the hair cycle is beyond the objective of this project, but worthy of further investigation.

4.2 Discovered light receptors are mediator of hair cycle regulation

4.2.1 CRY1 delays hair follicle catagen entry via CDK6

Increasing evidence suggest a fundamental role for the clock machinery in the regulation of the hair cycle (Al-Nuaimi et al. 2014; Plikus et al. 2013). HF growth consists of cyclic events of degeneration and regeneration, mainly regulated by signaling between DP and HF stem cells (Rompolas and Greco 2014). The master regulators of the timing between different hair cycles phases have not been clearly identified yet. A role for the circadian clock in hair cycle control has been hypothesized: Clock and Bmal1 mutant mice exhibit a delay in anagen progression (Lin et al. 2009); downregulation of the same genes in HF organ culture determine prolongation of the anagen phase (Al-Nuaimi et al. 2014); a different susceptibility of HFs to γ-irradiation during the day disappears in

Cry1−/−; Cry2−/− mutant mice, suggesting a role for CRYs in preventing hair loss induced by the external stressors (Plikus et al. 2013).

In our experiments, stabilization of CRY1 protein delayed anagen to catagen transition *ex vivo* (Figure 3-7), while downregulation of CRY1 promoted early entrance into the catagen phase (Figure 3-8). Marked reduction in proliferative events in the hair matrix and the ORS layer was observed after CRY1 silencing (Figure 3-8 D). Stabilization of Cryptochromes was performed using the small synthetic molecule KL001 (Figure 3-6 A) (Hirota et al. 2012) that specifically binds to CRY proteins preventing ubiquitin-dependent degradation of CRY (Hirota et al. 2012). The opportunity to use a tool that selectively targets one of the core clock proteins allowed us to study the role of CRY in hair physiology. Treatment with KL001 significantly decreased levels of *PER1* in HF organ culture (Figure 3-6). The same effect was consistently observed in unsynchronized U2OS cells, where KL001 resulted in the decline of PER1 levels at transcript and protein levels, while nuclear protein levels of CRY1 and 2 were increased, despite a reduction in mRNA expression (Hirota et al. 2012). Recently Al-Nuaimi et al found that PER1 expression is upregulated in catagen HF, and that PER1 silencing prolongs anagen phase in HF organ culture (Al-Nuaimi et al. 2014). Therefore, CRY1 may promote anagen maintenance inhibiting the expression of PER1, which leads to stimulation of keratinocytes proliferation.

Impairment of clock machinery has well known effects on cell cycle. For example, liver regeneration was impaired in Cry1 and 2 deficient mice (Matsuo et al. 2003); the molecular analysis suggested that the circadian clock may affect cell division by regulating the expression of the E-box–containing gene

Wee1, which encodes a kinase involved in timing of M phase entry (Matsuo et al. 2003). In Cry1 and 2 double knock-out mice proliferative Pcna-positive cell population is expanded distally above the Auber line in anagen hair follicle, compared with wild type. Nevertheless no increase in the total number of mitotic events was observed in double mutant mice (Plikus et al. 2013). This was explained by inability of ectopic PCNA+ cells to complete mitosis, due to pro-differentiation signaling via non circadian mechanism that would counteract the effect of clock oscillator's disruption. In our experiments, only CRY1 was targeted that resulted in the significant decrease in cell proliferation that lead to pre-mature catagen initiation (Figure 3-8).

Several studies demonstrated a tissue-specific regulation of gene expression by clock transcription factors (Balsalobre et al. 1998; Storch et al. 2002). 10% of the genes expressed in liver and 8% of the genes expressed in the heart showed circadian regulation; liver and heart circadian gene sets revealed very little overlap, suggesting a tissue specific gene expression regulation of circadian clocks (Storch et al. 2002). In synchronized fibroblasts, 81 novel genes following a robust circadian pattern were identified; interestingly, within this group, several transcripts belonged to the genes involved in cell cycle regulation such as Cyclin D3 and CDK4, known to play a role in the G1/S transition (Grundschober et al. 2001). Double Cry1 and 2 knock-out mice exhibited constant and arrhythmic expression of important players in the cell cycle regulation, such as Cyclin-dependent kinase 2 protein (CDK2) (Plikus et al. 2013), making clear the link between the clock machinery and cell cycle regulation.

To evaluate if specific mediators of the cell cycle were activated by CRY1 in the HF cells we performed microarray analysis after CRY1 silencing. We confirmed that in primary ORS cells downregulation of CRY1 also significantly suppressed proliferation (Figure 3-9 D). Silencing of CRY1 did not affect the expression of any of the others clock genes with similar function, CRY2 and PER1, suggesting that the analysis is restricted to the genes that are specifically targeted by CRY1 (Figure 3-9 C). CRY1 silencing significantly reduced expression of genes involved in cell cycle regulation: Pleckstrin 2 (PLEK2), cyclin-dependent kinase 6 (CDK6), proteasome 26S subunit, non-ATPase 2 (PSMD2), transmembrane BAX inhibitor motif containing 6 (TMBIM6), KDEL Endoplasmic Reticulum Protein Retention Receptor 1 (KDELR1) (Figure 3-10 B). Nothing is known about these genes in relation to hair physiology but all genes were shown to be involved in promoting cell proliferation in other models. PSMD2, in addition to participation in proteasome function, may be involved in the TNFα signaling pathway, interacting with the tumor necrosis factor type 1 receptor (TNFR) (Dunbar et al. 1997). TNFα is known to promote catagen, as shown by its inhibitory effect on hair growth *in vitro* (Philpott et al. 1996). TNFR is also involved in HF fate regulation: deficient mice for the receptor have defects in HF induction, lack sweat glands and exhibit tooth malformation (Botchkarev and Sharov 2004; Headon and Overbeek 1999). PLEK2 interacts with the actin cytoskeleton to induce cell spreading (Hamaguchi et al. 2007): increased levels in PLEK2 expression were found in melanoma patients, suggesting a fundamental role for this protein in sustaining proliferation (Luo et al. 2011). TMBIM6 is a multi-transmembrane domain-spanning endoplasmic reticulum (ER)-located protein that is evolutionarily conserved: TMBIM6 protects

against apoptosis (Xu and Reed 1998), is a negative regulator of the endoplasmic reticulum stress (Lisbona et al. 2009) and reduces the production of reactive oxygen species through direct interaction with NADPH-P450 reductase (Kim et al. 2009), a member of the microsomal monooxygenase system.

CDK6 is a member of the cyclin-dependent protein kinase (CDK) family that includes CDK4 and CDK2 kinases. CDK proteins are involved in the control of the cell cycle and differentiation. CDK6 promotes G1/S transition via phosphorylation of pRB/RB1 and NPM1 (Sherr and Roberts 1999; Weinberg 1995). CDK6 is also involved in the initiation and maintenance of cell cycle exit during cell differentiation (Grossel and Hinds 2006).

Since the role of CDK6 in HF is still unknown, we performed immunofluorescence analysis to characterize localization of this kinase in healthy full thickness skin. Surprisingly, we discovered that CDK6 specifically is localized in the cytoplasmic compartment of the IRS cells of anagen HFs (Figure 3-11 B), while we have been able to detect nuclear signal for CDK6 in primary ORS cells (Figure 3-10 C). A cytoplasmic localization for CDK6 has been shown in U2OS cells (Grossel et al. 1999), T cells (Mahony et al. 1998; Nagasawa et al. 1997) and mouse astrocytes (Ericson et al. 2003) that is similar to our observations in the HF. Specific compartmentalization of CDK6 can be related to its ability to create a functional complex that are translocated into the nucleus (Grossel et al. 1999; Mahony et al. 1998), or an alternative cytoplasmic role for CDK6 was suggested: cdk6 protein was found to be located in the ruffling edge of spreading cells in MRC5 human fibroblast and the ability to suppress p16INK4a-mediated inhibition of cell division was shown, indicating a

function in controlling matrix-dependent cell spreading. (Fåhraeus and Lane 1999).

Our results demonstrated a correlation between CRY1 expression and levels of CDK6, which could suggest that CRY1 alters cell proliferation in HF *ex-vivo* via CDK6 activity. The hypothesis that the cellular clock regulates the cell cycle via interaction with CDK/Cyclin molecular gates has previously been evaluated: Plikus et al work suggests that clock generates daily mitotic rhythmicity in hair matrix by synchronizing Cdc2/Cyclin B-mediated G2/M checkpoint (Plikus et al. 2013). It has also been shown a pro-proliferative effect for CDK6, which activity was elevated in squamous cell carcinomas (Timmermann et al. 1997).

However, it is not clear why CDK6 is specifically localized in the IRS of anagen HF, a region of differentiated cells, and how this could affect the proliferating matrix cells. Nevertheless, recent findings indicate a novel and specific role for CDK6 in regulation of differentiation in multiple cell types. Sustained expression of CDK6, but not of CDK4 kinase, blocked differentiation of mouse erythroid leukemia cells (Matushansky et al. 2000; Matushansky et al. 2003). In mouse, aberrant levels of CDK6 in the astrocytes caused rapid changes in morphology from a more differentiated to a precursor-like state; this was also confirmed by an altered expression of differentiation markers (Ericson et al. 2003). BMP2-SMAD signaling-induced differentiation in mouse osteoblasts was associated with strongly down-regulated CDK6 expression (Ogasawara et al. 2004b). In osteoclasts, CDK6 was found to be a key determinant of the differentiation rate and act as a downstream effector of NF-kappa B signaling (Ogasawara et al. 2004a). However, the precise mechanism by which CDK6 regulates cell differentiation is still not fully clear.

Interestingly, inhibition of CDK4/6 in the skin completely blocks HF growth and differentiation (Benjamin et al. 2003). However, this effect was only observed when CDK4/6 were inhibited at the time of the hair cycle induction by epilation (day 0 of epilation), while CDK4/6 were dispensable for hair cycle progression. This evidence suggest that hair cycle can be activated by CDKs pathway only within a specific temporal window (Benjamin et al. 2003). Therefore, we are tempted to speculate, that differences in timing and activity of CDK6 during hair cycle could be regulated by the clock machinery system, and specifically by CRY1.

4.2.2 OPN3 is involved in the regulation of keratinocytes proliferation in the hair follicle

We have demonstrated that OPN3 exerts a positive effect on ORS cells proliferation (Figure 3-12 E). *In vitro* analysis of the effect of OPN3 downregulation revealed the significant decrease in the number of proliferative EdU positive cells, compared to the corresponding controls (Figure 3-12 E). Transcriptomic analysis detected that silencing of OPN3 expression in the proliferating ORS keratinocytes leads to the altered expression of genes involved in the control of stem cell activity in skin and HF (Figure 3-13). For example, the expression of p21-activated kinase 2 (PAK2) and follistatin-like1 (FSTL1) was downregulated due to OPN3 silencing. PAK2 plays a role in a variety of different signalling pathways including cytoskeleton regulation, cell motility, apoptosis or proliferation. PAK2 acts as a downstream effector of RAC1 that leads to the inhibition of c-Myc (Benitah et al. 2004; Huang et al. 2004). Both RAC1 and c-Myc are implicated in the control of epidermal stem cell

(Benitah et al. 2005). In epidermal stem cells c-Myc activation causes a progressive reduction in the growth rate *in vitro* without inducing apoptosis due to a marked stimulation of terminal differentiation (Gandarillas and Watt 1997; Watt 2000). c-Myc overexpression in vivo promotes basal keratinocytes exit from the stem cell compartment, inducing preferential differentiation into sebocytes lineages at the expenses of hair differentiation (Arnold and Watt 2001). Interestingly, c-Myc was found to be expressed in several compartments of the anagen human HF, including the hair bulb, proximal IRS and the bulge region (Bull et al. 2001; Rumio et al. 2000). Evidence about c-Myc localization in the IRS and our finding about *PAK2* downregulation caused by OPN3 silencing suggest the possible functional link between OPN3 and c-Myc in the regulation of HF cell proliferation/differentiation. FSTL1 is another very attractive OPN3 target gene, because it is known that FSTL1 inhibits bone morphogenetic protein (BMP) suppressive effects in telogen HF stem cells allowing the initiation of the new hair cycle (McDowall et al. 2008).

These findings highlighted a novel previously unrecognised role for OPN3 in cell cycle modulation in the HF cells. Taken together, the identified light-sensitive receptors in the HF, Cryptochromes and Opsins, can be involved in the hair cycle control.

4.3 Blue light prolong anagen ex vivo and its stimulatory effect can be mediated by OPN3

In recent years, several molecules have emerged as novel mediators of light activation in non-photosensitive tissues, such as nitrosated proteins regulating nitric oxide (NO) (Liebmann et al. 2010; Oplander et al. 2013), the flavoprotein-containing Cryptochromes (Bouly et al. 2007) and Opsins (Wicks et al. 2011). Despite such a long list of potential absorbers of blue light, the shorter-wavelength UV-free part of the electromagnetic spectrum remains to be relatively unexplored. The latter could possibly be explained by a relatively short penetration depth of this part of the electromagnetic spectrum. However, 450 nm light is successfully used for treatment of cutaneous diseases, including psoriasis and eczema (Keemss et al. 2016; Pfaff et al. 2015), suggesting sufficient blue light penetration into the skin. A novel device has recently been developed for percutaneous light delivery. This device incorporates a microlens array that focuses the light through the needle tips at specific points and can achieve the required intensity profile within the tissue, overcoming the limitation of blue light penetration in the skin (Kim et al. 2016). A 9-fold enhancement of light delivery was achieved in bovine tissues that could be approximated to 1.3 - 2.5 mm depth penetration through the human skin (Kim et al. 2016). Similar additional optical beam manipulations might allow the photons of blue light at sufficient density to reach HF epithelial cells, including the bulge stem cells located in the outer root sheath or DP and matrix cells of miniaturized AGA HFs.

Photosensitivity of visual Opsins requires binding of the 11-cis-retinal chromophore to a Lysine residue of the G protein coupled receptors. While 11-

cis retinal is abundantly present in the eye to ensure the formation of a functional receptor, all-trans retinal are mostly present in non-photosensitive tissues (Koyanagi et al. 2013; Miyagi et al. 2001). Nevertheless, it has been reported that homologs of vertebrate OPN3 in pufferfish and mosquito becomes light sensitive when they bind to 13-cis-retinal, and they might function as photoreceptors in many tissues (Miyagi et al. 2001). Photosensitivity of Cryptochromes in mammals has been largely debated (Grossel and Hinds 2006) but is now considered that they perform both light-dependent and light-independent functions in the regulation of the circadian clock (Lin and Todo 2005). In addition has been shown that their role in the light entrainment of the circadian clock can be carried out redundantly by other photoreceptors, more likely Opsins (Panda et al. 2002).

Therefore, the expression of CRY1 and 2, OPN2 and OPN3 in the different HF compartments and their role in hair physiology, stimulated our interest in understanding their possible involvement in light sensing capability of the HF.

It has been demonstrated that keratinocyte irradiation with blue light of 412-426 nm at relatively high radiant exposure causes toxic effects (Liebmann et al. 2010). In addition, 41.4 J/cm2 453 nm blue light irradiation rapidly induces ROS production and anti-proliferative effects (Becker et al. 2016; Liebmann et al. 2010). In our study, we observed that low level of light at 453 nm wavelength (which falls within Opsins and Cryptochromes absorption spectrum) promote anagen phase in HF *ex vivo* associated with sustained proliferation in the hair matrix keratinocytes compared with untreated control (Figure 3-14). Interestingly, low radiant exposure of 3.2 J/cm^2 stimulated metabolic activity in the ORS cells in vitro 24 hours after treatment, and promotion of cell

proliferation was significant only 8 hours after light irradiation (Figure 3-15 A-B). This suggests that light exerts a long term effect that is likely to be triggered by changes in gene expression levels in the affected cells. A positive effect of low levels (2 J/cm^2) of 453 nm blue light has recently been demonstrated in the dermal fibroblasts: the activation of metabolic activity and even more, the increased collagen production by papillary fibroblasts (Mignon et al. 2016b), and increased total protein synthesis (Masson-Meyers et al. 2016). Therefore, these reports suggest that low levels of blue light could promote positive effects on cell growth and functions. In line with it, our study demonstrated that 3.2 J/cm^2 of blue light with 453 nm central wavelength exert beneficial effect on anagen maintenance of HF *ex vivo*.

Despite numerous existing publications about responsiveness of HFs and HF cells to red light and existing commercial red light-emitting devices for hair growth stimulation, in our study 3.2 J/cm^2 of 689 nm light (red light) did not significantly affect hair growth *ex vivo* (p=0.7). However, this lack of statistical significance does not necessarily serve as evidence of the absence of positive effect of red light (Figure 3-14). A recent viewpoint review (Mignon et al. 2016a) that summarizes the investigation of 90 reports published between 1985 and 2015, mostly based on application of red and near-infrared light, identified major inconsistencies in optical parameters between the published studies. A variety of the optical ranges of photon density applied in *in vitro* and *ex vivo* settings has been shown to encompass over two orders of magnitude. Strikingly, same or very similar optical parameters used in different studies have been reported to trigger diverse effects on the cell (Liebmann et al. 2010; Pellicioli et al. 2014; Prabhu ; Song et al. 2003). It has also been shown that culture conditions can

have a huge impact on the outcome of the experiments with light (Mignon et al. 2016b). Therefore, even if the beneficial effect of blue light at low radiant exposure on hair growth raises a possibility to use these parameters for future therapeutic solutions, it is important to emphasize the limit of selected experimental conditions when translating *in vitro* results into *in vivo* scenarios.

Importantly, the stimulatory effect of blue light on ORS cell proliferation was abrogated by silencing of OPN3; downregulation of OPN3 *in vitro* dramatically reduced proliferation rate, which was otherwise induced by blue light treatment in primary ORS cells (Figure 3-15 C).

These findings support our hypothesis that positive effects of blue light on hair growth could be mediated, at least in part, by light-sensitive receptors such as OPN3. Further investigation will be required to understand the role of others light mediators, if light effects are triggered by a specific photoreceptor, or more likely by a cascade of pathways activated by different receptors.

5 Conclusions

In this project, a novel role for light-sensitive receptors in the control of human hair growth was identified. Based on the data obtained in this study the following conclusions can be made:

1. The light-sensitive receptors, such as CRY1, CRY2, OPN2 and OPN3 are expressed in the distinct compartments of the human HF. CRY1 is ubiquitously expressed throughout the HF; OPN2 and OPN3 are localized in the ORS and the IRS layers of the anagen HF, respectively; *CRY1, CRY2, OPN2* and *OPN3* transcripts were also detected in the HF stem cells.
2. CRY1 prolongs anagen phase by stimulating cell proliferation, at least in part via cell cycle kinase CDK6: CRY1 stabilization induced by KL001 treatment in HF *ex vivo* lengthens anagen phase; CRY1 silencing promotes early entrance into catagen phase associated with substantial reduction in cell proliferation; CRY1 silencing dampens CDK6 expression; KL001-mediated anagen prolongation is accompanied with the enhanced CDK6 expression.
3. OPN3 could have a positive effect on hair growth: OPN3 silencing in primary ORS cells negatively impacts proliferation, due to the altered expression of genes involved in the regulation of proliferative and apoptotic pathways.
4. Blue light (3,2 J/cm^2 , 453nm) exerts a positive effect on hair growth *ex vivo,* potentially via interaction with OPN3: blue light increases the mean

survival time of HF *ex vivo*, stimulating proliferation of the hair matrix cells. 3,2 J/cm^2 of blue light also boosts the metabolic activity in primary ORS and significantly promotes *in vitro* cell proliferation, which is abrogated by silencing of OPN3.

Taken together, the data obtained in this project suggest that human HF exhibits the expression of a variety of light-sensitive receptors that could mediate the effects of light on hair growth. The further research should be conducted to decipher direct interactions between blue light and Cryptochromes and Opsin receptors in the HFs, as well as to investigate a role of other blue-light acceptors in the control of hair growth. The beneficial effect of blue light at low radiant exposure on hair growth raises a possibility of increasing therapeutic efficacy when combined with topical chemistry used for management of hair growth disorders.

6 Publications, Meeting presentations, and Travel Awards

I. Journal articles

a. Buscone S, Mardaryev AN, Raafs B, Bikker JW, Sticht C, Gretz N, Farjo N, Uzunbajakava NE, Botchkareva NV. *A new path in defining light parameters for hair growth: Discovery and modulation of photoreceptors in human hair follicle*. Lasers Surg Med. **2017**. doi: 10.1002/lsm.22673. PMID: 28418107

II. Oral presentations

a. S. Buscone, I. Castellano, C. Mignon, N. Uzunbajakava, J. Thornton, D.Tobin, N. Botchkareva. **2015** *Expression of photo-receptors in human skin: implications for light-based therapies for hair and skin health*. 16th Congress of the European Society for Photobiology, Aveiro, Portugal.

b. S. Buscone, B. Raafs, M.A.A. van Vlimmeren, A. Mardaryev, N. E. Uzunbajakava, N.V. Botchkareva. **2016** A new path in defining light parameters for hair growth: discovery and modulation of light sensitive receptors in human hair follicles. 36th Annual Conference of the American Society for Laser Medicine and Surgery, Boston, MA, USA.

III. Poster presentations

a. S. Buscone, I. Castellano, C. Mignon, N. Uzunbajakava, J. Thornton, D.Tobin, N. Botchkareva. **2015**. *Expression of photo-receptors in human skin: implications for light-based therapies for hair and skin health*. 16th Congress of the European Society for Photobiology, Aveiro, Portugal.

b. S. Buscone, N.E. Uzunbajakava, G.Westgate, N.Farjo, A.N. Mardaryev, N.V. Botchkareva. **2015**. *Can Hair Follicles "See" the Light? Analysis of Light-Sensitive Receptors in Human Hair Follicles*. 9th World Congress for Hair Research, Miami, USA

c. C. Mignon, N. E. Uzunbajakava, B.Raafs, M. van Vlimmeren, M. Zeitouny, N.V. Botchkareva, A. Mardaryev, J. Thornton, S. Buscone, I. Castellano, D.J. Tobin. **2015**. A systematic approach to unravel how light impacts primary human dermal fibroblasts. 35th Annual Conference of the American Society for Laser Medicine and Surgery, Kissemmee, FL, USA

d. S. Buscone, M.A.A. van Vlimmeren, A. Mardaryev, N.E. Uzunbajakava, N.V. Botchkareva. **2016**. Photoreceptors in human hair follicle: investigating presence and functionality towards superior light-based therapies for hair disorders. 46th European Society for Dermatological Research, Munich, Germany

e. S. Buscone, J.W. Bikker, B. Raafs, N.V. Botchkareva, N. E. Uzunbajakava. **2016**. A novel statistical approach to evaluate effects of low level light on anagen to catagen transition in hair

follicle organ culture model. 7th International Bi-Annual Conference on Applied Hair Science, New Jersey, USA

f. N. E. Uzunbajakava, I. Castellano, C. Mignon, S. Buscone, D.J Tobin, N.V. Botchkareva, M.J. Thornton. **2016**. Human skin and hair can see light: unravelling expression of photoreceptors towards improved light therapies for hair and skin disorders. 36th Annual Conference of the American Society for Laser Medicine and Surgery, Boston, MA, USA

g. H. Siiskonen, S. Buscone, I. Castellano, J. Scheffel, N. E. Uzunbajakava, N.V. Botchkareva, M. Maurer. **2016**. *Human skin mast cells express photoreceptors*. 33rd Nordic congress in dermatology and venereology, Trondheim, Finland

IV. Travel Awards

a. 9th World Congress for Hair Research, **2015**. Miami, USA

b. 36th Annual Conference of the American Society for Laser Medicine and Surgery, **2016**. Boston, MA, USA.

7 References

Ahmad, W., ul Haque, M. F., Brancolini, V., Tsou, H. C., Ul Haque, S., Lam, H., Aita, V. M., Owen, J., Frank, J., and Cserhalmi-Friedman, P. B. (1998). "Alopecia universalis associated with a mutation in the human hairless gene." *Science*, 279(5351), 720-724.

Al-Nuaimi, Y., Hardman, J. A., Bíró, T., Haslam, I. S., Philpott, M. P., Tóth, B. I., Farjo, N., Farjo, B., Baier, G., and Watson, R. E. (2014). "A meeting of two chronobiological systems: circadian proteins Period1 and BMAL1 modulate the human hair cycle clock." *Journal of Investigative Dermatology*, 134(3), 610-619.

Albert, E. S., Bec, J. M., Desmadryl, G., Chekroud, K., Travo, C., Gaboyard, S., Bardin, F., Marc, I., Dumas, M., and Lenaers, G. (2012). "TRPV4 channels mediate the infrared laser-evoked response in sensory neurons." *Journal of neurophysiology*, 107(12), 3227-3234.

AlGhamdi, K. M., Kumar, A., and Moussa, N. A. (2012). "Low-level laser therapy: a useful technique for enhancing the proliferation of various cultured cells." *Lasers in medical science*, 27(1), 237-249.

Alkhalifah, A., Alsantali, A., Wang, E., McElwee, K. J., and Shapiro, J. (2010). "Alopecia areata update: part II. Treatment." *J Am Acad Dermatol*, 62(2), 191-202, quiz 203-4.

Anand, S. N., Maywood, E. S., Chesham, J. E., Joynson, G., Banks, G. T., Hastings, M. H., and Nolan, P. M. (2013). "Distinct and separable roles for endogenous CRY1 and CRY2 within the circadian molecular

clockwork of the suprachiasmatic nucleus, as revealed by the Fbxl3Afh mutation." *Journal of Neuroscience*, 33(17), 7145-7153.

Anders, J. J., Lanzafame, R. J., and Arany, P. R. (2015). "Low-level light/laser therapy versus photobiomodulation therapy." *Photomed Laser Surg*, 33(4), 183-4.

Arnold, I., and Watt, F. M. (2001). "c-Myc activation in transgenic mouse epidermis results in mobilization of stem cells and differentiation of their progeny." *Current biology*, 11(8), 558-568.

Avci, P., Gupta, A., Sadasivam, M., Vecchio, D., Pam, Z., Pam, N., and Hamblin, M. R. (2013). "Low-level laser (light) therapy (LLLT) in skin: stimulating, healing, restoring." *Semin Cutan Med Surg*, 32(1), 41-52.

Avci, P., Gupta, G. K., Clark, J., Wikonkal, N., and Hamblin, M. R. (2014). "Low-level laser (light) therapy (LLLT) for treatment of hair loss." *Lasers Surg Med*, 46(2), 144-51.

Bachmann, L., Zezell, D. M., Ribeiro, A. d. C., Gomes, L., and Ito, A. S. (2006). "Fluorescence spectroscopy of biological tissues—a review." *Applied Spectroscopy Reviews*, 41(6), 575-590.

Baehr, W., Wu, S. M., Bird, A. C., and Palczewski, K. (2003). "The retinoid cycle and retina disease." *Vision Res*, 43(28), 2957-8.

Baggs, J. E., Price, T. S., DiTacchio, L., Panda, S., Fitzgerald, G. A., and Hogenesch, J. B. (2009). "Network features of the mammalian circadian clock." *PLoS Biol*, 7(3), e52.

Ball, K. A., Castello, P. R., and Poyton, R. O. (2011). "Low intensity light stimulates nitrite-dependent nitric oxide synthesis but not oxygen

consumption by cytochrome c oxidase: Implications for phototherapy." *Journal of Photochemistry and Photobiology B: Biology*, 102(3), 182-191.

Balsalobre, A., Brown, S. A., Marcacci, L., Tronche, F., Kellendonk, C., Reichardt, H. M., Schütz, G., and Schibler, U. (2000). "Resetting of circadian time in peripheral tissues by glucocorticoid signaling." *Science*, 289(5488), 2344-2347.

Balsalobre, A., Damiola, F., and Schibler, U. (1998). "A serum shock induces circadian gene expression in mammalian tissue culture cells." *Cell*, 93(6), 929-937.

Banka, N., Bunagan, M. K., and Shapiro, J. (2013). "Pattern hair loss in men: diagnosis and medical treatment." *Dermatologic clinics*, 31(1), 129-140.

Becker, A., Klapczynski, A., Kuch, N., Arpino, F., Simon-Keller, K., De La Torre, C., Sticht, C., van Abeelen, F. A., Oversluizen, G., and Gretz, N. (2016). "Gene expression profiling reveals aryl hydrocarbon receptor as a possible target for photobiomodulation when using blue light." *Sci Rep*, 6, 33847.

Benitah, S. A., Frye, M., Glogauer, M., and Watt, F. M. (2005). "Stem cell depletion through epidermal deletion of Rac1." *Science*, 309(5736), 933-5.

Benitah, S. A., Valeron, P. F., van Aelst, L., Marshall, C. J., and Lacal, J. C. (2004). "Rho GTPases in human cancer: an unresolved link to upstream and downstream transcriptional regulation." *Biochim Biophys Acta*, 1705(2), 121-32.

Benjamin, D. Y., Becker-Hapak, M., Snyder, E. L., Vooijs, M., Denicourt, C., and Dowdy, S. F. (2003). "Distinct and nonoverlapping roles for pRB and

cyclin D: cyclin-dependent kinases 4/6 activity in melanocyte survival." *Proceedings of the National Academy of Sciences*, 100(25), 14881-14886.

Bikle, D. D., Elalieh, H., Chang, S., Xie, Z., and Sundberg, J. P. (2006). "Development and progression of alopecia in the vitamin D receptor null mouse." *J Cell Physiol*, 207(2), 340-53.

Blomhoff, R., and Blomhoff, H. K. (2006). "Overview of retinoid metabolism and function." *J Neurobiol*, 66(7), 606-30.

Bodemer, C., Peuchmaur, M., Fraitaig, S., Chatenoud, L., Brousse, N., and De Prost, Y. (2000). "Role of cytotoxic T cells in chronic alopecia areata." *J Invest Dermatol*, 114(1), 112-6.

Botchkarev, V. A. (2003). "Bone morphogenetic proteins and their antagonists in skin and hair follicle biology." *J Invest Dermatol*, 120(1), 36-47.

Botchkarev, V. A., Botchkareva, N. V., Nakamura, M., Huber, O., Funa, K., Lauster, R., Paus, R., and Gilchrest, B. A. (2001). "Noggin is required for induction of the hair follicle growth phase in postnatal skin." *FASEB J*, 15(12), 2205-14.

Botchkarev, V. A., and Kishimoto, J. (2003). "Molecular control of epithelial-mesenchymal interactions during hair follicle cycling." *J Investig Dermatol Symp Proc*, 8(1), 46-55.

Botchkarev, V. A., and Sharov, A. A. (2004). "BMP signaling in the control of skin development and hair follicle growth." *Differentiation*, 72(9-10), 512-526.

Botchkareva, N. V., Ahluwalia, G., and Shander, D. (2006). "Apoptosis in the hair follicle." *J Invest Dermatol*, 126(2), 258-64.

Boulnois, J.-L. (1986). "Photophysical processes in recent medical laser developments: a review." *Lasers in Medical Science*, 1(1), 47-66.

Bouly, J. P., Schleicher, E., Dionisio-Sese, M., Vandenbussche, F., Van Der Straeten, D., Bakrim, N., Meier, S., Batschauer, A., Galland, P., Bittl, R., and Ahmad, M. (2007). "Cryptochrome blue light photoreceptors are activated through interconversion of flavin redox states." *J Biol Chem*, 282(13), 9383-91.

Brown, S. A., Fleury-Olela, F., Nagoshi, E., Hauser, C., Juge, C., Meier, C. A., Chicheportiche, R., Dayer, J.-M., Albrecht, U., and Schibler, U. (2005). "The period length of fibroblast circadian gene expression varies widely among human individuals." *PLoS Biol*, 3(10), e338.

Buhl, A. E. (1991). "Minoxidil's action in hair follicles." *J Invest Dermatol*, 96(5), 73S-74S.

Buhl, A. E., Conrad, S. J., Waldon, D. J., and Brunden, M. N. (1993). "Potassium channel conductance as a control mechanism in hair follicles." *J Invest Dermatol*, 101(1 Suppl), 148S-152S.

Buhr, E. D., and Takahashi, J. S. (2013). "Molecular components of the Mammalian circadian clock." *Handb Exp Pharmacol*(217), 3-27.

Bull, J. J., Mïller-Röver, S., Patel, S. V., Chronnell, C. M., McKay, I. A., and Philpott, M. P. (2001). "Contrasting localization of c-Myc with other Myc superfamily transcription factors in the human hair follicle and during the hair growth cycle." *Journal of investigative dermatology*, 116(4), 617-622.

Cashmore, A. R., Jarillo, J. A., Wu, Y.-J., and Liu, D. (1999). "Cryptochromes: blue light receptors for plants and animals." *Science*, 284(5415), 760-765.

Cetin, E. D., Savk, E., Uslu, M., Eskin, M., and Karul, A. (2009). "Investigation of the inflammatory mechanisms in alopecia areata." *Am J Dermatopathol*, 31(1), 53-60.

Chase, H. (1965). "Cycles and waves of hair growth." *Biology of the Skin and Hair Growth*, 461-465.

Chaudhry, H., Lynch, M., Schomacker, K., Birngruber, R., Gregory, K., and Kochevar, I. (1993). "RELAXATION OF VASCULAR SMOOTH MUSCLE INDUCED BY LOW-POWER LASER RADIATION." *Photochemistry and photobiology*, 58(5), 661-669.

Chaves, I., Pokorny, R., Byrdin, M., Hoang, N., Ritz, T., Brettel, K., Essen, L.-O., van der Horst, G. T., Batschauer, A., and Ahmad, M. (2011). "The cryptochromes: blue light photoreceptors in plants and animals." *Annual review of plant biology*, 62, 335-364.

Chen, W., Zouboulis, C. C., Fritsch, M., Kodelja, V., and Orfanos, C. E. (1998). "Heterogeneity and quantitative differences of type 1 5 alpha-reductase expression in cultured skin epithelial cells." *Dermatology*, 196(1), 51-2.

Chung, H., Dai, T., Sharma, S. K., Huang, Y.-Y., Carroll, J. D., and Hamblin, M. R. (2012). "The nuts and bolts of low-level laser (light) therapy." *Annals of biomedical engineering*, 40(2), 516-533.

Cline, D. J. (1988). "Changes in hair color." *Dermatol Clin*, 6(2), 295-303.

Cotsarelis, G. (2006). "Gene expression profiling gets to the root of human hair follicle stem cells." *J Clin Invest*, 116(1), 19-22.

Cotsarelis, G., and Millar, S. E. (2001). "Towards a molecular understanding of hair loss and its treatment." *Trends Mol Med*, 7(7), 293-301.

Cotsarelis, G., Sun, T. T., and Lavker, R. M. (1990). "Label-retaining cells reside in the bulge area of pilosebaceous unit: implications for follicular stem cells, hair cycle, and skin carcinogenesis." *Cell*, 61(7), 1329-37.

DeVillez, R. L., Jacobs, J. P., Szpunar, C. A., and Warner, M. L. (1994). "Androgenetic alopecia in the female. Treatment with 2% topical minoxidil solution." *Arch Dermatol*, 130(3), 303-7.

Dierickx, C. C., and Anderson, R. R. (2005). "Visible light treatment of photoaging." *Dermatol Ther*, 18(3), 191-208.

Dressel, D., Brutt, C. H., Manfras, B., Zollner, T. M., Wunderlich, A., Bohm, B. O., and Boehncke, W. H. (1997). "Alopecia areata but not androgenetic alopecia is characterized by a restricted and oligoclonal T-cell receptor-repertoire among infiltrating lymphocytes." *J Cutan Pathol*, 24(3), 164-8.

Dunbar, J. D., Song, H. Y., Guo, D., Wu, L.-W., and Donner, D. B. (1997). "Two-hybrid cloning of a gene encoding TNF receptor-associated protein 2, a protein that interacts with the intracellular domain of the type 1 TNF receptor: identity with subunit 2 of the 26S protease." *The Journal of Immunology*, 158(9), 4252-4259.

Ehrreich, S. J., and Furchgott, R. F. (1968). "Relaxation of mammalian smooth muscles by visible and ultraviolet radiation." *Nature*, 218(5142), 682-684.

Ellis, J. A., Stebbing, M., and Harrap, S. B. (2001). "Polymorphism of the androgen receptor gene is associated with male pattern baldness." *J Invest Dermatol*, 116(3), 452-5.

Ericson, K. K., Krull, D., Slomiany, P., and Grossel, M. J. (2003). "Expression of Cyclin-Dependent Kinase 6, but not Cyclin-Dependent Kinase 4, Alters Morphology of Cultured Mouse Astrocytes11NSF under CAREER grant#

9984454 to Martha J. Grossel." *Molecular Cancer Research*, 1(9), 654-664.

Fåhraeus, R., and Lane, D. P. (1999). "The p16INK4a tumour suppressor protein inhibits αvβ3 integrin-mediated cell spreading on vitronectin by blocking PKC-dependent localization of αvβ3 to focal contacts." *The EMBO journal*, 18(8), 2106-2118.

Foitzik, K., Krause, K., Nixon, A. J., Ford, C. A., Ohnemus, U., Pearson, A. J., and Paus, R. (2003). "Prolactin and its receptor are expressed in murine hair follicle epithelium, show hair cycle-dependent expression, and induce catagen." *Am J Pathol*, 162(5), 1611-21.

Foitzik, K., Spexard, T., Nakamura, M., Halsner, U., and Paus, R. (2005). "Towards dissecting the pathogenesis of retinoid-induced hair loss: all-trans retinoic acid induces premature hair follicle regression (catagen) by upregulation of transforming growth factor-β2 in the dermal papilla." *Journal of investigative dermatology*, 124(6), 1119-1126.

Gaddameedhi, S., Selby, C. P., Kaufmann, W. K., Smart, R. C., and Sancar, A. (2011). "Control of skin cancer by the circadian rhythm." *Proceedings of the National Academy of Sciences*, 108(46), 18790-18795.

Gandarillas, A., and Watt, F. M. (1997). "c-Myc promotes differentiation of human epidermal stem cells." *Genes & development*, 11(21), 2869-2882.

Gao, X., and Xing, D. (2009). "Molecular mechanisms of cell proliferation induced by low power laser irradiation." *J Biomed Sci*, 16(4), 1-16.

Garza, L. A., Liu, Y., Yang, Z., Alagesan, B., Lawson, J. A., Norberg, S. M., Loy, D. E., Zhao, T., Blatt, H. B., Stanton, D. C., Carrasco, L., Ahluwalia, G., Fischer, S. M., FitzGerald, G. A., and Cotsarelis, G. (2012).

"Prostaglandin D2 inhibits hair growth and is elevated in bald scalp of men with androgenetic alopecia." *Sci Transl Med*, 4(126), 126ra34.

Garza, L. A., Yang, C. C., Zhao, T., Blatt, H. B., Lee, M., He, H., Stanton, D. C., Carrasco, L., Spiegel, J. H., Tobias, J. W., and Cotsarelis, G. (2011). "Bald scalp in men with androgenetic alopecia retains hair follicle stem cells but lacks CD200-rich and CD34-positive hair follicle progenitor cells." *J Clin Invest*, 121(2), 613-22.

Geyfman, M., Gordon, W., Paus, R., and Andersen, B. (2012a). "Identification of telogen markers underscores that telogen is far from a quiescent hair cycle phase." *J Invest Dermatol*, 132(3 Pt 1), 721-4.

Geyfman, M., Kumar, V., Liu, Q., Ruiz, R., Gordon, W., Espitia, F., Cam, E., Millar, S. E., Smyth, P., and Ihler, A. (2012b). "Brain and muscle Arnt-like protein-1 (BMAL1) controls circadian cell proliferation and susceptibility to UVB-induced DNA damage in the epidermis." *Proceedings of the National Academy of Sciences*, 109(29), 11758-11763.

Gilhar, A., Etzioni, A., and Paus, R. (2012). "Alopecia areata." *N Engl J Med*, 366(16), 1515-25.

Gilhar, A., Landau, M., Assy, B., Shalaginov, R., Serafimovich, S., and Kalish, R. S. (2001). "Melanocyte-associated T cell epitopes can function as autoantigens for transfer of alopecia areata to human scalp explants on Prkdc(scid) mice." *J Invest Dermatol*, 117(6), 1357-62.

Gilliam, A. C., Kremer, I. B., Yoshida, Y., Stevens, S. R., Tootell, E., Teunissen, M. B., Hammerberg, C., and Cooper, K. D. (1998). "The human hair follicle: a reservoir of CD40+ B7-deficient Langerhans cells that

repopulate epidermis after UVB exposure." *Journal of Investigative Dermatology*, 110(4), 422-427.

Giovani, B., Byrdin, M., Ahmad, M., and Brettel, K. (2003). "Light-induced electron transfer in a cryptochrome blue-light photoreceptor." *Nature Structural & Molecular Biology*, 10(6), 489.

Goh, C., Finkel, M., Christos, P. J., and Sinha, A. A. (2006). "Profile of 513 patients with alopecia areata: associations of disease subtypes with atopy, autoimmune disease and positive family history." *J Eur Acad Dermatol Venereol*, 20(9), 1055-60.

Gollapalli, D. R., and Rando, R. R. (2004). "The specific binding of retinoic acid to RPE65 and approaches to the treatment of macular degeneration." *Proc Natl Acad Sci U S A*, 101(27), 10030-5.

Golombek, D. A., and Rosenstein, R. E. (2010). "Physiology of circadian entrainment." *Physiological reviews*, 90(3), 1063-1102.

Greco, V., Chen, T., Rendl, M., Schober, M., Pasolli, H. A., Stokes, N., Dela Cruz-Racelis, J., and Fuchs, E. (2009). "A two-step mechanism for stem cell activation during hair regeneration." *Cell Stem Cell*, 4(2), 155-69.

Grossel, M. J., Baker, G. L., and Hinds, P. W. (1999). "Cdk6 can shorten G1 phase dependent upon the N-terminal INK4 interaction domain." *Journal of Biological Chemistry*, 274(42), 29960-29967.

Grossel, M. J., and Hinds, P. W. (2006). "Beyond the cell cycle: a new role for Cdk6 in differentiation." *Journal of cellular biochemistry*, 97(3), 485-493.

Grundschober, C., Delaunay, F., Pühlhofer, A., Triqueneaux, G., Laudet, V., Bartfai, T., and Nef, P. (2001). "Circadian regulation of diverse gene

products revealed by mRNA expression profiling of synchronized fibroblasts." *Journal of Biological Chemistry*, 276(50), 46751-46758.

Gu, Q., Wang, L., Huang, F., and Schwarz, W. (2012). "Stimulation of TRPV1 by green laser light." *Evidence-Based Complementary and Alternative Medicine*, 2012.

Gundogan, C., Greve, B., and Raulin, C. (2004). "Treatment of alopecia areata with the 308-nm xenon chloride excimer laser: case report of two successful treatments with the excimer laser." *Lasers Surg Med*, 34(2), 86-90.

Gupta, A. K., Filonenko, N., Salansky, N., and Sauder, D. N. (1998). "The use of low energy photon therapy (LEPT) in venous leg ulcers: a double-blind, placebo-controlled study." *Dermatol Surg*, 24(12), 1383-6.

Halford, S., Freedman, M. S., Bellingham, J., Inglis, S. L., Poopalasundaram, S., Soni, B. G., Foster, R. G., and Hunt, D. M. (2001). "Characterization of a novel human opsin gene with wide tissue expression and identification of embedded and flanking genes on chromosome 1q43." *Genomics*, 72(2), 203-8.

Haltaufderhyde, K., Ozdeslik, R. N., Wicks, N. L., Najera, J. A., and Oancea, E. (2015). "Opsin expression in human epidermal skin." *Photochem Photobiol*, 91(1), 117-23.

Hamaguchi, N., Ihara, S., Ohdaira, T., Nagano, H., Iwamatsu, A., Tachikawa, H., and Fukui, Y. (2007). "Pleckstrin-2 selectively interacts with phosphatidylinositol 3-kinase lipid products and regulates actin organization and cell spreading." *Biochemical and biophysical research communications*, 361(2), 270-275.

Hamblin, M. R., and Demidova, T. N. "Mechanisms of low level light therapy." *Presented at Biomedical Optics 2006*.

Hamm, H., and Traupe, H. (1989). "Loose anagen hair of childhood: the phenomenon of easily pluckable hair." *J Am Acad Dermatol*, 20(2 Pt 1), 242-8.

Hansen, L. A., Alexander, N., Hogan, M. E., Sundberg, J. P., Dlugosz, A., Threadgill, D. W., Magnuson, T., and Yuspa, S. H. (1997). "Genetically null mice reveal a central role for epidermal growth factor receptor in the differentiation of the hair follicle and normal hair development." *The American journal of pathology*, 150(6), 1959.

Hardie, R. C. (2014). "Photosensitive TRPs", *Mammalian Transient Receptor Potential (TRP) Cation Channels*. Springer, pp. 795-826.

Hardman, J. A., Tobin, D. J., Haslam, I. S., Farjo, N., Farjo, B., Al-Nuaimi, Y., Grimaldi, B., and Paus, R. (2015). "The peripheral clock regulates human pigmentation." *Journal of Investigative Dermatology*, 135(4), 1053-1064.

Harries, M. J., Sun, J., Paus, R., and King, L. E., Jr. (2010). "Management of alopecia areata." *BMJ*, 341, c3671.

Hawkins, D., Houreld, N., and Abrahamse, H. (2005). "Low level laser therapy (LLLT) as an effective therapeutic modality for delayed wound healing." *Annals of the New York Academy of Sciences*, 1056(1), 486-493.

Headon, D. J., and Overbeek, P. A. (1999). "Involvement of a novel Tnf receptor homologue in hair follicle induction." *Nature genetics*, 22(4), 370-374.

Hebert, J. M., Rosenquist, T., Gotz, J., and Martin, G. R. (1994). "FGF5 as a regulator of the hair growth cycle: evidence from targeted and spontaneous mutations." *Cell*, 78(6), 1017-25.

Higgins, C. A., Petukhova, L., Harel, S., Ho, Y. Y., Drill, E., Shapiro, L., Wajid, M., and Christiano, A. M. (2014). "FGF5 is a crucial regulator of hair length in humans." *Proc Natl Acad Sci U S A*, 111(29), 10648-53.

Higgins, C. A., Westgate, G. E., and Jahoda, C. A. (2011). "Modulation in proteolytic activity is identified as a hallmark of exogen by transcriptional profiling of hair follicles." *Journal of Investigative Dermatology*, 131(12), 2349-2357.

Hirota, T., Lee, J. W., St John, P. C., Sawa, M., Iwaisako, K., Noguchi, T., Pongsawakul, P. Y., Sonntag, T., Welsh, D. K., Brenner, D. A., Doyle, F. J., 3rd, Schultz, P. G., and Kay, S. A. (2012). "Identification of small molecule activators of cryptochrome." *Science*, 337(6098), 1094-7.

Hoang, N., Schleicher, E., Kacprzak, S., Bouly, J. P., Picot, M., Wu, W., Berndt, A., Wolf, E., Bittl, R., and Ahmad, M. (2008). "Human and Drosophila cryptochromes are light activated by flavin photoreduction in living cells." *PLoS Biol*, 6(7), e160.

Hopkins, J. T., McLoda, T. A., Seegmiller, J. G., and Baxter, G. D. (2004). "Low-level laser therapy facilitates superficial wound healing in humans: a triple-blind, sham-controlled study." *Journal of Athletic training*, 39(3), 223.

Hsu, D. S., Zhao, X., Zhao, S., Kazantsev, A., Wang, R.-P., Todo, T., Wei, Y.-F., and Sancar, A. (1996). "Putative human blue-light photoreceptors hCRY1 and hCRY2 are flavoproteins." *Biochemistry*, 35(44), 13871-13877.

Huang, Y.-Y., Chen, A. C.-H., Carroll, J. D., and Hamblin, M. R. (2009). "Biphasic dose response in low level lightherapy." *Dose-Response*, 7(4), 358-383.

Huang, Z., Traugh, J. A., and Bishop, J. M. (2004). "Negative control of the Myc protein by the stress-responsive kinase Pak2." *Mol Cell Biol*, 24(4), 1582-94.

Huelsken, J., Vogel, R., Erdmann, B., Cotsarelis, G., and Birchmeier, W. (2001). "beta-Catenin controls hair follicle morphogenesis and stem cell differentiation in the skin." *Cell*, 105(4), 533-45.

Inoue, K., Aoi, N., Sato, T., Yamauchi, Y., Suga, H., Eto, H., Kato, H., Araki, J., and Yoshimura, K. (2009). "Differential expression of stem-cell-associated markers in human hair follicle epithelial cells." *Lab Invest*, 89(8), 844-56.

Inoue, K., and Yoshimura, K. (2013). "Skin stem cells." *Methods Mol Biol*, 989, 305-13.

Ito, M., Cotsarelis, G., Kizawa, K., and Hamada, K. (2004). "Hair follicle stem cells in the lower bulge form the secondary germ, a biochemically distinct but functionally equivalent progenitor cell population, at the termination of catagen." *Differentiation*, 72(9–10), 548-557.

Ito, M., Liu, Y., Yang, Z., Nguyen, J., Liang, F., Morris, R. J., and Cotsarelis, G. (2005). "Stem cells in the hair follicle bulge contribute to wound repair but not to homeostasis of the epidermis." *Nat Med*, 11(12), 1351-4.

Jabbari, A., Dai, Z., Xing, L., Cerise, J. E., Ramot, Y., Berkun, Y., Sanchez, G. A., Goldbach-Mansky, R., Christiano, A. M., Clynes, R., and Zlotogorski,

A. (2015). "Reversal of Alopecia Areata Following Treatment With the JAK1/2 Inhibitor Baricitinib." *EBioMedicine*, 2(4), 351-5.

Jacobs, J. P., Szpunar, C. A., and Warner, M. L. (1993). "Use of topical minoxidil therapy for androgenetic alopecia in women." *Int J Dermatol*, 32(10), 758-62.

Jacques, S. L. (2013). "Optical properties of biological tissues: a review." *Physics in medicine and biology*, 58(11), R37.

Jahoda, C. A., Horne, K. A., and Oliver, R. F. (1984). "Induction of hair growth by implantation of cultured dermal papilla cells." *Nature*, 311(5986), 560-2.

Jaworsky, C., Kligman, A. M., and Murphy, G. F. (1992). "Characterization of inflammatory infiltrates in male pattern alopecia: implications for pathogenesis." *Br J Dermatol*, 127(3), 239-46.

Jimenez, J. J., Wikramanayake, T. C., Bergfeld, W., Hordinsky, M., Hickman, J. G., Hamblin, M. R., and Schachner, L. A. (2014). "Efficacy and safety of a low-level laser device in the treatment of male and female pattern hair loss: a multicenter, randomized, sham device-controlled, double-blind study." *Am J Clin Dermatol*, 15(2), 115-27.

Johnstone, M. A., and Albert, D. M. (2002). "Prostaglandin-induced hair growth." *Surv Ophthalmol*, 47 Suppl 1, S185-202.

Joshi, R. S. (2011). "The Inner Root Sheath and the Men Associated with it Eponymically." *Int J Trichology*, 3(1), 57-62.

Kajagar, B. M., Godhi, A. S., Pandit, A., and Khatri, S. (2012). "Efficacy of low level laser therapy on wound healing in patients with chronic diabetic foot ulcers-a randomised control trial." *Indian J Surg*, 74(5), 359-63.

Kaneko, Y., and Szallasi, A. (2014). "Transient receptor potential (TRP) channels: a clinical perspective." *British journal of pharmacology*, 171(10), 2474-2507.

Karu, T. (1989). "Photobiology of low-power laser effects." *Health Phys*, 56(5), 691-704.

Karu, T. (1999). "Primary and secondary mechanisms of action of visible to near-IR radiation on cells." *J Photochem Photobiol B*, 49(1), 1-17.

Karu, T., and Kolyakov, S. (2005). "Exact action spectra for cellular responses relevant to phototherapy." *Photomedicine and Laser Therapy*, 23(4), 355-361.

Karu, T. I. (2011). "Light Coherence. Is this Property Important for Photomedicine? Photobiological Sciences Online (KC Smith, ed.) American Society for Photobiology". City.

Karu, T. I. (2014). "Cellular and Molecular Mechanisms of Photobiomodulation (Low-Power Laser Therapy)." *IEEE JOURNAL OF SELECTED TOPICS IN QUANTUM ELECTRONICS*, 20(2).

Karu, T. I., Pyatibrat, L. V., and Afanasyeva, N. I. (2004). "A novel mitochondrial signaling pathway activated by visible-to-near infrared radiation." *Photochem Photobiol*, 80(2), 366-72.

Karu, T. I., Pyatibrat, L. V., and Afanasyeva, N. I. (2005). "Cellular effects of low power laser therapy can be mediated by nitric oxide." *Lasers in surgery and medicine*, 36(4), 307-314.

Kasus-Jacobi, A., Ou, J., Birch, D. G., Locke, K. G., Shelton, J. M., Richardson, J. A., Murphy, A. J., Valenzuela, D. M., Yancopoulos, G. D., and Edwards, A. O. (2005). "Functional characterization of mouse RDH11 as

a retinol dehydrogenase involved in dark adaptation in vivo." *Journal of Biological Chemistry*, 280(21), 20413-20420.

Keemss, K., Pfaff, S. C., Born, M., Liebmann, J., Merk, H. F., and von Felbert, V. (2016). "Prospective, Randomized Study on the Efficacy and Safety of Local UV-Free Blue Light Treatment of Eczema." *Dermatology*, 232(4), 496-502.

Kennedy Crispin, M., Ko, J. M., Craiglow, B. G., Li, S., Shankar, G., Urban, J. R., Chen, J. C., Cerise, J. E., Jabbari, A., Winge, M. C., Marinkovich, M. P., Christiano, A. M., Oro, A. E., and King, B. A. (2016). "Safety and efficacy of the JAK inhibitor tofacitinib citrate in patients with alopecia areata." *JCI Insight*, 1(15), e89776.

Khan, I., and Arany, P. (2015). "Biophysical Approaches for Oral Wound Healing: Emphasis on Photobiomodulation." *Adv Wound Care (New Rochelle)*, 4(12), 724-737.

Kim, D.-K., and Holbrook, K. A. (1995). "The appearance, density, and distribution of Merkel cells in human embryonic and fetal skin: their relation to sweat gland and hair follicle development." *Journal of investigative dermatology*, 104(3), 411-416.

Kim, H.-R., Lee, G.-H., Cho, E. Y., Chae, S.-W., Ahn, T., and Chae, H.-J. (2009). "Bax inhibitor 1 regulates ER-stress-induced ROS accumulation through the regulation of cytochrome P450 2E1." *Journal of cell science*, 122(8), 1126-1133.

Kim, H., Choi, J. W., Kim, J. Y., Shin, J. W., Lee, S. J., and Huh, C. H. (2013a). "Low-level light therapy for androgenetic alopecia: a 24-week,

randomized, double-blind, sham device-controlled multicenter trial." *Dermatol Surg*, 39(8), 1177-83.

Kim, H. J., Son, E. D., Jung, J. Y., Choi, H., Lee, T. R., and Shin, D. W. (2013b). "Violet light down-regulates the expression of specific differentiation markers through Rhodopsin in normal human epidermal keratinocytes." *PLoS One*, 8(9), e73678.

Kim, M., An, J., Kim, K. S., Choi, M., Humar, M., Kwok, S. J., Dai, T., and Yun, S. H. (2016). "Optical lens-microneedle array for percutaneous light delivery." *Biomed Opt Express*, 7(10), 4220-4227.

Kim, T. S., Maeda, A., Maeda, T., Heinlein, C., Kedishvili, N., Palczewski, K., and Nelson, P. S. (2005). "Delayed Dark Adaptation in 11-cis-Retinol Dehydrogenase-deficient Mice A ROLE OF RDH11 IN VISUAL PROCESSES IN VIVO." *Journal of Biological Chemistry*, 280(10), 8694-8704.

Kleinpenning, M. M., Smits, T., Frunt, M. H., van Erp, P. E., van de Kerkhof, P. C., and Gerritsen, R. M. (2010). "Clinical and histological effects of blue light on normal skin." *Photodermatol Photoimmunol Photomed*, 26(1), 16-21.

Kloepper, J. E., Tiede, S., Brinckmann, J., Reinhardt, D. P., Meyer, W., Faessler, R., and Paus, R. (2008). "Immunophenotyping of the human bulge region: the quest to define useful in situ markers for human epithelial hair follicle stem cells and their niche." *Exp Dermatol*, 17(7), 592-609.

Ko, C. H., and Takahashi, J. S. (2006). "Molecular components of the mammalian circadian clock." *Hum Mol Genet*, 15 Spec No 2, R271-7.

Kowalska, E., and Brown, S. "Peripheral clocks: keeping up with the master clock." *Presented at Cold Spring Harbor Symposia on Quantitative Biology*.

Koyanagi, M., Takada, E., Nagata, T., Tsukamoto, H., and Terakita, A. (2013). "Homologs of vertebrate Opn3 potentially serve as a light sensor in nonphotoreceptive tissue." *Proc Natl Acad Sci U S A*, 110(13), 4998-5003.

Krause, K., and Foitzik, K. (2006). "Biology of the hair follicle: the basics." *Semin Cutan Med Surg*, 25(1), 2-10.

Kreplak, L., Merigoux, C., Briki, F., Flot, D., and Doucet, J. (2001). "Investigation of human hair cuticle structure by microdiffraction: direct observation of cell membrane complex swelling." *Biochim Biophys Acta*, 1547(2), 268-74.

Kuchabal, S. D., and Kuchabal, D. S. (2010). "Alopecia Areata Associated with Localized Vitiligo." *Case Rep Dermatol*, 2(1), 27-31.

Kurtev, A., and Iliev, E. (2005). "Thyroid autoimmunity in children and adolescents with alopecia areata." *Int J Dermatol*, 44(6), 457-61.

Lachgar, S., Charveron, M., Gall, Y., and Bonafe, J. L. (1998). "Minoxidil upregulates the expression of vascular endothelial growth factor in human hair dermal papilla cells." *Br J Dermatol*, 138(3), 407-11.

Lanzafame, R. J., Blanche, R. R., Bodian, A. B., Chiacchierini, R. P., Fernandez-Obregon, A., and Kazmirek, E. R. (2013). "The growth of human scalp hair mediated by visible red light laser and LED sources in males." *Lasers Surg Med*, 45(8), 487-95.

Lanzafame, R. J., Blanche, R. R., Chiacchierini, R. P., Kazmirek, E. R., and Sklar, J. A. (2014). "The growth of human scalp hair in females using visible red light laser and LED sources." *Lasers Surg Med*, 46(8), 601-7.

Leavitt, M., Charles, G., Heyman, E., and Michaels, D. (2009). "HairMax LaserComb laser phototherapy device in the treatment of male androgenetic alopecia: A randomized, double-blind, sham device-controlled, multicentre trial." *Clinical drug investigation*, 29(5), 283-92.

Liebmann, J., Born, M., and Kolb-Bachofen, V. (2010). "Blue-light irradiation regulates proliferation and differentiation in human skin cells." *J Invest Dermatol*, 130(1), 259-69.

Lin, C., and Todo, T. (2005). "The cryptochromes." *Genome biology*, 6(5), 220.

Lin, K. K., Kumar, V., Geyfman, M., Chudova, D., Ihler, A. T., Smyth, P., Paus, R., Takahashi, J. S., and Andersen, B. (2009). "Circadian clock genes contribute to the regulation of hair follicle cycling." *PLoS Genet*, 5(7), e1000573.

Lisbona, F., Rojas-Rivera, D., Thielen, P., Zamorano, S., Todd, D., Martinon, F., Glavic, A., Kress, C., Lin, J. H., and Walter, P. (2009). "BAX inhibitor-1 is a negative regulator of the ER stress sensor IRE1α." *Molecular cell*, 33(6), 679-691.

Luck, M., Mathes, T., Bruun, S., Fudim, R., Hagedorn, R., Tran Nguyen, T. M., Kateriya, S., Kennis, J. T., Hildebrandt, P., and Hegemann, P. (2012). "A photochromic histidine kinase rhodopsin (HKR1) that is bimodally switched by ultraviolet and blue light." *J Biol Chem*, 287(47), 40083-90.

Luo, Y., Robinson, S., Fujita, J., Siconolfi, L., Magidson, J., Edwards, C. K., Wassmann, K., Storm, K., Norris, D. A., and Bankaitis-Davis, D. (2011).

"Transcriptome profiling of whole blood cells identifies PLEK2 and C1QB in human melanoma." *PloS one*, 6(6), e20971.

Lyle, S., Christofidou-Solomidou, M., Liu, Y., Elder, D. E., Albelda, S., and Cotsarelis, G. (1998). "The C8/144B monoclonal antibody recognizes cytokeratin 15 and defines the location of human hair follicle stem cells." *J Cell Sci*, 111 (Pt 21), 3179-88.

Mahe, Y. F., Michelet, J. F., Billoni, N., Jarrousse, F., Buan, B., Commo, S., Saint-Leger, D., and Bernard, B. A. (2000). "Androgenetic alopecia and microinflammation." *Int J Dermatol*, 39(8), 576-84.

Mahony, D., Parry, D. A., and Lees, E. (1998). "Active cdk6 complexes are predominantly nuclear and represent only a minority of the cdk6 in T cells." *Oncogene*, 16(5).

Martinez-Mir, A., Zlotogorski, A., Gordon, D., Petukhova, L., Mo, J., Gilliam, T. C., Londono, D., Haynes, C., Ott, J., Hordinsky, M., Nanova, K., Norris, D., Price, V., Duvic, M., and Christiano, A. M. (2007). "Genomewide scan for linkage reveals evidence of several susceptibility loci for alopecia areata." *Am J Hum Genet*, 80(2), 316-28.

Masson-Meyers, D. S., Bumah, V. V., and Enwemeka, C. S. (2016). "Blue light does not impair wound healing in vitro." *J Photochem Photobiol B*, 160, 53-60.

Matsuo, T., Yamaguchi, S., Mitsui, S., Emi, A., Shimoda, F., and Okamura, H. (2003). "Control Mechanism of the Circadian Clock for Timing of Cell Division in Vivo." *Science*, 302(5643), 255-259.

Matushansky, I., Radparvar, F., and Skoultchi, A. I. (2000). "Reprogramming leukemic cells to terminal differentiation by inhibiting specific cyclin-

dependent kinases in G1." *Proceedings of the National Academy of Sciences*, 97(26), 14317-14322.

Matushansky, I., Radparvar, F., and Skoultchi, A. I. (2003). "CDK6 blocks differentiation: coupling cell proliferation to the block to differentiation in leukemic cells." *Oncogene*, 22(27), 4143-4149.

McDowall, M., Edwards, N. M., Jahoda, C. A., and Hynd, P. I. (2008). "The role of activins and follistatins in skin and hair follicle development and function." *Cytokine Growth Factor Rev*, 19(5-6), 415-26.

McElwee, K. J., Kissling, S., Wenzel, E., Huth, A., and Hoffmann, R. (2003). "Cultured peribulbar dermal sheath cells can induce hair follicle development and contribute to the dermal sheath and dermal papilla." *Journal of investigative dermatology*, 121(6), 1267-1275.

Menon, S. T., Han, M., and Sakmar, T. P. (2001). "Rhodopsin: structural basis of molecular physiology." *Physiol Rev*, 81(4), 1659-88.

Mester, E., Szende, B., and Tota, J. (1967). "Effect of laser on hair growth of mice." *Kiserl Orvostud*, 19, 628-631.

Metelitsa, A. I., and Green, J. B. (2011). "Home-use laser and light devices for the skin: an update." *Semin Cutan Med Surg*, 30(3), 144-7.

Mignon, C., Botchkareva, N. V., Uzunbajakava, N. E., and Tobin, D. J. (2016a). "Photobiomodulation devices for hair regrowth and wound healing: a therapy full of promise but a literature full of confusion." *Experimental dermatology*, 25(10), 745-749.

Mignon, C., Uzunbajakava, N. E., Raafs, B., Botchkareva, N. V., Moolenaar, M., and Tobin, D. J. "Photobiomodulation of distinct lineages of human dermal fibroblasts: a rational approach towards the selection of effective

light parameters for skin rejuvenation and wound healing." *Presented at Mechanisms of Photobiomodulation Therapy XI*, SPIE 9695, Mechanisms of Photobiomodulation Therapy XI, 969508.

Millar, S. E. (2002). "Molecular mechanisms regulating hair follicle development." *J Invest Dermatol*, 118(2), 216-25.

Milner, Y., Sudnik, J., Filippi, M., Kizoulis, M., Kashgarian, M., and Stenn, K. (2002). "Exogen, shedding phase of the hair growth cycle: characterization of a mouse model." *J Invest Dermatol*, 119(3), 639-44.

Mishina, Y. (2003). "Function of bone morphogenetic protein signaling during mouse development." *Front Biosci*, 8, d855-69.

Mittermayr, R., Osipov, A., Piskernik, C., Haindl, S., Dungel, P., Weber, C., Vladimirov, Y. A., Redl, H., and Kozlov, A. V. (2007). "Blue laser light increases perfusion of a skin flap via release of nitric oxide from hemoglobin." *MOLECULAR MEDICINE-CAMBRIDGE MA THEN NEW YORK-*, 13(1/2), 22.

Miyagi, M., Yokoyama, H., Shiraishi, H., Matsumoto, M., and Ishii, H. (2001). "Simultaneous quantification of retinol, retinal, and retinoic acid isomers by high-performance liquid chromatography with a simple gradiation." *J Chromatogr B Biomed Sci Appl*, 757(2), 365-8.

Moore, P., Ridgway, T. D., Higbee, R. G., Howard, E. W., and Lucroy, M. D. (2005). "Effect of wavelength on low-intensity laser irradiation-stimulated cell proliferation in vitro." *Lasers in surgery and medicine*, 36(1), 8-12.

Morris, R. J., Liu, Y., Marles, L., Yang, Z., Trempus, C., Li, S., Lin, J. S., Sawicki, J. A., and Cotsarelis, G. (2004). "Capturing and profiling adult hair follicle stem cells." *Nat Biotechnol*, 22(4), 411-7.

Muller-Rover, S., Handjiski, B., van der Veen, C., Eichmuller, S., Foitzik, K., McKay, I. A., Stenn, K. S., and Paus, R. (2001). "A comprehensive guide for the accurate classification of murine hair follicles in distinct hair cycle stages." *J Invest Dermatol*, 117(1), 3-15.

Müller, G., Dörschel, K., and Kar, H. (1991). "Biophysics of the photoablation process." *Lasers in Medical Science*, 6(3), 241-254.

Munck, A., Gavazzoni, M. F., and Trueb, R. M. (2014). "Use of low-level laser therapy as monotherapy or concomitant therapy for male and female androgenetic alopecia." *Int J Trichology*, 6(2), 45-9.

Mysore, V. (2012). "Finasteride and sexual side effects." *Indian Dermatol Online J*, 3(1), 62-5.

Naeser, M. A. (2006). "Photobiomodulation of pain in carpal tunnel syndrome: review of seven laser therapy studies." *Photomed Laser Surg*, 24(2), 101-10.

Nagasawa, M., Melamed, I., Kupfer, A., Gelfand, E. W., and Lucas, J. J. (1997). "Rapid nuclear translocation and increased activity of cyclin-dependent kinase 6 after T cell activation." *The Journal of Immunology*, 158(11), 5146-5154.

Norwood, O. T. (1975). "Male pattern baldness: classification and incidence." *South Med J*, 68(11), 1359-65.

Norwood, O. T. (2001). "Incidence of female androgenetic alopecia (female pattern alopecia)." *Dermatol Surg*, 27(1), 53-4.

Ogasawara, T., Katagiri, M., Yamamoto, A., Hoshi, K., Takato, T., Nakamura, K., Tanaka, S., Okayama, H., and Kawaguchi, H. (2004a). "Osteoclast Differentiation by RANKL Requires NF-κB-Mediated Downregulation of

Cyclin-Dependent Kinase 6 (Cdk6)." *Journal of Bone and Mineral Research*, 19(7), 1128-1136.

Ogasawara, T., Kawaguchi, H., Jinno, S., Hoshi, K., Itaka, K., Takato, T., Nakamura, K., and Okayama, H. (2004b). "Bone morphogenetic protein 2-induced osteoblast differentiation requires Smad-mediated down-regulation of Cdk6." *Molecular and cellular biology*, 24(15), 6560-6568.

Ohyama, M., Terunuma, A., Tock, C. L., Radonovich, M. F., Pise-Masison, C. A., Hopping, S. B., Brady, J. N., Udey, M. C., and Vogel, J. C. (2006). "Characterization and isolation of stem cell-enriched human hair follicle bulge cells." *J Clin Invest*, 116(1), 249-60.

Okada, T., Le Trong, I., Fox, B. A., Behnke, C. A., Stenkamp, R. E., and Palczewski, K. (2000). "X-ray diffraction analysis of three-dimensional crystals of bovine rhodopsin obtained from mixed micelles." *Journal of structural biology*, 130(1), 73-80.

Olsen, E. A., Hordinsky, M. K., Price, V. H., Roberts, J. L., Shapiro, J., Canfield, D., Duvic, M., King, L. E., Jr., McMichael, A. J., Randall, V. A., Turner, M. L., Sperling, L., Whiting, D. A., Norris, D., and National Alopecia Areata, F. (2004). "Alopecia areata investigational assessment guidelines--Part II. National Alopecia Areata Foundation." *J Am Acad Dermatol*, 51(3), 440-7.

Ong, W. K., Chen, H. F., Tsai, C. T., Fu, Y. J., Wong, Y. S., Yen, D. J., Chang, T. H., Huang, H. D., Lee, O. K., Chien, S., and Ho, J. H. (2013). "The activation of directional stem cell motility by green light-emitting diode irradiation." *Biomaterials*, 34(8), 1911-20.

Oplander, C., Deck, A., Volkmar, C. M., Kirsch, M., Liebmann, J., Born, M., van Abeelen, F., van Faassen, E. E., Kroncke, K. D., Windolf, J., and Suschek, C. V. (2013). "Mechanism and biological relevance of blue-light (420-453 nm)-induced nonenzymatic nitric oxide generation from photolabile nitric oxide derivates in human skin in vitro and in vivo." *Free Radic Biol Med*, 65, 1363-77.

Oshima, T., Yamanaka, I., Kumar, A., Yamaguchi, J., Nishiwaki-Ohkawa, T., Muto, K., Kawamura, R., Hirota, T., Yagita, K., Irle, S., Kay, S. A., Yoshimura, T., and Itami, K. (2015). "C-H activation generates period-shortening molecules that target cryptochrome in the mammalian circadian clock." *Angew Chem Int Ed Engl*, 54(24), 7193-7.

Oshimori, N., and Fuchs, E. (2012). "Paracrine TGF-β signaling counterbalances BMP-mediated repression in hair follicle stem cell activation." *Cell stem cell*, 10(1), 63-75.

Ota, Y., Saitoh, Y., Suzuki, S., Ozawa, K., Kawano, M., and Imamura, T. (2002). "Fibroblast growth factor 5 inhibits hair growth by blocking dermal papilla cell activation." *Biochemical and biophysical research communications*, 290(1), 169-176.

Palmer, H. G., Martinez, D., Carmeliet, G., and Watt, F. M. (2008). "The vitamin D receptor is required for mouse hair cycle progression but not for maintenance of the epidermal stem cell compartment." *J Invest Dermatol*, 128(8), 2113-7.

Panda, S., Sato, T. K., Castrucci, A. M., Rollag, M. D., DeGrip, W. J., Hogenesch, J. B., Provencio, I., and Kay, S. A. (2002). "Melanopsin

(Opn4) requirement for normal light-induced circadian phase shifting." *Science*, 298(5601), 2213-2216.

Panteleyev, A. A., van der Veen, C., Rosenbach, T., Muller-Rover, S., Sokolov, V. E., and Paus, R. (1998). "Towards defining the pathogenesis of the hairless phenotype." *J Invest Dermatol*, 110(6), 902-7.

Paschotta, R. (2008). *Field Guide to Lasers*: SPIE press.

Pastore, D., Di Martino, C., Bosco, G., and Passarella, S. (1995). "Plant Mitochondria are Sensitive to Helium-Neon Laser Light." *Plant Biosystem*, 129(4), 1075-1076.

Pastore, D., Greco, M., Petragallo, V., and Passarella, S. (1994). "Increase in<-- H+/e-ratio of the cytochrome c oxidase reaction in mitochondria irradiated with helium-neon laser." *Biochemistry and molecular biology international*, 34(4), 817-826.

Pastore, M. G., S. Passarella, D. (2000). "Specific helium-neon laser sensitivity of the purified cytochrome c oxidase." *International journal of radiation biology*, 76(6), 863-870.

Paus, R., and Cotsarelis, G. (1999). "The biology of hair follicles." *N Engl J Med*, 341(7), 491-7.

Paus, R., and Foitzik, K. (2004). "In search of the "hair cycle clock": a guided tour." *Differentiation*, 72(9-10), 489-511.

Paus, R., Nickoloff, B. J., and Ito, T. (2005). "A 'hairy' privilege." *Trends Immunol*, 26(1), 32-40.

Paus, R., Slominski, A., and Czarnetzki, B. M. (1993). "Is alopecia areata an autoimmune-response against melanogenesis-related proteins, exposed

by abnormal MHC class I expression in the anagen hair bulb?" *Yale J Biol Med*, 66(6), 541-54.

Pellicioli, A. C., Martins, M. D., Dillenburg, C. S., Marques, M. M., Squarize, C. H., and Castilho, R. M. (2014). "Laser phototherapy accelerates oral keratinocyte migration through the modulation of the mammalian target of rapamycin signaling pathway." *J Biomed Opt*, 19(2), 028002.

Petukhova, L., Duvic, M., Hordinsky, M., Norris, D., Price, V., Shimomura, Y., Kim, H., Singh, P., Lee, A., Chen, W. V., Meyer, K. C., Paus, R., Jahoda, C. A., Amos, C. I., Gregersen, P. K., and Christiano, A. M. (2010). "Genome-wide association study in alopecia areata implicates both innate and adaptive immunity." *Nature*, 466(7302), 113-7.

Pfaff, S., Liebmann, J., Born, M., Merk, H. F., and von Felbert, V. (2015). "Prospective Randomized Long-Term Study on the Efficacy and Safety of UV-Free Blue Light for Treating Mild Psoriasis Vulgaris." *Dermatology*, 231(1), 24-34.

Philpott, M., Sanders, D., Bowen, J., and Kealey, T. (1996). "Effects of interleukins, colony-stimulating factor and tumour necrosis factor on human hair follicle growth in vitro: a possible role for interleukin-1 and tumour necrosis factor-α in alopecia areata." *British journal of dermatology*, 135(6), 942-948.

Philpott, M., Sanders, D., and Kealey, T. (1994a). "Effects of insulin and insulin-like growth factors on cultured human hair follicles: IGF-I at physiologic concentrations is an important regulator of hair follicle growth in vitro." *Journal of Investigative Dermatology*, 102(6), 857-861.

Philpott, M. P., Sanders, D., Westgate, G. E., and Kealey, T. (1994b). "Human hair growth in vitro: a model for the study of hair follicle biology." *J Dermatol Sci*, 7 Suppl, S55-72.

Plikus, M. V. (2012). "New activators and inhibitors in the hair cycle clock: targeting stem cells' state of competence." *Journal of Investigative Dermatology*, 132(5), 1321-1324.

Plikus, M. V., Baker, R. E., Chen, C.-C., Fare, C., de la Cruz, D., Andl, T., Maini, P. K., Millar, S. E., Widelitz, R., and Chuong, C.-M. (2011). "Self-organizing and stochastic behaviors during the regeneration of hair stem cells." *Science*, 332(6029), 586-589.

Plikus, M. V., Mayer, J. A., de la Cruz, D., Baker, R. E., Maini, P. K., Maxson, R., and Chuong, C. M. (2008). "Cyclic dermal BMP signalling regulates stem cell activation during hair regeneration." *Nature*, 451(7176), 340-4.

Plikus, M. V., Vollmers, C., de la Cruz, D., Chaix, A., Ramos, R., Panda, S., and Chuong, C. M. (2013). "Local circadian clock gates cell cycle progression of transient amplifying cells during regenerative hair cycling." *Proc Natl Acad Sci U S A*, 110(23), E2106-15.

Prabhu, V. R., Bola Sadashiva S.; Mahato, Krishna Kishore. "Alterations in cell migration and cell viability of wounded human skin fibroblasts following visible red light exposure." *Proceedings of the SPIE*, 8932.

Price, V. H. (1999). "Treatment of hair loss." *N Engl J Med*, 341(13), 964-73.

Price, V. H. (2003). "Androgenetic alopecia in women." *J Investig Dermatol Symp Proc*, 8(1), 24-7.

Purba, T. S., Haslam, I. S., Poblet, E., Jimenez, F., Gandarillas, A., Izeta, A., and Paus, R. (2014). "Human epithelial hair follicle stem cells and their

progeny: current state of knowledge, the widening gap in translational research and future challenges." *Bioessays*, 36(5), 513-25.

Quigley, C. A. (1998). "The androgen receptor: physiology and pathophysiology", *Testosterone*. Springer, pp. 33-106.

Rando, R. R. (1996). "Polyenes and vision." *Chemistry & biology*, 3(4), 255-262.

Rietschel, R. L., and Duncan, S. H. (1987). "Safety and efficacy of topical minoxidil in the management of androgenetic alopecia." *J Am Acad Dermatol*, 16(3 Pt 2), 677-85.

Rinaldi, F. (2008). "Laser: a review." *Clin Dermatol*, 26(6), 590-601.

Rittmaster, R. S. (1994). "Finasteride." *N Engl J Med*, 330(2), 120-5.

Rompolas, P., and Greco, V. (2014). "Stem cell dynamics in the hair follicle niche." *Semin Cell Dev Biol*, 25-26, 34-42.

Rose, P. T. (2015). "Hair restoration surgery: challenges and solutions." *Clin Cosmet Investig Dermatol*, 8, 361-70.

Rumio, C., Donetti, E., Imberti, A., Barajon, I., Prosperi, E., Brivio, M., Boselli, A., Lavezzari, E., Veraldi, S., and Bignotto, M. (2000). "c-Myc expression in human anagen hair follicles." *British journal of dermatology*, 142(6), 1092-1099.

Safavi, K. (1992). "Prevalence of alopecia areata in the First National Health and Nutrition Examination Survey." *Arch Dermatol*, 128(5), 702.

Safavi, K. H., Muller, S. A., Suman, V. J., Moshell, A. N., and Melton, L. J., 3rd. (1995). "Incidence of alopecia areata in Olmsted County, Minnesota, 1975 through 1989." *Mayo Clin Proc*, 70(7), 628-33.

Sakamoto, K., Nagase, T., Fukui, H., Horikawa, K., Okada, T., Tanaka, H., Sato, K., Miyake, Y., Ohara, O., and Kako, K. (1998). "Multitissue

circadian expression of rat periodhomolog (rPer2) mRNA is governed by the mammalian circadian clock, the suprachiasmatic nucleus in the brain." *Journal of Biological Chemistry*, 273(42), 27039-27042.

Sancar, A. (2000). "Cryptochrome: the second photoactive pigment in the eye and its role in circadian photoreception." *Annu Rev Biochem*, 69, 31-67.

Sato, M., Matsuo, T., Atmore, H., and Akashi, M. (2014). "Possible contribution of chronobiology to cardiovascular health." *Frontiers in physiology*, 4, 409.

Sato, N., Leopold, P. L., and Crystal, R. G. (1999). "Induction of the hair growth phase in postnatal mice by localized transient expression of Sonic hedgehog." *J Clin Invest*, 104(7), 855-64.

Sawaya, M. E., and Hordinsky, M. K. (1995). "Glucocorticoid regulation of hair growth in alopecia areata." *J Invest Dermatol*, 104(5 Suppl), 30S.

Sawaya, M. E., and Price, V. H. (1997). "Different levels of 5alpha-reductase type I and II, aromatase, and androgen receptor in hair follicles of women and men with androgenetic alopecia." *J Invest Dermatol*, 109(3), 296-300.

Sazonov, A., Romanov, G., Portnoĭ, L., Odinokova, V., and Karu, T. (1985). "Low-intensity noncoherent red light in the complex treatment of peptic ulcer." *Sovetskaia meditsina*(12), 42.

Schmutz, I., Albrecht, U., and Ripperger, J. A. (2012). "The role of clock genes and rhythmicity in the liver." *Molecular and cellular endocrinology*, 349(1), 38-44.

Schneider, M. R., Schmidt-Ullrich, R., and Paus, R. (2009). "The hair follicle as a dynamic miniorgan." *Curr Biol*, 19(3), R132-42.

Sehgal, V. N., and Jain, S. (2003). "Alopecia areata: clinical perspective and an insight into pathogenesis." *J Dermatol*, 30(4), 271-89.

Sekharan, S., and Morokuma, K. (2011). "Why 11-cis-retinal? Why not 7-cis-, 9-cis-, or 13-cis-retinal in the eye?" *J Am Chem Soc*, 133(47), 19052-5.

Selby, C. P., Thompson, C., Schmitz, T. M., Van Gelder, R. N., and Sancar, A. (2000). "Functional redundancy of cryptochromes and classical photoreceptors for nonvisual ocular photoreception in mice." *Proceedings of the National Academy of Sciences*, 97(26), 14697-14702.

Sequeira, I., and Nicolas, J. F. (2012). "Redefining the structure of the hair follicle by 3D clonal analysis." *Development*, 139(20), 3741-51.

Severi, G., Sinclair, R., Hopper, J. L., English, D. R., McCredie, M. R., Boyle, P., and Giles, G. G. (2003). "Androgenetic alopecia in men aged 40-69 years: prevalence and risk factors." *Br J Dermatol*, 149(6), 1207-13.

Shapiro, J., and Price, V. H. (1998). "Hair regrowth. Therapeutic agents." *Dermatol Clin*, 16(2), 341-56.

Sherr, C. J., and Roberts, J. M. (1999). "CDK inhibitors: positive and negative regulators of G1-phase progression." *Genes & development*, 13(12), 1501-1512.

Singh, B., and Goldberg, L. J. (2016). "Autologous Platelet-Rich Plasma for the Treatment of Pattern Hair Loss." *Am J Clin Dermatol*, 17(4), 359-67.

Singh, G., and Lavanya, M. (2010). "Topical immunotherapy in alopecia areata." *International journal of trichology*, 2(1), 36.

Slominski, A., Tobin, D. J., Shibahara, S., and Wortsman, J. (2004). "Melanin pigmentation in mammalian skin and its hormonal regulation." *Physiol Rev*, 84(4), 1155-228.

Snippert, H. J., Haegebarth, A., Kasper, M., Jaks, V., van Es, J. H., Barker, N., van de Wetering, M., van den Born, M., Begthel, H., Vries, R. G., Stange, D. E., Toftgard, R., and Clevers, H. (2010). "Lgr6 marks stem cells in the hair follicle that generate all cell lineages of the skin." *Science*, 327(5971), 1385-9.

Song, S., Zhang, Y., Fong, C.-C., Tsang, C.-H., Yang, Z., and Yang, M. (2003). "cDNA microarray analysis of gene expression profiles in human fibroblast cells irradiated with red light." *Journal of Investigative Dermatology*, 120(5), 849-857.

Steiner, R. (1993). "Thermal and non-thermal laser dissection." *Endoscopic surgery and allied technologies*, 2(3-4), 214-220.

Steiner, R. (2011). "Laser-tissue interactions", *Laser and IPL Technology in Dermatology and Aesthetic Medicine*. Springer, pp. 23-36.

Stenn, K. S., and Paus, R. (2001). "Controls of hair follicle cycling." *Physiol Rev*, 81(1), 449-494.

Storch, K.-F., Lipan, O., Leykin, I., Viswanathan, N., Davis, F. C., Wong, W. H., and Weitz, C. J. (2002). "Extensive and divergent circadian gene expression in liver and heart." *Nature*, 417(6884), 78-83.

Straile, W. E., Chase, H. B., and Arsenault, C. (1961). "Growth and differentiation of hair follicles between periods of activity and quiescence." *J Exp Zool*, 148, 205-21.

Sugihara, T., Nagata, T., Mason, B., Koyanagi, M., and Terakita, A. (2016). "Absorption Characteristics of Vertebrate Non-Visual Opsin, Opn3." *PLoS One*, 11(8), e0161215.

Tan, E., Tay, Y. K., Goh, C. L., and Chin Giam, Y. (2002). "The pattern and profile of alopecia areata in Singapore--a study of 219 Asians." *Int J Dermatol*, 41(11), 748-53.

Tanioka, M., Yamada, H., Doi, M., Bando, H., Yamaguchi, Y., Nishigori, C., and Okamura, H. (2009). "Molecular clocks in mouse skin." *Journal of Investigative Dermatology*, 129(5), 1225-1231.

Templeton, S. F., and Solomon, A. R. (1994). "Scarring alopecia: a classification based on microscopic criteria." *Journal of cutaneous pathology*, 21(2), 97-109.

Terakita, A. (2005). "The opsins." *Genome Biol*, 6(3), 213.

Thresher, R. J., Vitaterna, M. H., Miyamoto, Y., Kazantsev, A., Hsu, D. S., Petit, C., Selby, C. P., Dawut, L., Smithies, O., and Takahashi, J. S. (1998). "Role of mouse cryptochrome blue-light photoreceptor in circadian photoresponses." *Science*, 282(5393), 1490-1494.

Timmermann, S., Hinds, P. W., and Munger, K. (1997). "Elevated activity of cyclin-dependent kinase 6 in human squamous cell carcinoma lines." *Cell Growth and Differentiation-Publication American Association for Cancer Research*, 8(4), 361-370.

Tobin, D. J., and Bystryn, J. C. (1996). "Different populations of melanocytes are present in hair follicles and epidermis." *Pigment cell research*, 9(6), 304-310.

Tosti, A., and Duque-Estrada, B. (2009). "Treatment strategies for alopecia." *Expert Opin Pharmacother*, 10(6), 1017-26.

Tosti, A., and Piraccini, B. M. (2002). "Loose anagen hair syndrome and loose anagen hair." *Arch Dermatol*, 138(4), 521-2.

Tosti, A., Whiting, D., Iorizzo, M., Pazzaglia, M., Misciali, C., Vincenzi, C., and Micali, G. (2008). "The role of scalp dermoscopy in the diagnosis of alopecia areata incognita." *J Am Acad Dermatol*, 59(1), 64-7.

Trempus, C. S., Morris, R. J., Bortner, C. D., Cotsarelis, G., Faircloth, R. S., Reece, J. M., and Tennant, R. W. (2003). "Enrichment for living murine keratinocytes from the hair follicle bulge with the cell surface marker CD34." *J Invest Dermatol*, 120(4), 501-11.

Treuting, P. M., and Dintzis, S. M. (2011). *Comparative Anatomy and Histology: A Mouse and Human Atlas (Expert Consult)*: Academic Press.

Trueb, R. M. (2002). "Molecular mechanisms of androgenetic alopecia." *Exp Gerontol*, 37(8-9), 981-90.

Tsutsumi, M., Ikeyama, K., Denda, S., Nakanishi, J., Fuziwara, S., Aoki, H., and Denda, M. (2009). "Expressions of rod and cone photoreceptor-like proteins in human epidermis." *Exp Dermatol*, 18(6), 567-70.

Van Der Horst, G. T., Muijtjens, M., Kobayashi, K., Takano, R., Kanno, S.-i., Takao, M., de Wit, J., Verkerk, A., Eker, A. P., and van Leenen, D. (1999). "Mammalian Cry1 and Cry2 are essential for maintenance of circadian rhythms." *Nature*, 398(6728), 627-630.

Van Gelder, R. N., Wee, R., Lee, J. A., and Tu, D. C. (2003). "Reduced pupillary light responses in mice lacking cryptochromes." *Science*, 299(5604), 222-222.

Vladimirov Iu, A., Klebanov, G. I., Borisenko, G. G., and Osipov, A. N. (2004). "[Molecular and cellular mechanisms of the low intensity laser radiation effect]." *Biofizika*, 49(2), 339-50.

Wang, L. C., Liu, Z. Y., Gambardella, L., Delacour, A., Shapiro, R., Yang, J., Sizing, I., Rayhorn, P., Garber, E. A., Benjamin, C. D., Williams, K. P., Taylor, F. R., Barrandon, Y., Ling, L., and Burkly, L. C. (2000). "Regular articles: conditional disruption of hedgehog signaling pathway defines its critical role in hair development and regeneration." *J Invest Dermatol*, 114(5), 901-8.

Wang, S. J., Shohat, T., Vadheim, C., Shellow, W., Edwards, J., and Rotter, J. I. (1994). "Increased risk for type I (insulin-dependent) diabetes in relatives of patients with alopecia areata (AA)." *Am J Med Genet*, 51(3), 234-9.

Wang, Y., Huang, Y. Y., Wang, Y., Lyu, P., and Hamblin, M. R. (2016). "Photobiomodulation (blue and green light) encourages osteoblastic-differentiation of human adipose-derived stem cells: role of intracellular calcium and light-gated ion channels." *Sci Rep*, 6, 33719.

Wasserman, D., Guzman-Sanchez, D. A., Scott, K., and McMichael, A. (2007). "Alopecia areata." *Int J Dermatol*, 46(2), 121-31.

Watt, F. M. (2000). "Epidermal stem cells as targets for gene transfer." *Human gene therapy*, 11(16), 2261-2266.

Weinberg, R. A. (1995). "The retinoblastoma protein and cell cycle control." *Cell*, 81(3), 323-330.

Weinstabl, A., Hoff-Lesch, S., Merk, H. F., and von Felbert, V. (2011). "Prospective randomized study on the efficacy of blue light in the treatment of psoriasis vulgaris." *Dermatology*, 223(3), 251-9.

White, J. H., Chiano, M., Wigglesworth, M., Geske, R., Riley, J., White, N., Hall, S., Zhu, G., Maurio, F., Savage, T., Anderson, W., Cordy, J., Ducceschi, M., investigators, G., Vestbo, J., and Pillai, S. G. (2008). "Identification of

a novel asthma susceptibility gene on chromosome 1qter and its functional evaluation." *Hum Mol Genet*, 17(13), 1890-903.

Whiting, D. A. (1993). "Diagnostic and predictive value of horizontal sections of scalp biopsy specimens in male pattern androgenetic alopecia." *J Am Acad Dermatol*, 28(5 Pt 1), 755-63.

Whiting, D. A. (2003). "Histopathologic features of alopecia areata: a new look." *Arch Dermatol*, 139(12), 1555-9.

Wicks, N. L., Chan, J. W., Najera, J. A., Ciriello, J. M., and Oancea, E. (2011). "UVA phototransduction drives early melanin synthesis in human melanocytes." *Curr Biol*, 21(22), 1906-11.

Wong-Riley, M. T., Liang, H. L., Eells, J. T., Chance, B., Henry, M. M., Buchmann, E., Kane, M., and Whelan, H. T. (2005). "Photobiomodulation directly benefits primary neurons functionally inactivated by toxins: role of cytochrome c oxidase." *J Biol Chem*, 280(6), 4761-71.

Xing, L., Dai, Z., Jabbari, A., Cerise, J. E., Higgins, C. A., Gong, W., de Jong, A., Harel, S., DeStefano, G. M., Rothman, L., Singh, P., Petukhova, L., Mackay-Wiggan, J., Christiano, A. M., and Clynes, R. (2014). "Alopecia areata is driven by cytotoxic T lymphocytes and is reversed by JAK inhibition." *Nat Med*, 20(9), 1043-9.

Xu, Q., and Reed, J. C. (1998). "Bax inhibitor-1, a mammalian apoptosis suppressor identified by functional screening in yeast." *Molecular cell*, 1(3), 337-346.

Yamazaki, S., Numano, R., Abe, M., Hida, A., Takahashi, R.-i., Ueda, M., Block, G. D., Sakaki, Y., Menaker, M., and Tei, H. (2000). "Resetting central

and peripheral circadian oscillators in transgenic rats." *Science*, 288(5466), 682-685.

Yoo, S.-H., Yamazaki, S., Lowrey, P. L., Shimomura, K., Ko, C. H., Buhr, E. D., Siepka, S. M., Hong, H.-K., Oh, W. J., and Yoo, O. J. (2004). "PERIOD2:: LUCIFERASE real-time reporting of circadian dynamics reveals persistent circadian oscillations in mouse peripheral tissues." *Proceedings of the National Academy of Sciences of the United States of America*, 101(15), 5339-5346.

Yu, W., Naim, J. O., and Lanzafame, R. J. (1997). "Effects of photostimulation on wound healing in diabetic mice." *Lasers in surgery and medicine*, 20(1), 56-63.

Zanello, S. B., Jackson, D. M., and Holick, M. F. (2000). "Expression of the circadian clock genes clock and period1 in human skin." *Journal of investigative dermatology*, 115(4), 757-760.

Zhang, E. E., Liu, A. C., Hirota, T., Miraglia, L. J., Welch, G., Pongsawakul, P. Y., Liu, X., Atwood, A., Huss, J. W., and Janes, J. (2009). "A genome-wide RNAi screen for modifiers of the circadian clock in human cells." *Cell*, 139(1), 199-210.